Chapter 1

Introduction

Chaos is either undesirable or desirable in various engineering problems. Many researchers have devoted themselves to finding new ways to control chaos more efficiently. Chaotic phenomena are quite useful in many applications such as fluid mixing [1], human brain dynamics [2], and heart beat regulation [3], information processing, etc. Therefore, making a periodic dynamical system chaotic, or preserving chaos of a chaotic dynamical system, is very meaningful and worthy to be investigated.

Chaos synchronization has been applied in many fields such as secure communication [4,5], chemical and biological systems [6,7], etc. A lot of researchers have studied synchronization between two identical chaotic systems[10-16]. But up to now, the studies are mostly concentrated on complete synchronization. Hence a large number of researches have not been carried out for anticipated and lag synchronization which became an important part of this thesis.

The object studied of this thesis is brushless dc motor (BLDCM). The major advantage of BLDCM is the elimination of the physical contact between the brushes and the commutators. BLDCM has been widely applied in direct-drive applications such as robotics [8], aerospace [9], etc. In this thesis, (a) its synchronization by linear feedback control and adaptive control via a system variable, and global synchronization of three coupled chaotic systems with ring connection, (b) we investigate anticipated chaotic synchronization of BLDCM and lag chaotic synchronization and complete chaos synchronization of identical systems in different ways (c) chaos synchronization for fractional order motor system.

This thesis is organized as follows. Chapter 2 contains the dynamic equation of BLDCM. First, the system model is described. Second, the system equations are transformed

to a compact form. In Chapter 3, the synchronization of two identical chaotic systems is accomplished via control of a single variable, by a linear feedback controller and an adaptive controller, and the method of ring connection is applied for three BLDCM chaotic systems for synchronization. Numerical results are presented. In Chapter 4, two methods are investigated to achieve anticipated synchronization and complete synchronization. Three methods are used to achieve lag synchronization. In Chapter 5, chaos analysis, chaos control of fractional order system and synchronization for identical and different fractional order system are presented, and numerical results are shown.

Chapter 2

Regular and Chaotic Dynamics of Brushless DC Motor

In this Chapter, the dynamic characteristics[18-19] of BLDCM are investigated. First, the dynamic system model is given. Second, the state equations are transformed to a compact form. Finally, we present the numerical analysis of periodic and chaotic behavior of BLDCM.

2.1 Description of the System Model and Differential Equation of Motion

BLDCM is an electromechanical system. The physical model of BLDCM is shown in Fig. 2.1 [17].

where

$Q_{1,3}$: light transistor,

$Q_{4,9}$: transistor,

D : light diode,

$L_{1,3}$: stator winding,

$H_{1,3}$: light sensor.

The equation of electrical dynamics can be described by [11-12]

$$\frac{d}{dt}\mathbf{I}(t)=\frac{1}{\mathbf{L}(\theta)}[\mathbf{V}(t)-\mathbf{R}\mathbf{I}(t)-(\frac{d\mathbf{L}(\theta)}{d\theta}\mathbf{I}(t)+\frac{d\mathbf{\Lambda}_M(\theta)}{d\theta})\frac{d\theta}{dt}] \quad (2.1.1)$$

where

$\mathbf{I}(t)$: the phase current vector,

$\mathbf{L}(\theta)$: the inductance matrix,

$\mathbf{V}(t)$: the vector corresponding to the voltages across the phase windings,

$\mathbf{R}$: the winding resistance matrix,

$\mathbf{\Lambda}_M(\theta)$: the flux linkage vector due to the presence of permanent magnets,

θ : the displacement variable,

and the equation of mechanical dynamics can be describe by

$$\frac{d}{dt}\omega = \frac{1}{J}\left[T(\mathbf{I},\theta) - T_l(t)\right] \tag{2.1.2}$$

where

ω : the rotator angular velocity,

J : the inertia of rotator,

$T(\mathbf{I},\theta)$: the electromagnetic torque,

$T_l(t)$: the external torques imposed on the rotator shaft.

Accounting for viscous damping friction, the external torques can be described by

$$T_l(t) = b\omega + T_L \tag{2.1.3}$$

where

b : the viscous damping coefficient,

T_L : the torque due to external load, cogging effect, coulomb friction, etc.

Up to now, Eq. (2.1.1) and Eq.(2.1.2) explicitly depend on θ. This is not expected, since the solutions are hard to obtain. Therefore, we transform the above equations to the rotating frame via Park's transformation, and the explicit dependence on θ can be eliminated. We can obtain

$$\frac{d}{dt}i_q = \frac{1}{L_q}[-Ri_q - n\omega(L_d i_d + k_t) + v_q] \tag{2.1.4}$$

$$\frac{d}{dt}i_d = \frac{1}{L_d}[-Ri_d + nL_q\omega i_q + v_d] \tag{2.1.5}$$

and the electromagnetic torque is described by

$$T(i_q, i_d) = n[k_t i_q + (L_d - L_q)i_q i_d] \tag{2.1.6}$$

where

i_q, i_d : the quadrature-axis and direct-axis current,

v_q, v_d : the quadrature-axis and direct-axis voltage,

L_q, L_d : the fictitious inductance on the quadrature-axis and direct-axis,

R : winding resistance,

n : number of permanent pole pairs,

$k_t = \sqrt{\frac{3}{2}}k_e$: k_e is the permanent-magnet flux constant.

2.2 Single Time Scale Representation of the Equations of Motion

In this section, we transform the system equations to a compact form, through an affine transformation and a single time scale transformation [20].

$$\mathbf{x} = \mathbf{\Phi}\hat{\mathbf{x}} + \varsigma \tag{2.2.1}$$

$$t = \tau\hat{t} \tag{2.2.2}$$

where

$\mathbf{x}$: the m-dimensional state vector,

$\mathbf{\Phi}$: $m \times m$ constant non-singular matrix,

ς : $m \times 1$ constant vector.

Transformation matrix has not to be a specified form, for our purposes and simplicity, we choose

$$\mathbf{\Phi} = \begin{bmatrix} \sigma_1 & 0 & 0 \\ 0 & \sigma_2 & 0 \\ 0 & 0 & \sigma_3 \end{bmatrix}, \quad \varsigma = \begin{bmatrix} \varsigma_1 \\ \varsigma_2 \\ \varsigma_3 \end{bmatrix} \tag{2.2.3}$$

where

$$\sigma_1 = \frac{-\delta k_t \pm \sqrt{\delta^2 k_t^2 - 4\rho\delta\Delta\tau b\sigma_3^2}}{2\rho\delta\Delta}, \quad \sigma_2 = \delta\sigma_1, \quad \sigma_3 = \frac{1}{n\tau},$$

$$\varsigma_1 = 0, \quad \varsigma_2 = -\rho\sigma_2 - \frac{k_t}{L_d}, \quad \varsigma_3 = 0,$$

$$\tau = \frac{L_q}{R}, \quad \Delta = L_d - L_q, \quad \delta = \frac{L_q}{L_d}, \quad \rho \text{ is a free parameter.}$$

Combining Eq.(2.2.1)-(2.2.3) and Eq.(2.1.2)-(2.1.6), we obtain the equations in compact forms. The numbers of parameters are greatly reduced.

$$\begin{aligned} \frac{d}{d\hat{t}}\hat{x}_1 &= \hat{v}_q - \hat{x}_1 - \hat{x}_2\hat{x}_3 + \rho\hat{x}_3 \\ \frac{d}{d\hat{t}}\hat{x}_2 &= \hat{v}_d - \delta\hat{x}_2 + \hat{x}_1\hat{x}_3 \\ \frac{d}{d\hat{t}}\hat{x}_3 &= \sigma(\hat{x}_1 - \hat{x}_3) + \eta\hat{x}_1\hat{x}_2 - \hat{T}_L \end{aligned} \tag{2.2.4}$$

where

$$\hat{v}_q = \frac{\tau}{\sigma_1 L_q} v_q,\ \hat{v}_d = \frac{\tau}{\sigma_2 L_d}(v_d - R\varsigma_2),\ \hat{T}_L = \frac{\tau}{J\sigma_3} T_L,$$

$$\sigma = \frac{\tau b}{J},\ \eta = \frac{\Delta\sigma_1\sigma_2}{J\sigma_3^2}.$$

Here we have to assert that Eq.(2.2.4) is nondimensionalized. In the Chapters below, a variety of different control inputs added on Eq.(2.2.4) are also nondimensionalized. However, if we transform them to the original forms, each control input is dimensional and has its practically physical meaning.

In addition, BLDCM is an autonomous system. It means that the period of the system is not explicitly known, so different choice of Poincaré section would lead to different bifurcation diagram. In the Chapters below, adding control inputs changes the dynamics of the system, thus we have to modify the choice of Poincaré section. Modifying Poincaré section, we obtain almost the same bifurcation diagram. The only difference is the shift in $\hat{x}_3$ axis. Therefore, we just present the original bifurcation diagram.

At last, we present the numerical results. The parameters in numerical simulation are L_q =1.125×10^{-3}, L_d =1.725×10^{-3}, R =0.9, n =4, v_q =5, v_d =-43.5, J =5×10^{-6}, k_t =49.4×10^{-3}, b =22.6×10^{-3}, T_L =0.1, ρ =60, $\hat{v}_q$ =0.168, $\hat{v}_d$ =20.66, δ =0.875, η =0.26, $\hat{T}_L$ =0.53, and the initial condition is $\hat{x}_1(0)=\hat{x}_2(0)=\hat{x}_3(0)=0.01$. The phase portrait whose Poincaré section is plane x_1x_3 , bifurcation diagram, and Lyapunov exponents are shown in Fig. 2.2-2.4, respectively. It can be observed that the motion is period 1 for σ=4.05, period 2 for σ=4.15, and period 4 for σ=4.21. For σ=4.55, the motion is chaotic.

Chapter 3

The Synchronization of Chaotic BLDCM System via Control of a Single Variable

Two methods to achieve synchronization of chaotic BLDCM are presented[21]. The synchronization of two identical chaotic systems is accomplished via control of a single variable [21], by a linear feedback controller[22] and an adaptive controller[23-26]. Numerical results are presented. Chaos synchronization of three coupled chaos systems with ring connection is studied[27,28]. Chaos synchronizations are given by using unidirectional coupling or bidirectional coupling respectively.

3.1 Synchronization by Linear Feedback Control via a Single Variable

First, we add a controller in third equation of Eq. (2.2.4). Then the drive system and the response system are as follows:

$$\begin{aligned} \dot{x}_1 &= v_q - x_1 - x_2 x_3 + \rho x_3 \\ \dot{x}_2 &= v_d - \delta x_2 + x_1 x_3 \\ \dot{x}_3 &= \sigma(x_1 - x_3) + \eta x_1 x_2 - T_L \end{aligned} \tag{3.1.1}$$

$$\begin{aligned} \dot{y}_1 &= v_q - y_1 - y_2 y_3 + \rho y_3 \\ \dot{y}_2 &= v_d - \delta y_2 + y_1 y_3 \\ \dot{y}_3 &= \sigma(y_1 - y_3) + \eta y_1 y_2 - T_L + u_3 \end{aligned} \tag{3.1.2}$$

Let $e_1 = y_1 - x_1, e_2 = y_2 - x_2, e_3 = y_3 - x_2$ be the synchronization errors between the drive and response systems. Suppose that M_1 is the upper bound of the absolute value of variables,

x_1 (since a chaotic system has bounded trajectories, constant M_1 exists) then the two BLDCM systems will be synchronized under the control $u_1 = u_2 = 0$, $u_3 = -g_s e_3$ as follows.

From Eq. (3.1.1) and Eq. (3.1.2) error dynamics can be obtained:

$$\begin{aligned} \dot{e}_1 &= -e_1 + \rho e_3 + (x_2 x_3 - y_2 y_3) \\ \dot{e}_2 &= -\delta e_2 + (y_1 y_3 - x_1 x_3) \\ \dot{e}_3 &= \sigma(e_1 - e_3) + \eta(y_1 y_2 - x_1 x_2) - g_s e_3 \end{aligned} \tag{3.1.3}$$

Choose the following Lyapunov function

$$V = \frac{1}{2}(e_1^2 + e_2^2 + \frac{1}{\eta} e_3^2) \geq 0 \tag{3.1.4}$$

Where η > 0. V is positive definite. The derivative of V along trajectories of Eq. (3.1.3) is

$$\begin{aligned} \dot{V} &= e_1 \dot{e}_1 + e_2 \dot{e}_2 + \frac{1}{\eta} e_3 \dot{e}_3 \\ &= -e_1^2 - \delta e_2^2 - \frac{1}{\eta}(\sigma + g_s) e_3^2 + (\rho + \frac{\sigma}{\eta}) e_1 e_3 + 2 x_1 e_2 e_3 + e_1 e_2 e_3 \end{aligned} \tag{3.1.5}$$

For sufficient small $\mathbf{e} = [e_1 \; e_2 \; e_3]^T$, the term of third degree of **e** can be neglected for judge stability, then

$$\begin{aligned} \dot{V} &\leq -e_1^2 - \delta e_2^2 - \frac{1}{\eta}(\sigma + g_s) e_3^2 + (\rho + \frac{\sigma}{\eta}) |e_1 e_3| + 2 M_1 |e_2 e_3| \\ &= -\mathbf{e}^T P \mathbf{e} \end{aligned} \tag{3.1.6}$$

The negative coefficient matrix for the quadratic form in right hand side of Eq. (3.1.6) is

$$P = \begin{bmatrix} 1 & 0 & -\frac{1}{2}(\rho + \frac{\sigma}{\eta}) \\ 0 & \delta & -M_1 \\ -\frac{1}{2}(\rho + \frac{\sigma}{\eta}) & -M_1 & \frac{1}{\eta}(\sigma + g_s) \end{bmatrix}$$

Obviously, to ensure that the origin of error system Eq.(3.1.3) is asymptotically stable, the

matrix P should be positive definite, this is the case if and only if the following three inequalities hold：

$(A)\ \ \delta > 0$

$(B)\ \ \dfrac{\delta(\sigma + g_s)}{\eta} - \dfrac{\delta}{4}(\rho + \dfrac{\sigma}{\eta})^2 - M_1^2 > 0$

According, if $g_s > \dfrac{(\rho\eta + \sigma)^2 + 4M_1^2\eta^2 - 4\eta\delta\sigma}{4\eta\delta}$, then the matrix P is positive definite. $\dot{V}$ is negative definite, which implies that the origin of error system Eq. (3.1.3) is asymptotically stable for sufficiently small **e**. Therefore, the response Eq.(3.1.2) is synchronized with the drive Eq.(3.1.1). The numerical simulation result is shown in Fig.3.1.

3.2 Adaptive Control for Synchronization of BLDCM System

First, we add a controller $u_3 = -(\sigma + g)e_3$ in the third Eq. (2.2.4), the driver system and the response system are as follows:

$$\begin{aligned} \dot{x}_1 &= v_q - x_1 - x_2 x_3 + \rho x_3 \\ \dot{x}_2 &= v_d - \delta x_2 + x_1 x_3 \\ \dot{x}_3 &= \sigma(x_1 - x_3) + \eta x_1 x_2 - T_L \end{aligned} \tag{3.2.1}$$

$$\begin{aligned} \dot{y}_1 &= v_q - y_1 - y_2 y_3 + \rho y_3 \\ \dot{y}_2 &= v_d - \delta y_2 + y_1 y_3 \\ \dot{y}_3 &= \sigma(y_1 - y_3) + \eta y_1 y_2 - T_L + u_3 \end{aligned} \tag{3.2.2}$$

Suppose that M_1 is the upper bound of the absolute value of x_1, (since a chaotic system has bounded trajectories, constant M_1 exists) then the two systems will be synchronized under the control $u_1 = u_2 = 0$, $u_3 = -(a + g)e_3$ where $\dot{g} = e_3^2$ as follows.

The error dynamics is

$$\begin{aligned}\dot{e}_1 &= -e_1 + \rho e_3 + (x_2 x_3 - y_2 y_3)\\ \dot{e}_2 &= -\delta e_2 + (y_1 y_3 - x_1 x_3)\\ \dot{e}_3 &= \sigma(e_1 - e_3) + \eta(y_1 y_2 - x_1 x_2) - (\sigma + g)e_3\end{aligned} \tag{3.2.3}$$

Choose the following Lyapunov function ：

$$V = \frac{1}{2}\left[e_1^2 + e_2^2 + \frac{1}{\eta} e_3^2 + \frac{(g - g^*)^2}{\eta} \right] \geq 0 \tag{3.2.4}$$

where g^* is constant, then the differentiation of V along trajectories of Eq.(3.2.3) is

$$\begin{aligned}\dot{V} &= e_1\dot{e}_1 + e_2\dot{e}_2 + \frac{1}{\eta} e_3\dot{e}_3 + \frac{1}{\eta}(g - g^*)\dot{g}\\ &= -e_1^2 - \delta e_2^2 - \frac{1}{\eta}(\sigma + g^*)e_3^2 + \frac{(\rho\eta + \sigma)}{\eta} e_1 e_3 + 2x_1 e_2 e_3 + e_1 e_2 e_3\end{aligned} \tag{3.2.5}$$

For sufficient small **e**=$\left[e_1\ e_2\ e_3\right]^T$, the term of third degree of **e** can be neglected for judge stability, then

$$\begin{aligned}\dot{V} &\leq -e_1^2 - \delta e_2^2 - \frac{1}{\eta}(\sigma + g^*)e_3^2 + \frac{(\rho\eta + \sigma)}{\eta}\left|e_1 e_3\right| + 2M_1\left|e_2 e_3\right|\\ &= -\mathbf{e}^{\mathrm{T}} P_a \mathbf{e}\end{aligned} \tag{3.2.6}$$

The negative coefficient matrix for the quadratic form in right hand side of Eq. (3.2.4) is

$$P_a = \begin{bmatrix} 1 & 0 & \frac{-(\rho\eta + \sigma)}{2\eta} \\ 0 & \delta & -M_1 \\ \frac{-(\rho\eta + \sigma)}{2\eta} & -M_1 & (\sigma + \frac{g^*}{\eta}) \end{bmatrix}$$

Obviously, to ensure that the origin of error system Eq.(3.2.3) is asymptotically stable, the matrix P_a should be positive definite, this is the case if and only if the following three inequalities hold：

$(A)\ \ \delta > 0$

$(B)\ \ \delta(\sigma + \frac{g^*}{\eta}) - \frac{\delta(\rho\eta + \sigma)^2}{4\eta^2} - M_1^2 > 0$

Accordingly, if $g^* > \frac{\delta(\rho\eta + \sigma)^2 + 4M_1^2\eta^2 - 4\eta^2\delta\sigma}{4\eta\delta}$, then the matrix P_a is positive definite, $\dot{V}$ is negative definite, which implies that the origin of error system Eq.(3.2.3) is asymptotically stable for sufficiently small **e**. Therefore, the response Eq.(3.2.2) is synchronized with the drive Eq.(3.2.1). The numerical simulation result is shown in Fig.3.2.

3.3 Global Synchronization of Three Coupled BLDCM Chaos Systems with Ring Connection

In this section, chaos synchronization of three coupled chaos systems with ring connection[27-28] is studied. Chaos synchronizations are given by using unidirectional coupling or bidirectional coupling respectively.

3.3.1 Chaos Synchronization of Three Chaotic Systems With Unidirectional Coupling

The three coupled BLDCM chaos systems by the unidirectional ring connection can be described as following.

$$\begin{aligned}
\dot{x}_1 &= v_q - x_1 - x_2x_3 + \rho x_3 + k_{11}(z_1 - x_1) \\
\dot{x}_2 &= v_d - \delta x_2 + x_1x_3 + k_{12}(z_2 - x_2) \\
\dot{x}_3 &= \sigma(x_1 - x_3) + \eta x_1x_2 - T_L + k_{13}(z_3 - x_3)
\end{aligned} \tag{3.3.1}$$

$$\begin{aligned}
\dot{y}_1 &= v_q - y_1 - y_2y_3 + \rho y_3 + k_{21}(x_1 - y_1) \\
\dot{y}_2 &= v_d - \delta y_2 + y_1y_3 + k_{22}(x_1 - y_1) \\
\dot{y}_3 &= \sigma(y_1 - y_3) + \eta y_1y_2 - T_L + k_{23}(x_1 - y_1)
\end{aligned} \tag{3.3.2}$$

And

$$\begin{aligned}\dot{z}_1 &= v_q - z_1 - z_2 z_3 + \rho z_3 + k_{31}(y_1 - z_1)\\ \dot{z}_2 &= v_d - \delta z_2 + z_1 z_3 + k_{32}(y_2 - z_2)\\ \dot{z}_3 &= \sigma(z_1 - z_3) + \eta z_1 z_2 - T_L + k_{33}(y_3 - z_3)\end{aligned} \tag{3.3.3}$$

Subtracting (3.3.1) and (3.3.2) from (3.3.2) and (3.3.3), respectively, we can obtain the following error dynamics system:

$$\dot{e} = \begin{pmatrix}\dot{e}_1\\ \dot{e}_2\end{pmatrix} = \begin{pmatrix}M_{11} & M_{12}\\ M_{21} & M_{22}\end{pmatrix}\begin{pmatrix}e_1\\ e_2\end{pmatrix} \tag{3.3.4}$$

where

$$e_1 = (e_{11}, e_{12}, e_{13})^{\mathrm{T}} = (y_1 - x_1, y_2 - x_2, y_3 - x_3)^{\mathrm{T}}, e_2 = (e_{21}, e_{22}, e_{23})^{\mathrm{T}} = (z_1 - y_1, z_2 - y_2, z_3 - y_3)^{\mathrm{T}},$$

Let

$$B = \begin{pmatrix}M_{11} & M_{12}\\ M_{21} & M_{22}\end{pmatrix}. \tag{3.3.5}$$

Choosing $G = diag(g_1, g_2, g_3, g_4, g_5, g_6)$ in which $g_i > 0, i = 1, 2, \ldots 6.$

Then $Q = B^{\mathrm{T}}G + GB + \varepsilon I$ is negative definite if and only if it satisfies

$$(-1)^i{}_i \Delta_i > 0, \quad i = 1, 2, \ldots, 6, \tag{3.3.6}$$

where Δ_i represents the *i*th order sequential sub-determinant of matrix Q. The Eq.(3.3.6) is applied from [27].

Let $v_q = 0.168, vV_d = 20.66, T_l = 0.53, \sigma = 4.55$ and choose $k_{11} = 1, k_{12} = 1, k_{13} = 0.5,$ $k_{21} = 1, k_{22} = 0.5, k_{23} = 1, k_{31} = 0.5, k_{32} = 2, k_{33} = 1,$ so that the inequality Eq.(3.3.5) can be held. The initial values of three coupled BLDCM systems are taken as $x_1(0) = 5, x_2(0) = 6, x_3(0) = 20, y_1(0) = 6, y_2(0) = 6, y_3(0) = 9, z_1(0) = 0.5, z_2 = 1, z_3 = 1.5$ .With the coupled parameters increase, the synchronization of three coupled BLDCM systems can be done more quickly. As we can see in Fig. 3-3 and Fig. 3.4 the synchronization occurs at time t = 3.5sec. when the coupled parameters is much larger $k_{11}=4, k_{12}=2, k_{13}=2, k_{21}=3, k_{22}=1, k_{23}=2, k_{31}=2, k_{32}=2, k_{33}=1,$ with the same initial values , the synchronization occurs more quickly at time t = 1sec.We can

see in Fig.3.5 and Fig.3.6.

3.3.2 Chaos Synchronization of Three Chaotic Systems With Bidirectional Coupling

The three coupled BLDCM chaos systems using the unidirectional ring connection can be described as following.

$$\begin{aligned}\dot{x}_1 &= v_q - x_1 - x_2x_3 + \rho x_3 + k_{11}(-2x_1 + y_1 + z_1)\\ \dot{x}_2 &= v_d - \delta x_2 + x_1x_3 + k_{12}(-2x_2 + y_2 + z_2)\\ \dot{x}_3 &= \sigma(x_1 - x_3) + \eta x_1x_2 - T_L + k_{13}(-2x_3 + y_3 + z_3)\end{aligned} \tag{3.4.1}$$

$$\begin{aligned}\dot{y}_1 &= v_q - y_1 - y_2y_3 + \rho y_3 + k_{21}(-2y_1 + x_1 + z_1)\\ \dot{y}_2 &= v_d - \delta y_2 + y_1y_3 + k_{22}(-2y_2 + x_2 + z_2)\\ \dot{y}_3 &= \sigma(y_1 - y_3) + \eta y_1y_2 - T_L + k_{23}(-2y_3 + x_3 + z_3)\end{aligned} \tag{3.4.2}$$

And

$$\begin{aligned}\dot{z}_1 &= v_q - z_1 - z_2z_3 + \rho z_3 + k_{31}(-2z_1 + x_1 + y_1)\\ \dot{z}_2 &= v_d - \delta z_2 + z_1z_3 + k_{32}(-2z_2 + x_2 + y_2)\\ \dot{z}_3 &= \sigma(z_1 - z_3) + \eta z_1z_2 - T_L + k_{33}(-2z_3 + x_3 + y_3)\end{aligned} \tag{3.4.3}$$

Subtracting Eq.(3.4.1) and Eq.(3.4.2) from Eq.(3.4.2) and Eq.(3.4.3), respectively, we can obtain the following error dynamics system:

$$\dot{e} = \begin{pmatrix}\dot{e}_1\\ \dot{e}_2\end{pmatrix} = \begin{pmatrix}A_{11} & A_{12}\\ A_{21} & A_{22}\end{pmatrix}\begin{pmatrix}e_1\\ e_2\end{pmatrix} \tag{3.4.4}$$

where

$$e_1 = (e_{11}, e_{12}, e_{13})^{\mathrm{T}} = (y_1 - x_1, y_2 - x_2, y_3 - x_3)^{\mathrm{T}}, e_2 = (e_{21}, e_{22}, e_{23})^{\mathrm{T}} = (z_1 - y_1, z_2 - y_2, z_3 - y_3)^{\mathrm{T}}, \tag{3.4.5}$$

Choose the positive definite symmetric constant matrix $G = diag(g_1, g_2, g_3, g_4, g_5, g_6)$, $g_i > 0, i = 1, 2, \ldots 6.$ and any constant ε>0, then $Q = B^{\mathrm{T}}G + GB + \varepsilon I$ is negative definite

if and only if $(-1)^i{}_i\Delta_i > 0, \quad i = 1, 2, \ldots, 6,$ (3.4.6)

Where Δ_i represents the *i*th order sequential sub-determinant of matrix Q, where

$$B = \begin{pmatrix} A_{11} & A_{12} \\ A_{21} & A_{22} \end{pmatrix}$$

We take $v_q = 0.168, v_d = 20.66, T_L = 0.53, \sigma = 4.55$ and choose .The initial values of three coupled BLDCM systems are taken as $x_1(0) = 1, x_2(0) = 3, x_3(0) = 5, y_1(0) = 2, y_2(0) = 4$, $y_3(0) = 6, z_1(0) = 3, z_2 = 6, z_3 = 9$. Let $\varepsilon > 0$ $g_i = 1, i = 1, 2, \ldots, 6$. The simulation can be seen in Figs. 3-7, Fig.3-8 and Fig3-9, Fig.3-10. One can notice that the synchronization among three BLDCM chaotic systems with ring connection can be realized when the coupled parameters k_{ij} is very small, and the synchronization can be realized more quickly when the parameters are much larger. In Fig.3-7 and Fig. 3-8 the synchronization is realized at time t = 1.8sec when coupled parameters are chosen as $k_{11} = 0.5, k_{12} = 1, k_{13} = 0.7, k_{21} = 1, k_{22} = 0.5, k_{23} = 1, k_{31} = 0.7,$ $k_{32} = 1, k_{33} = 0.5$. However, in Fig.3-9 and Fig. 3-10 the synchronization is realized at time t = 1.1sec when coupled parameters are chosen as $k_{11} = 3, k_{12} = 2, k_{13} = 3, k_{21} = 2, k_{22} = 2, k_{23} = 2, k_{31} = 2,$. $k_{32} = 3, k_{33} = 3$.

Chapter 4

Anticipated, Lag and Complete to BLDCM Synchronizations in Chaotic System

The complete, lag and anticipated synchronization of two identical autonomous chaotic systems are discussed in this chapter. Three methods are studied for achievement of complete and lag synchronizations. Two method is studies for anticipated synchronization.

4.1 Complete Synchronization of BLDCM System

4.1.1 Utlizing Pecora and Corroll Method for Synchronization

Firstly, we use Pecora and Corroll method [29-31] of synchronization for identical systems. The master and slave systems are described as follows:

$$\begin{aligned}\dot{x}_1 &= v_q - x_1 - x_2 x_3 + \rho x_3 \\ \dot{x}_2 &= v_d - \delta x_2 + x_1 x_3 \\ \dot{x}_3 &= \sigma(x_1 - x_3) + \eta x_1 x_2 - T_L\end{aligned} \tag{4.1.1}$$

$$\begin{aligned}\dot{y}_1 &= v_q - y_1 - y_2 y_3 + \rho y_3 \\ \dot{y}_2 &= v_d - \delta y_2 + y_1 y_3 \\ \dot{y}_3 &= \sigma(y_1 - y_3) + \eta y_1 y_2 - T_L\end{aligned} \tag{4.1.2}$$

First, we use the variable x_1 in Eq. (4.1.1) to replace variable y_1 in Eq. (4.1.2), then new slave system is described as follow.

$$\begin{aligned}\dot{y}_1 &= v_q - x_1 - y_2 y_3 + \rho y_3 \\ \dot{y}_2 &= v_d - \delta y_2 + x_1 y_3 \\ \dot{y}_3 &= \sigma(x_1 - y_3) + \eta x_1 y_2 - T_L\end{aligned} \tag{4.1.3}$$

Taking Eq. (4.1.1), Eq. (4.1.3) as a whole, the synchronization can be obtained by simulation which is shown in Fig. 4.1. Similarly, replacement of y_3 by x_3 can also obtain the synchronization of these two identical systems, as shown in Fig.4.2.

Lastly, it is found that the replacement of y_1 *and* y_2 by x_1 *and* x_2 or y_1 *and* y_3 by x_1 *and* x_3 can also obtain the synchronization as shown in Fig.4.3, 4.4 which shows that the x_1, x_2 case has less time for the accomplishment of synchronization.

4.1.2 Linear Coupling to Achieve Complete Synchronization

Using Eq. (4.1.1) as master and Eq. (4.1.2) with linear coupling as slave

$$\begin{aligned}\dot{y}_1 &= v_q - y_1 - y_2 y_3 + \rho\, y_3 + K_1(x_1 - y_1)\\ \dot{y}_2 &= v_d - \delta\, y_2 + y_1 y_3 + K_2(x_2 - y_2)\\ \dot{y}_3 &= \sigma(y_1 - y_3) + \eta\, y_1 y_2 - T_L + K_3(x_3 - y_3)\end{aligned} \quad . \qquad (4.1.4)$$

where $\mathbf{K} = [k_1\ k_2\ k_3]^T$ is a coupling strength matrix, synchronization can be obtained with rather small coupling strengths $K_1 = K_2 = K_3 = 1$, as shown in Fig.4.5. .

4.2 Lag Synchronization of BLDCM System

4.2.1 Utlizing Pecora and Corroll Method for Synchronization

The master system and slave systems are described[32] by Eq. (4.1.1) and Eq. (4.1.2). First, we take variable $x_1(t-\tau)$ in Eq. (4.1.1) to replace variable y_1 in Eq. (4.1.2), then new slave system is

$$\begin{aligned}\dot{y}_1 &= v_q - x_1(t-\tau) - y_2 y_3 + \rho\, y_3\\ \dot{y}_2 &= v_d - \delta\, y_2 + x_1(t-\tau) y_3\\ \dot{y}_3 &= \sigma(x_1(t-\tau) - y_3) + \eta\, x_1(t-\tau) y_2 - T_L\end{aligned} \qquad (4.2.1)$$

Taking Eq. (4.1.1), Eq. (4.1.3) as a whole, the synchronization can be obtained by simulations which are shown in Fig.4.6~ 4.8. By simulation result, it is found that range of delay time τ is

unlimited.

Variable $x_3(t-\tau)$ in Eq. (4.1.1) is used to replace variable y_3 in Eq. (4.1.2), the simulation results are in Fig. 4.9~ 4.11 .The lag phenomenon is quite clear in Fig 4.9 and Fig.4.10. it is found that range of delay time τ is unlimited also.

Variables $x_1(t-\tau), x_2(t-\tau)$ in Eq.(4.1.1) is used to replace variables y_1, y_2 in Eq. (4.1.2), the simulation results are in Fig.4.12 and Fig.4.13. It is found that range of delay time τ is unlimited also.

Variables $x_1(t-\tau), x_3(t-\tau)$ in Eq.(4.1.1) is used to replace variables y_1, y_3 in Eq. (4.1.2), then simulation results are in Fig. 4.14 and Fig.4.15.

Lastly, it is found that the accomplishments of synchronization obtained by replacement of y_1, y_2 by x_1, x_2 or y_1, y_3 by x_1, x_3 are faster than that obtained by replacement of single state, while the x_1, x_2 case is faster then x_1, x_3 case.

4.2.2 Linear Coupling Method to Achieve Lag Synchronization

We modify the coupling scheme proposed in for the dynamics of the master, $x(t)$, and slave, $y(t)$ as:

$$\begin{aligned} \dot{\mathbf{X}}(t) &= f(X(t)), \\ \dot{\mathbf{Y}}(t) &= f(Y(t)) + \mathbf{K}[X(t-\tau) - Y(t)], \end{aligned} \tag{4.2.2}$$

where $f(X(t))$ is an arbitrary function and **K** is a coupling strength matrix and τ is time delay. Using above method, simulation is made. Results are showed in Fig. 4.16~ 4.19. From simulation results, the range of time delay τ is 1 to 10, which has good performance.

4.3 Anticipated Synchronization of BLDCM

The synchronization of chaotic systems in a unidirectional coupling configuration has attracted great interest due to its potential applications to secure communication systems [34]. Particular attention has been paid to the so-called *anticipating synchronization* regime [35],

where two identical chaotic systems can be synchronized by unidirectional delayed coupling in such a manner that the ‘‘slave’’ (the system with coupling) anticipates the ‘‘master’’ (the one without coupling). More specifically, the coupling scheme proposed in [33] for the dynamics of the master $x(t)$ and slave $y(t)$ is the following:

$$\begin{aligned}\dot{\mathbf{X}}(t) &= \mathbf{F}(X(t)),\\ \dot{\mathbf{Y}}(t) &= \mathbf{F}(Y(t)) + \mathbf{K}[X(t) - Y(t-\tau)],\end{aligned} \tag{4.3.1}$$

In last section we investigated lag synchronization. In this section the same method as subsection (4.2.2) is used for anticipated synchronization. For BLDCM system, the master and slave are as follows:

$$\begin{aligned}\dot{x}_1 &= v_q - x_1 - x_2 x_3 + \rho x_3\\ \dot{x}_2 &= v_d - \delta x_2 + x_1 x_3\\ \dot{x}_3 &= \sigma(x_1 - x_3) + \eta x_1 x_2 - T_L\end{aligned} \tag{4.3.2}$$

$$\begin{aligned}\dot{y}_1 &= v_q - y_1 - y_2 y_3 + \rho y_3 + K_1(x_1 - y_1(t-\tau))\\ \dot{y}_2 &= v_d - \delta y_2 + y_1 y_3 + K_2(x_2 - y_2(t-\tau))\\ \dot{y}_3 &= \sigma(y_1 - y_3) + \eta y_1 y_2 - T_L + K_3(x_3 - y_3(t-\tau))\end{aligned} \tag{4.3.3}$$

where **x** and **y** are vectors, **F** is a vector function, τ is a delay time, **K** is a coupling strength matrix. For appropriate values of the delay time τ and coupling strength **K**, the basic result is that $y(t) \approx x(t+\tau)$, i.e., the slave ‘‘anticipates’’ by an amount τ the output of the master. The simulation results are shown in Fig.4.20, 4.21.

4-4 Using Active Control to Generalized Lag, Anticipated, and Complete Synchronization in BLDCM Chaos System

In this section, active control[37] is used to generalized lag, anticipated, and complete

Synchronization[36-42]. When generalized synchronization is accomplished, the response state y is a given function of the drive state x.We define a type of generalized (lag, anticipated, and complete) synchronization which is defined as the presence of certain relationship between the states of the drive and response systems, i.e., there exists a smooth vector function H such that y(t)=H(x(t-τ)) with $\tau \in R$, which includes generalized lag synchronization (GLS, $y(t) = H(x(t-\tau))$ *with*, $\tau \in R^{+}$)generalized anticipated synchronization (GAS, $y(t) = H(x(t-\tau))$ *with* $\tau \in R^{-}$), generalized complete synchronization GS($y(t)=H(x(t))$ with $\tau = 0$).Finally, numerical results are presented.

4-4-1 Linear Vector function

The drive and response system is as following.

$$\begin{Bmatrix} \dot{x}_1 \\ \dot{x}_2 \\ \dot{x}_3 \end{Bmatrix} = A \begin{Bmatrix} \dot{x}_1 \\ \dot{x}_2 \\ \dot{x}_3 \end{Bmatrix} + F(x), \quad A = \begin{bmatrix} -1 & 0 & \rho \\ 0 & -\delta & 0 \\ \sigma & 0 & -\sigma \end{bmatrix}, \quad F(x) = \begin{bmatrix} -x_2 x_3 + v_q \\ x_1 x_3 + v_d \\ \eta\, x_1 x_2 - T_L \end{bmatrix} \tag{4.4.1}$$

$$\begin{Bmatrix} \dot{y}_1 \\ \dot{y}_2 \\ \dot{y}_3 \end{Bmatrix} = B \begin{Bmatrix} y_1 \\ y_2 \\ y_3 \end{Bmatrix} + G(x) + U(x,y),$$

$$B = \begin{bmatrix} -1 & 0 & \rho \\ 0 & -\delta & 0 \\ \sigma & 0 & -\sigma \end{bmatrix}, \quad G(x) = \begin{bmatrix} -y_2 y_3 + v_q \\ y_1 y_3 + v_d \\ \eta\, y_1 y_2 - T_L \end{bmatrix}, \quad U(x,y) = \begin{bmatrix} U_1(x,y) \\ U_2(x,y) \\ U_3(x,y) \end{bmatrix}, \tag{4.4.2}$$

Let the error states $e(t) = y(t) - H(x(t-\tau))$, where $\tau \in R$ and $H(x(t-\tau)) = [H_1(x(t-\tau)),$ $H_2(x(t-\tau)), \ldots, H_n(x(t-\tau))]^{\mathrm{T}}$ is a smooth vector function. According to reference [42], we can obtain the error dynamic system and choose controller U(x,y) as following:

$$\begin{aligned} &\dot{e}(t) = Ae(t) + BH(x(t-\tau)) + G(y(t-\tau)) \\ &+DH(x(t-\tau))[Ax(t-\tau) + F(x(t-\tau)) + U(x,y) \end{aligned} \tag{4.4.3}$$

$$U = \Delta e - BH(x(t-\tau)) - G(y(t-\tau)) \\ +DH(x(t-\tau))[Ax(t-\tau) + F(x(t-\tau))] \tag{4.4.4}$$

We choose a linaer vector function $H(x(t-\tau))$ as following and $DH(x(t-\tau))$ is the Jacobian matrix of $H(x(t-\tau))$.

$$H(x_1, x_2, x_3) = \begin{pmatrix} h_{11} & 0 & 0 \\ 0 & h_{22} & 0 \\ 0 & 0 & h_{33} \end{pmatrix} \begin{pmatrix} x_1(t-\tau) \\ x_2(t-\tau) \\ x_3(t-\tau) \end{pmatrix} + \begin{pmatrix} c_1 \\ c_2 \\ c_3 \end{pmatrix} \tag{4.4.5}$$

Then the error dynamic system (4-4-3) becomes

$$\begin{Bmatrix} \dot{e}_1 \\ \dot{e}_2 \\ \dot{e}_3 \end{Bmatrix} = (B+\Delta) \begin{bmatrix} e_1 \\ e_2 \\ e_3 \end{bmatrix} = \begin{bmatrix} \Delta_{11} - 1 & \Delta_{12} & \Delta_{13} + \rho \\ \Delta_{21} & \Delta_{22} - \delta & \Delta_{23} \\ \Delta_{31} - \sigma & \Delta_{32} & \Delta_{33} + \sigma \end{bmatrix} \begin{bmatrix} e_1 \\ e_2 \\ e_3 \end{bmatrix}, \tag{4.4.6}$$

Proper Δ_{ij} can be obtain such that all eigenvalues of system (4.4.6) have negative real parts, that is to say, the system (4-4-6) is global asymptotically stable. First, we take the parameter in system(4.4.1) and (4.4.2) as $v_q = 0.168, v_d = 20.66, T_L = 0.53, \sigma = 4.55,\ \rho = 60$, $\eta = 0.26$ and choose a linear smooth vector function $H(x(t-\tau)) = [x_1 + 1, x_2 + 1, x_3 + 1]^{\mathrm{T}}$ .Let $\Delta_{11} = -3, \Delta_{12} = -2, \Delta_{13} = 3, \Delta_{21} = 0, \Delta_{22} = -30,\ \Delta_{23} = 2, \Delta_{31} = -4.55, \Delta_{32} = 0, \Delta_{33} = -30$,and the initial values of system (4.4.1) and (4.4.2) as $x_1 = 0.01, x_2 = 0.01$, $x_3 = 0.01$, $y_1 = 0.1,\ y_2 = -5,$ $y_3 = -10$. The time constant τ=1 and τ=-1.5 are used in lag and anticipated synchronization respectively. Finally, the dynamics of generalized lag, anticipated and complete synchronization errors for the drive system (4.4.1) and the response system (4.4.2) are shown in Fig.4.22, Fig.4.23, Fig.4.24, Fig.4.25, Fig.4.26, Fig.4.27 and Fig.4.28.

4-4-2 Nonlinear Vector function

The drive system and response system are also system(4.4.1) and (4.4.2). In this section, we choose nonlinear vector function $H(x(t-\tau))$ that is as following:

$$H(x_1,x_2,x_3)=\begin{pmatrix} 2x(t-\tau)_1 & 0 & 0 \\ 0 & 2x(t-\tau)_2 & 0 \\ 0 & 0 & 2x(t-\tau)_3 \end{pmatrix}\begin{pmatrix} x_1(t-\tau) \\ x_2(t-\tau) \\ x_3(t-\tau) \end{pmatrix} \quad (4.4.7)$$

We can obtain the error dynamic system (4-4-6) from system(4-4-1) and system(4-4-2), then choose proper Δ_{ij} such that all eigenvalues of system(4.4.6) have negative real parts, that is to say, the Eq.(4.4.6) is global asymptotically stable. We take the parameter in system(4.4.1) and (4.4.2) as $v_q=0.168, v_d=20.66, T_L=0.53, \sigma=4.55, \rho=60, \eta=0.26$ .Let $\Delta_{11}=-30, \Delta_{12}=2, \Delta_{13}=3, \Delta_{21}=0, \Delta_{22}=-30, \Delta_{23}=2, \Delta_{31}=-4.55, \Delta_{32}=0, \Delta_{33}=-33$, and the initial values of system (4.4.1) and (4.4.2) as $x_1=10, x_2=5, x_3=7$, and τ =0.5. $, y_1=21, y_2=30, y_3=15$. The time constant τ=0.5 and τ=-1 are used in lag and anticipated synchronization respectively. Finally the dynamics of generalized lag, anticipated and complete synchronization errors for the drive system (4.4.1) and the response system (4.4.2) are shown in Fig.4.29, Fig.4.30, Fig.4.31, Fig.4.32, Fig.4.33, Fig.4.34 and Fig.4.35.

4-4-3 Using Nonlinear Vector function for generalized synchronization of BLDCM and Lorenz chaotic system

In this section, we use nonlinear vector function $H(x(t-\tau))$ and different chaotic systems for generalized synchronization. The drive system is system(4.4.1) and the response system is Lorenz system：

$$\begin{Bmatrix} \dot{y}_1 \\ \dot{y}_2 \\ \dot{y}_3 \end{Bmatrix}=B\begin{Bmatrix} y_1 \\ y_2 \\ y_3 \end{Bmatrix}+G(y)+U, \quad B=\begin{bmatrix} -a & a & 0 \\ c & 0 & -1 \\ 0 & 0 & -b \end{bmatrix},$$

$$G(y)=\begin{bmatrix} 0 \\ -y_1y_3 \\ y_1y_2 \end{bmatrix}, \quad (4.4.8)$$

$$H(x_1, x_2, x_3) = \begin{pmatrix} 3 & 0 & 0 \\ 0 & 3 & 0 \\ 0 & 0 & 3 \end{pmatrix} \begin{pmatrix} \cos(x_1(t-\tau)) \\ \cos(x_2(t-\tau)) \\ \cos(x_3(t-\tau)) \end{pmatrix} \quad (4.4.9)$$

We can obtain the error dynamic system (4.4.6) from system(4.4.1) and (4.4.8), then choose proper Δ_{ij} such that all eigenvalues of system (4.4.6) have negative real parts, that is to say, the system (4.4.6) is global asymptotically stable. We take the parameter in system(4.4.1) and (4.4.8) as $v_q = 0.168, v_d = 20.66, T_L = 0.53, \sigma = 4.55, \rho = 60, \eta = 0.26,$ $a = 10, b = 8/3, c = 28,$ Let $\Delta_{11} = -5, \Delta_{12} = 2, \Delta_{13} = 5, \Delta_{21} = -28, \Delta_{22} = -5, \Delta_{23} = 1, \Delta_{31} = 0$, $\Delta_{32} = 0, \Delta_{33} = -5$, and the initial values of system (4.4.1) and (4.4.2) as $x_1 = -15, x_2 = 5, x_3 = 30$, $y_1 = -5, y_2 = -4, y_3 = 5$. The time constant τ=1 and τ=-0.2 are used in lag and anticipated synchronization respectively. Finally, the dynamics of generalized lag, anticipated and complete synchronization errors for the drive system (4.4.1) and the response system (4.4.2) are shown in Fig.4.34, Fig.4.35, Fig.4.36, Fig.4.37, Fig.4.38, Fig.4.39.

Chapter 5

Chaos in Fractional Order BLDCM and Its Control and Synchronization

Brief description about fractional derivative and its approximation are presented[43-49]. Phase portraits and bifurcation diagram are studied to show the chaotic behaviors of fractional order BLDCM. It is shown that fractional order chaotic systems can also be controlled and synchronized[50].

5-1 Fractional derivative and its approximation

Riemann-Liouville definition is frequently used in the several definitions of fractional derivative [43], which is described as following.

$$\frac{d^r f(t)}{dt^r} = \frac{1}{\Gamma(m-r)} \frac{d^m}{dt^m} \int_0^t \frac{f(\tau)}{(t-\tau)^{r-m+1}} d\tau \qquad (5.1.1)$$

where $\Gamma(m-r)$ is gamma function and $m-1 \le r < m$ .According to definition of fraction of differ-integral, it dose not allow direct implementation of fractional operators by time-domain simulations. Fortunately, the basic engineering tool for analyzing linear systems, the Laplace transform, is still applicable and works as one would expect;

$$L\left\{\frac{d^r f(t)}{dt^r}\right\} = s^r L\{f(t)\} - \sum_{k=0}^{m-1} s^k \left[\frac{d^{r-1-k} f(t)}{dt^{r-1-k}}\right]_{t=0} \qquad for\ all\ r,$$

where *n* is an integer such that *n* - 1 < r< *n*. Upon considering the initial conditions to be zero, this formula reduces to the more expected and comforting form as following

$$L\left\{\frac{d^r f(t)}{dt^r}\right\} = s^r L\{f(t)\} \tag{5.1.2}$$

It has other efficient method that is to approximate fractional operators by using standard integer order operators to avoid this problem. In reference [43-50], an effective algorithm is developed to approximate fractional order transfer functions. Basically, the idea is to approximate the system behavior in the frequency domain. By using frequency domain techniques based on Bode diagrams, one can obtain a linear approximation of the fractional order integrator, the order of which depends on the desired bandwidth and discrepancy between the actual and the approximate magnitude Bode diagrams. This approximation approach was adopted in [43-50]. In Table 1 of [51], approximations for $1/s^r$ with q 0.1–0.9 in steps 0.1 are given, with errors of approximately 2 dB. We also use these approximations in the following simulations.

5-2 The Chaos in Fractional Order BLDCM System

The fractional order BLDCM system is described as following:

$$\begin{aligned}
\frac{d^i x_1}{dt^r} &= v_q - x_1 - x_2 x_3 + \rho x_3 \\
\frac{d^j x_2}{dt^r} &= v_d - \delta x_2 + x_1 x_3 \\
\frac{d^k x_3}{dt^r} &= \sigma(x_1 - x_3) + \eta x_1 x_2 - T_L
\end{aligned} \tag{5.2.1}$$

When i, j, k are the fractional numbers. When i=1,j=1,k=1, system (5-2-1) is the original one with integral order, which is chaotic when $(v_q, v_d, \delta, \sigma, \eta, T_L) = (0.168, 20.66, -0.875, 4.55, 0.26, 0.53)$. The phase portraits are shown in Fig.5.1.

When i=0.9,j=1,k=0.9 , the fractional order of system (5.2.1) is 2.8, which is still chaotic when $(v_q, v_d, \delta, \sigma, \eta, T_L)$=(0.168,20.66,-0.875,11,0.26,0.53).The phase portraits and bifurcation are shown in Fig.5.2 and Fig.5.3.

When i = 0.9 , j = 1, k = 1 , the fractional order of system (5.2.1) is 2.9, which is still chaotic when $(v_q, v_d, \delta, \sigma, \eta, T_L)$=(0.168,20.66,-0.875,7,0.26,0.53) . The phase portraits and bifurcation are shown in Fig.5.4 and Fig.5.5.

When i = 1,j = 0.9 and 1.1, k = 1 , the fractional order of system (5.2.1) is 2.9 and 3.1, which is still chaotic when $(v_q, v_d, \delta, \eta, T_L)$= (0.168, 20.66, -0.875, 6,0.26,0.53) and σ=6 and 9. The phase portraits and bifurcation are shown in Fig.5.6, Fig.5.7, Fig.5.8 and Fig.5.9.

When i = 1,j = 1, k = 0.3~1.1 , the fractional order of system (5.2.1) is 2.3, 2.4,2.5,2.6,2.7,2.8,2.9,3.1 which is still chaotic when $(v_q, v_d, \delta, \eta, T_L)$= (0.168, 20.66, -0.875, 0.2,0.26,0.53) and σ = 0.2,1.5, 1.5, 4, 6, 7.2, 3,9.The phase portraits and bifurcation are shown in Fig.5.10, Fig.5.11, Fig.5.12, Fig.5.13, Fig.5.14, Fig.5.15, Fig.5.16, Fig.5.17, Fig.5.18, Fig.5.19, Fig.5.20 , Fig.5.21,Fig.5.22 ,Fig.5.23, Fig.5.24 and Fig.5.25 .

5-3 Control of fractional order system

Chaos control attracts more and more attentions from various disciplines in science and engineering, and has been extensively investigated during last decade. In this section, we will introduce control of fraction order of chaos[50].

The fractional order BLDCM system Eq.(5.2.1) in a compact from is as following:

$$\frac{d^{\alpha} X}{dt^{\alpha}} = f(x) \tag{5.3.1}$$

where $X = [x_1, x_2, x_3]^T$ and α=i, j, k. Eq.(5.3.1) with a simple linear state feedback controller can be show as

$$\frac{d^{\alpha}X}{dt^{\alpha}} = f(x) + u \tag{5.3.2}$$

Where u is a linear state feedback controller of the form as follow [43]. For simplicity, we assume $u = diag(k_1, k_2, k_3)$ is a diagonal matrix.

$$u = \begin{bmatrix} k_1 & 0 & 0 \\ 0 & k_2 & 0 \\ 0 & 0 & k_3 \end{bmatrix} (X - \bar{X}) \tag{5.3.3}$$

where $\bar{X}$ is the control target, and k_1, k_2, k_3 are constant parameters which can easily obtained from standard stability analysis. In this part, it lets $\bar{X}$ be equilibrium point of BLDCM system. Simulation results show that this controller can also stabilize the fractional order BLDCM system with order (i, j, k) = (0.9,1,1), (1,0.9,1), (1,1,0.9) and k_1, k_2, k_3 = (-15,-25,-30) are shown in Fig. 5.26, Fig. 5.27, Fig. 5.28, respectively. In these figures, the control signal is added at t=25sec. As we can see from three figure, the designed chaos controller can effectively control the fractional order BLDCM system to its equilibrium point.

5-4 Synchronization for Identical Fractional Order Chaotic System

In this section, we study the synchronization of identical fraction order chaotic system by feedback control method[50]. We will numerically investigate the topic here and present three cases. The driver system is described Eq.(5.2.1) and response system is as following:

$$\begin{aligned} \frac{d^{i}y_1}{d^{i}t} &= v_q - y_1 - y_2 y_3 + \rho y_3 + k_1(y_1 - x_1) \\ \frac{d^{j}y_1}{d^{j}t} &= v_d - \delta y_2 + y_1 y_3 + k_2(y_2 - x_2) \\ \frac{d^{k}y_1}{d^{k}t} &= \sigma(y_1 - y_3) + \eta y_1 y_2 - T_L + k_3(y_3 - x_3) \end{aligned} \tag{5.4.1}$$

Where k_1, k_2, k_3 are coupling parameters and $(v_q, v_d, \delta, \eta, T_L)$ =(0.168,20.66,0.875,0.26,0.53), σ takes different values for different systems. In this part, three cases for synchronization are

presented.

Case 1. Order of the drive system is (i, j, k) =(0.9,1,1) and the response system is(i,j,k)=(0.9,1,1). system parameters are $(v_q, v_d, \delta, \eta, T_L)$ =(0.168,20.66,0.875,0.26,0.53), σ=8 and k_1, k_2, k_3 = (-5,0,0) The numerical result is shown in Fig. 5.29.

Case 2. Order of the drive system is (i, j, k) =(1,0.9,1) and the response system is (i,j,k)=(1, 0.9,1). system parameters are $(v_q, v_d, \delta, \eta, T_L)$ =(0.168,20.66,0.875,0.26,0.53), σ=6 and k_1, k_2, k_3 = (-4,0,0) The numerical result is shown in Fig. 5.30.

Case 3. Order of the drive system is (i, j, k) =(1,1,0.9) and the response system is(i,j,k)=(1,1,0.9). system parameters are $(v_q, v_d, \delta, \eta, T_L)$ =(0.168,20.66,0.875,0.26,0.53), σ=8 and k_1, k_2, k_3 = (-6,0,0) The numerical result is shown in Fig. 5.31.

5-5 Synchronization for Different Fractional Order Chaotic System

In this section, we study the synchronization of different fraction order chaotic system. The analysis of fractioal order ststem is by no means trivial. So, we will numerically investigate the topic here and present three cases. The driver system is described Eq(5.2.1) and response system is described Eq.(5.4.1).

Where k_1, k_2, k_3 are coupling parameters and $(v_q, v_d, \delta, \eta, T_L)$ =(0.168,20.66,0.875, 0.26,0.53),σ takes different values for different systems.

Case 1. Order of the drive system is (i, j, k) =(1,1,1) and the response system is (i,j,k)=(1,1,0.9). system parameters are $(v_q, v_d, \delta, \eta, T_L)$ =(0.168,20.66,0.875,0.26,0.53), σ=4.55 and $(v_q, v_d, \delta, \eta, T_L)$ =(0.168,20.66,0.875,0.26,0.53), σ=3, for response respectively. The numerical result is shown in Fig. 5.32.

Case 2. Order of the drive system is (i, j, k) =(1,1,1) and the response system is

(i,j,k)=(1,1,0.7). system parameters are $(v_q, v_d, \delta, \eta, T_L)$ =(0.168,20.66,0.875,0.26,0.53), σ=4.55 and $(v_q, v_d, \delta, \eta, T_L)$ =(0.168,20.66,0.875,0.26,0.53), σ=6, for response respectively. The numerical result is shown in Fig. 5.33.

Case 3. Order of the drive system is (i, j, k) =(1,1,1) and the response system is (i,j,k)=(1,1,0.5). system parameters are $(v_q, v_d, \delta, \eta, T_L)$ =(0.168,20.66,0.875,0.26,0.53), σ=4.55 and $(v_q, v_d, \delta, \eta, T_L)$ =(0.168,20.66,0.875,0.26,0.53), σ=1.5 , for response respectively. The numerical result is shown in Fig. 5.34

From above numerical results, we can observe the system error which will increase as what order of system is to decrease.

Chapter 6 Conclusions

Brushless dc motor (BLDCM) is studied in this thesis. It is an autonomous third-order electromechanical system. Using different numerical analysis such as phase portrait、bifurcation diagram and Lyapunov exponent, chaotic behavior are studied.

In Chapter 3, controlling for synchronization of chaotic BLDCM system is via a single variable. Two control approaches, linear feedback control and adaptive control, are used. We use the same method for synchronization of three identical chaotic systems with ring connection via unidirectional or bidirectional linear error feedback. Chaos synchronization can be realized as the coupled parameter is small, and it can be done more quickly as the coupled parameter become lager from numerical results.

In Chapter 4, first, Pecora and Carroll method is applied to the complete and lag synchronization of BLDCM chaotic system, more number of state of response system replaced by states of drive system presents that, chaos synchronization can be done more quickly. Next, feedback control for complete and lag synchronization is applied in BLDCM chaotic system. As the coupled strength increases, error can quickly converge to zero, and range of time constant τ can be arbitrarily chosen. Using the same conception, anticipated synchronization can be achieved, but range of time constant has limitation. Third, the conception of generalized synchronization for identical and different chaotic system is achieved by linear and nonlinear vector function.

In Chapter 5, we found that chaos exists in the fractional order BLDCM system with less than 3. Adding linear feedback controller, controlling of fractional order BLDCM to its equilibrium point is achieved, and synchronization of identical and different fractional order chaotic system are also achieved. Error of synchronization for identical fractional order systems is smaller than that for different fractional order systems.

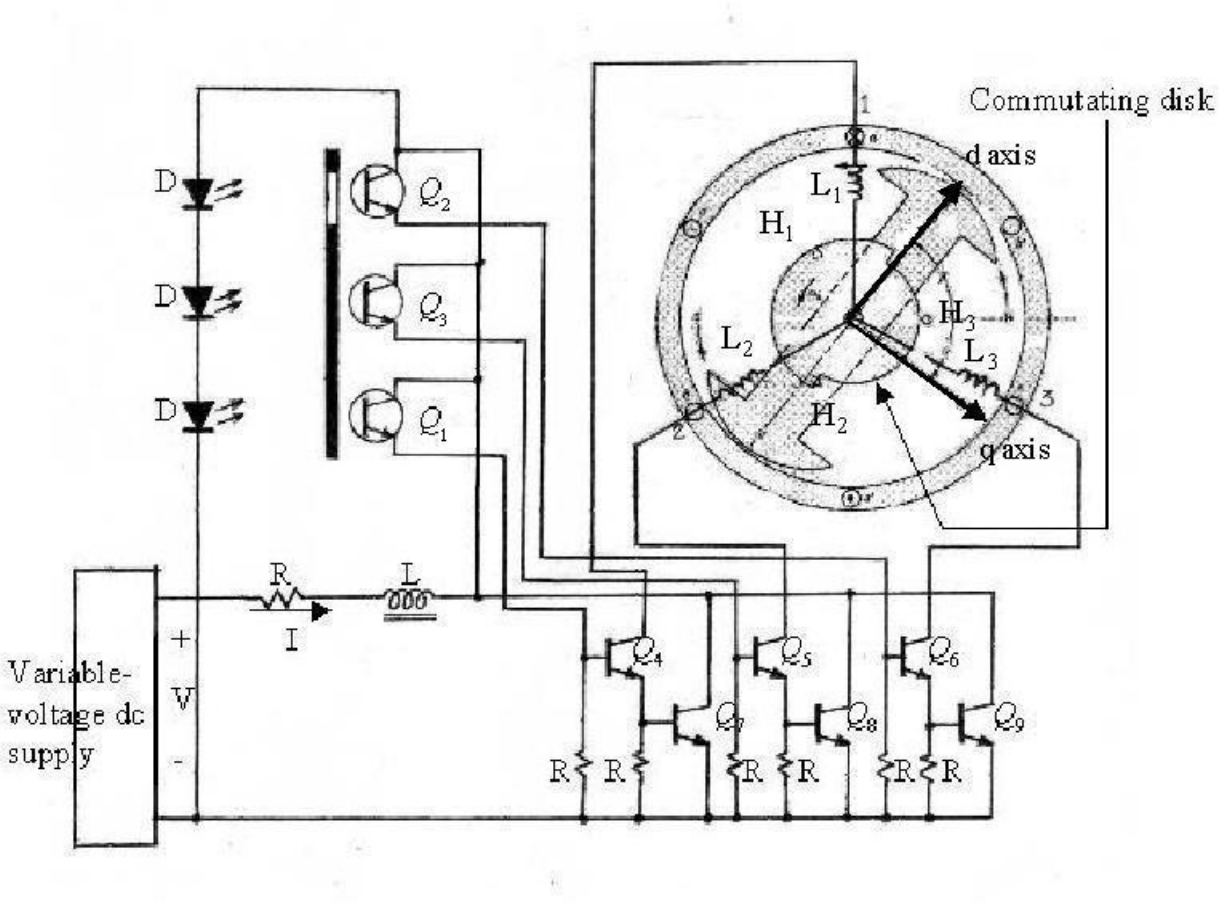

Fig.2.1 A schematic diagram of typical brushless dc motor

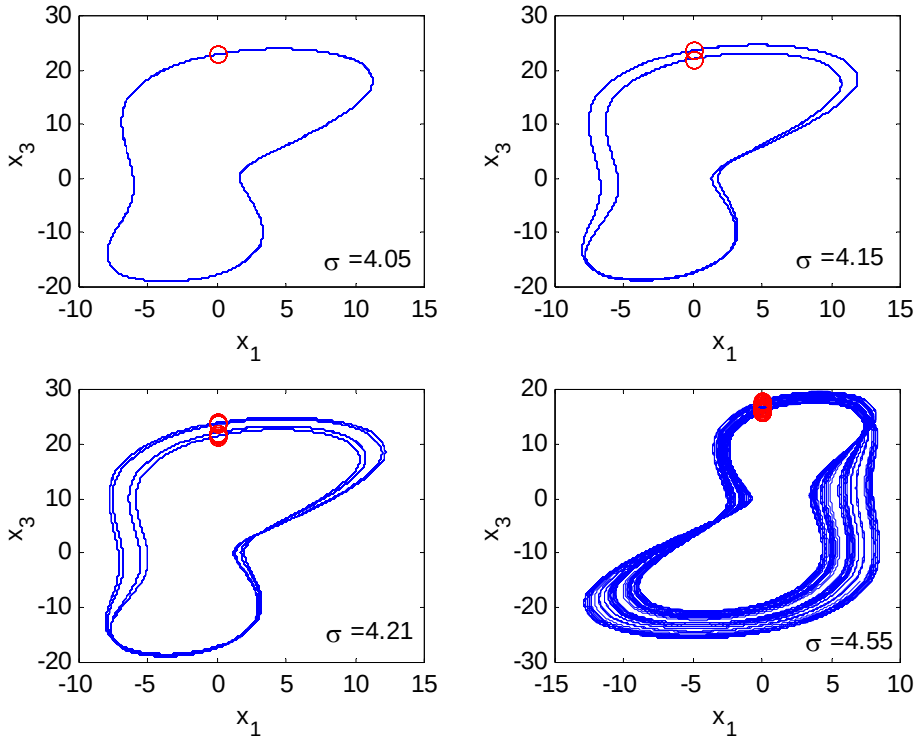

Fig. 2.2 Phase portrait for BLDCM.

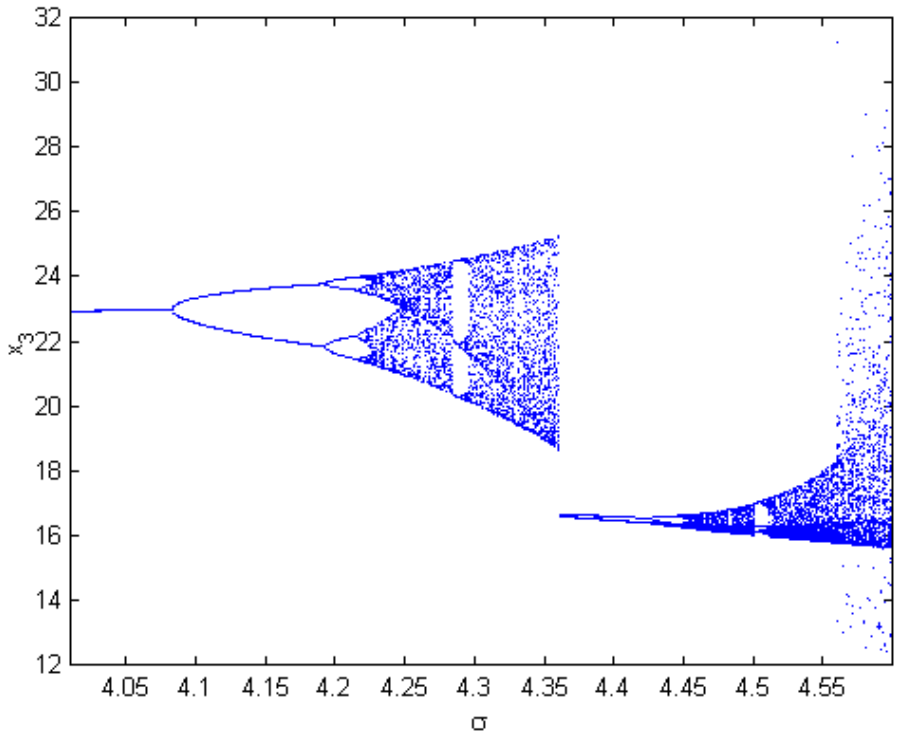

Fig. 2.3 Bifurcation diagram for BLDCM.

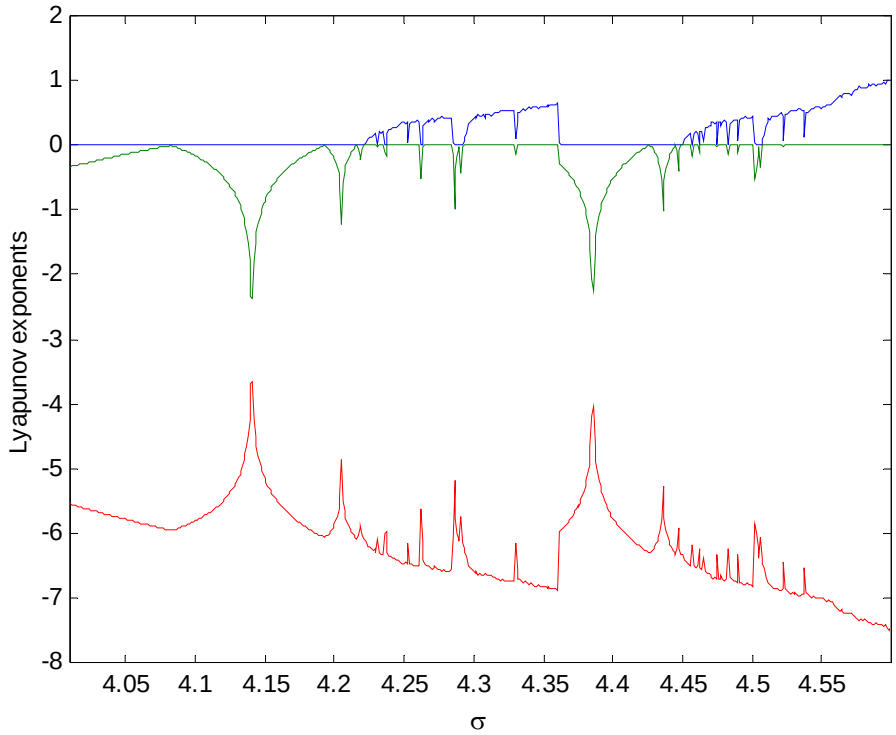

Fig. 2.4 Lyapunov exponents for BLDCM.

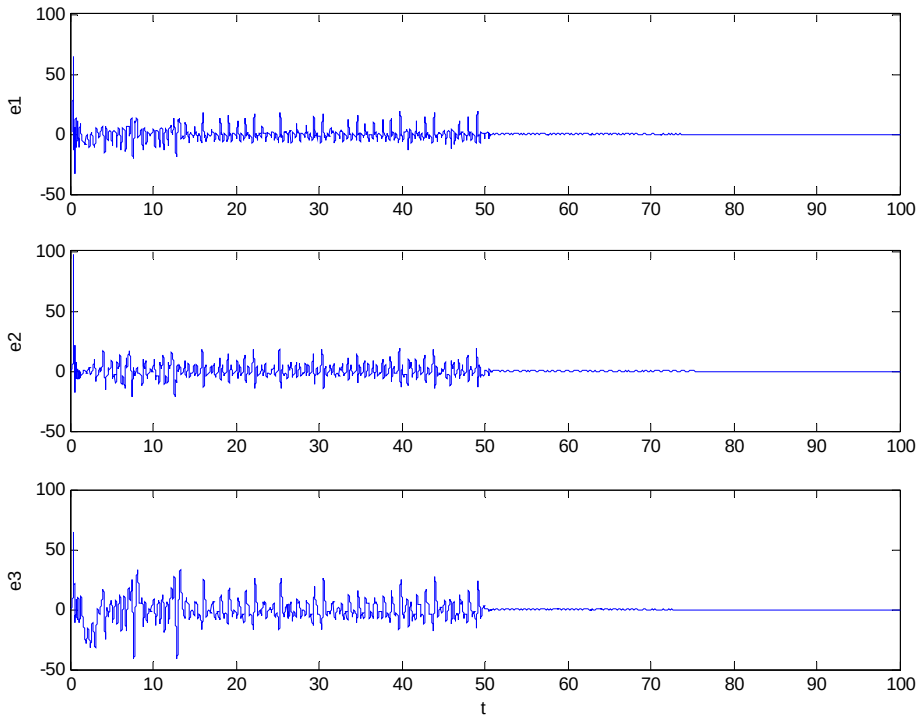

Fig 3.1 Time history of errors

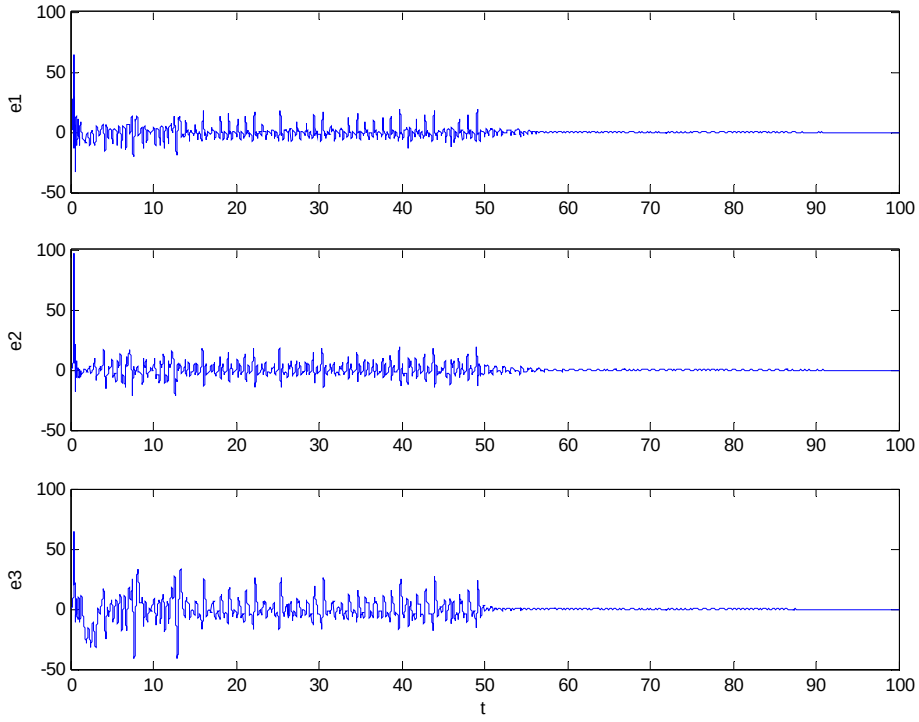

Fig 3.2 Time history of errors

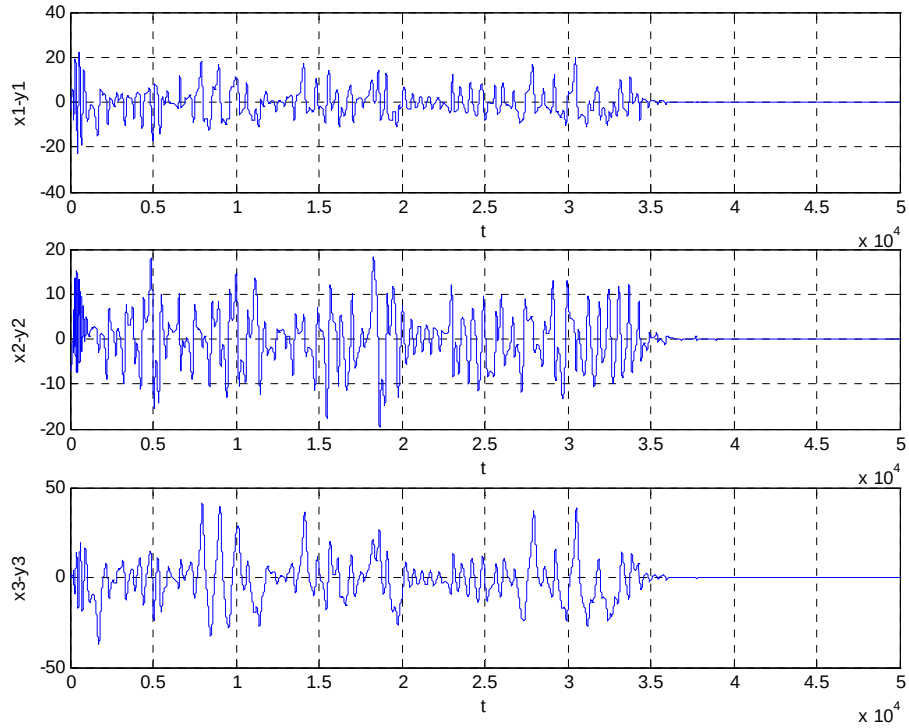

Fig. 3.3 Unidirectional coupling when the coupling parameters are $k_{11}=1, k_{12}=1, k_{13}=0.5, k_{21}=1, k_{22}=0.5, k_{23}=1, k_{31}=0.5, k_{32}=2, k_{33}=1$ with states x and y.

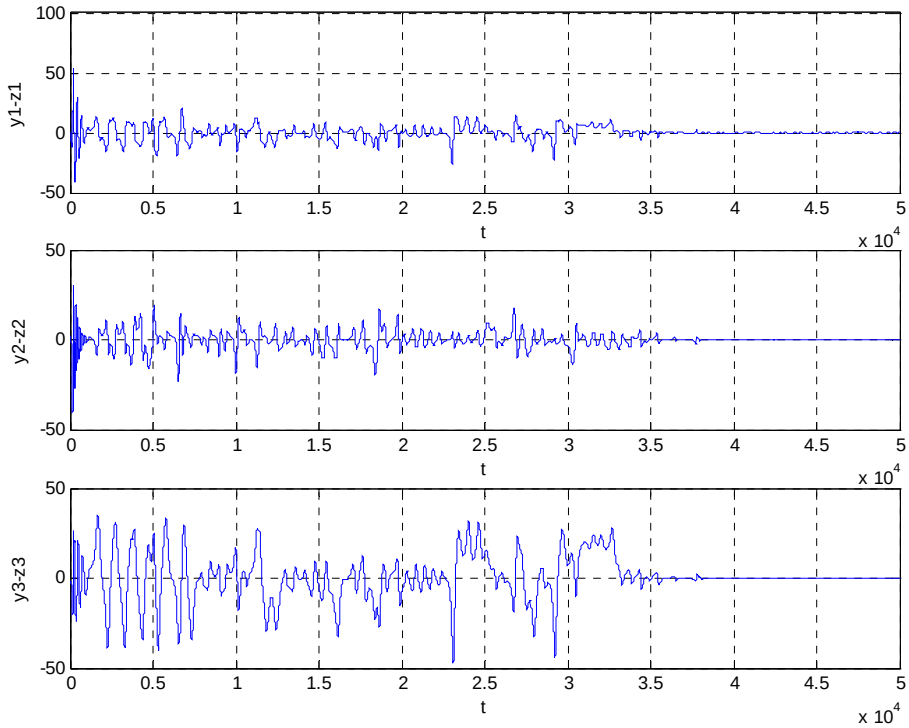

Fig. 3.4 Unidirectional coupling when the coupling parameter are $k_{11}=1, k_{12}=1, k_{13}=0.5, k_{21}=1, k_{22}=0.5, k_{23}=1, k_{31}=0.5, k_{32}=2, k_{33}=1$ with states y and z.

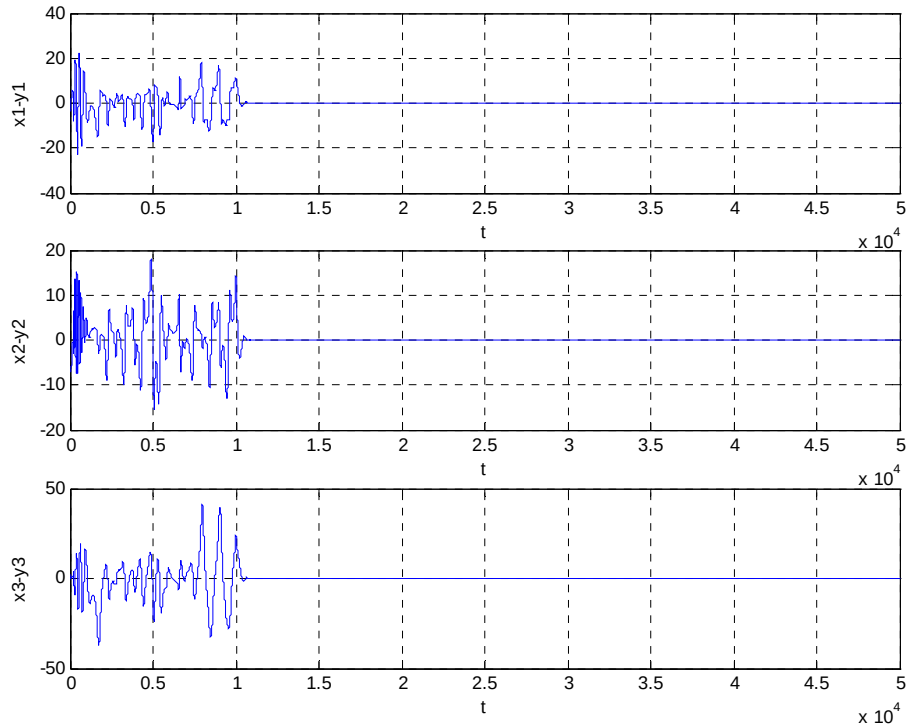

Fig. 3.5 Unidirectional coupling when the coupling parameter are $k_{11}=4, k_{12}=2, k_{13}=2, k_{21}=3, k_{22}=1, k_{23}=2, k_{31}=2, k_{32}=2, k_{33}=1$ with states x and y.

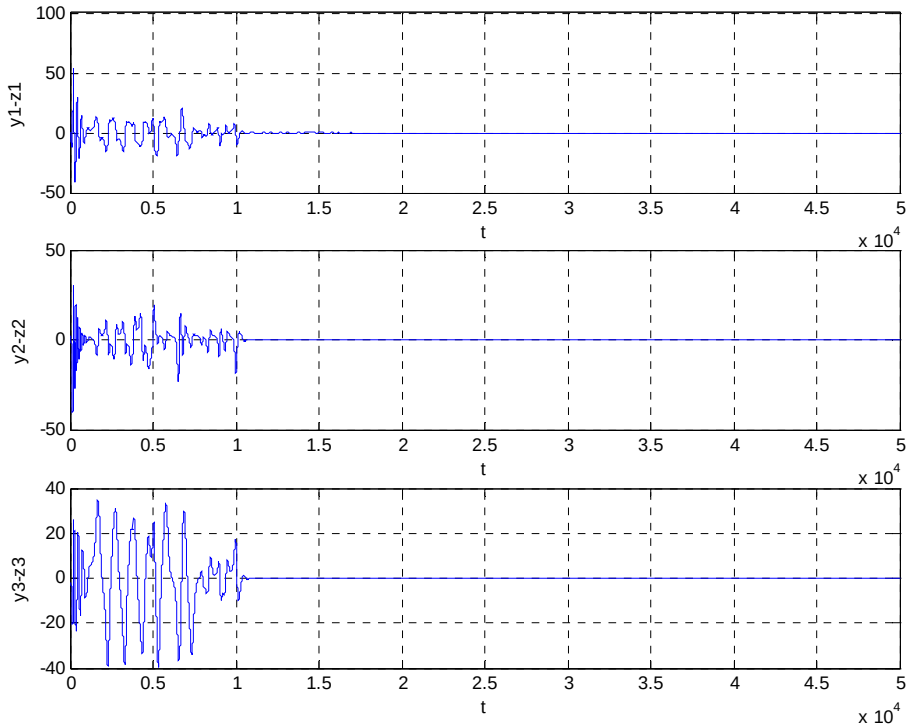

Fig. 3.6 Unidirectional coupling when the coupling parameters are $k_{11}=4, k_{12}=2, k_{13}=2, k_{21}=3, k_{22}=1, k_{23}=2, k_{31}=2, k_{32}=2, k_{33}=1$ with states y and z.

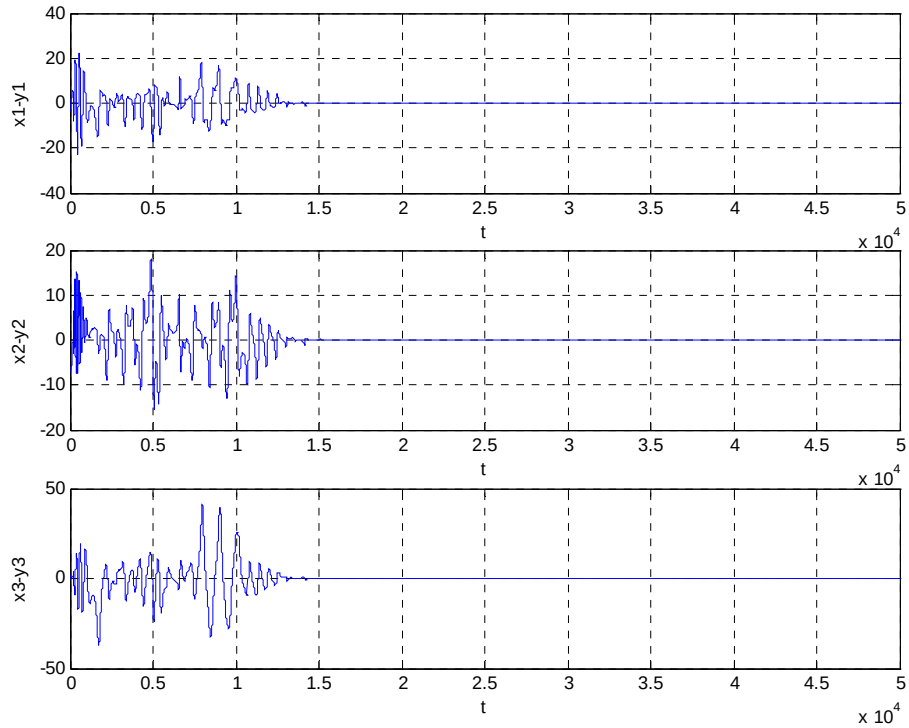

Fig. 3.7 bidirectional coupling when the coupling parameters are $k_{11}=0.5, k_{12}=1, k_{13}=0.7, k_{21}=1, k_{22}=0.5, k_{23}=1, k_{31}=0.7, k_{32}=1, k_{33}=0.5$ with states x and y.

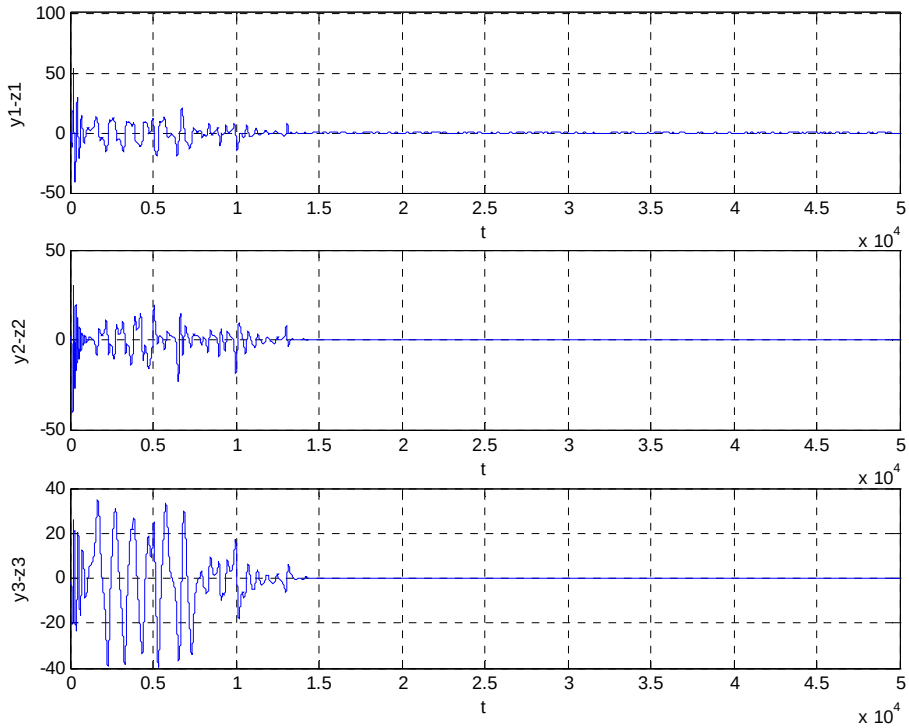

Fig. 3.8 bidirectional coupling when the coupling parameters are $k_{11}=0.5, k_{12}=1, k_{13}=0.7, k_{21}=1, k_{22}=0.5, k_{23}=1, k_{31}=0.7, k_{32}=1, k_{33}=0.5$ with states y and z.

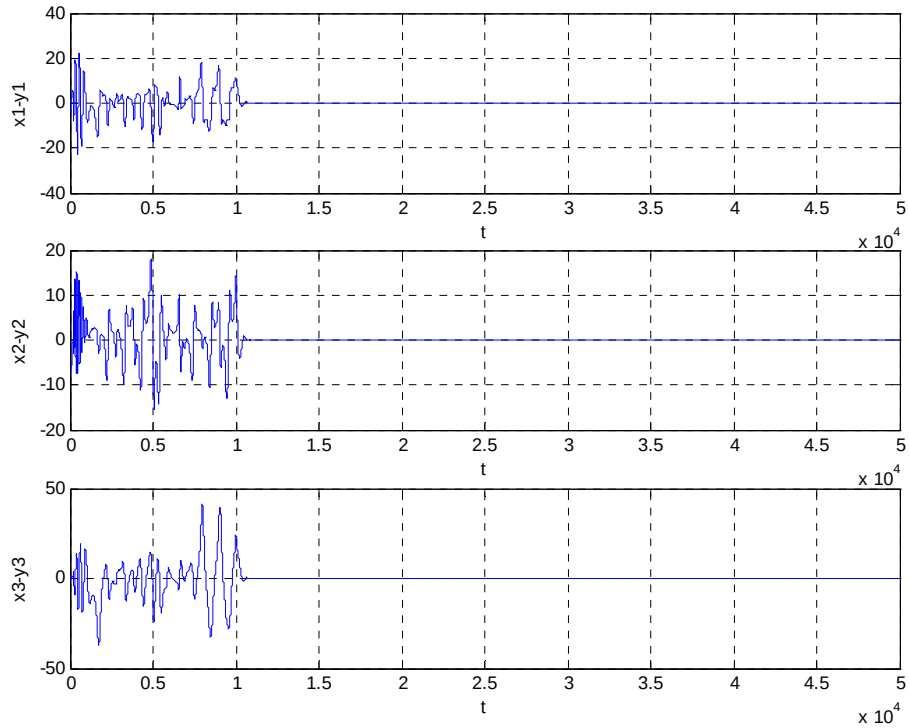

Fig. 3.9 Bidirectional coupling when the coupling parameter are $k_{11}=3, k_{12}=2, k_{13}=3, k_{21}=2, k_{22}=2, k_{23}=2, k_{31}=2, k_{32}=3, k_{33}=3$ with states x and y.

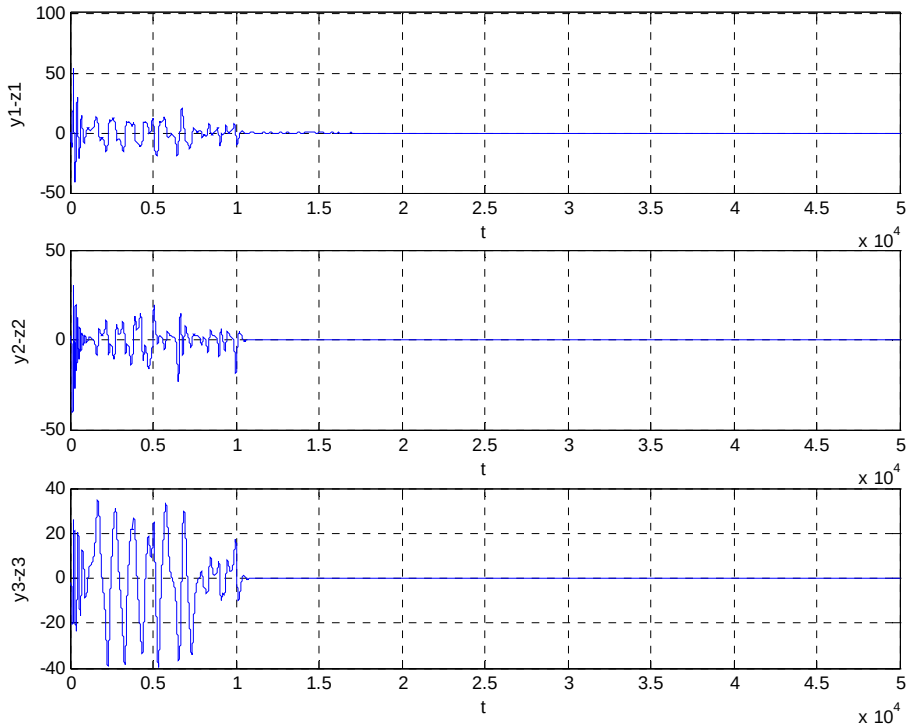

Fig. 3.10 Bidirectional coupling when the coupling parameters are $k_{11}=3, k_{12}=2, k_{13}=3, k_{21}=2, k_{22}=2, k_{23}=2, k_{31}=2, k_{32}=3, k_{33}=3$ with states y and z.

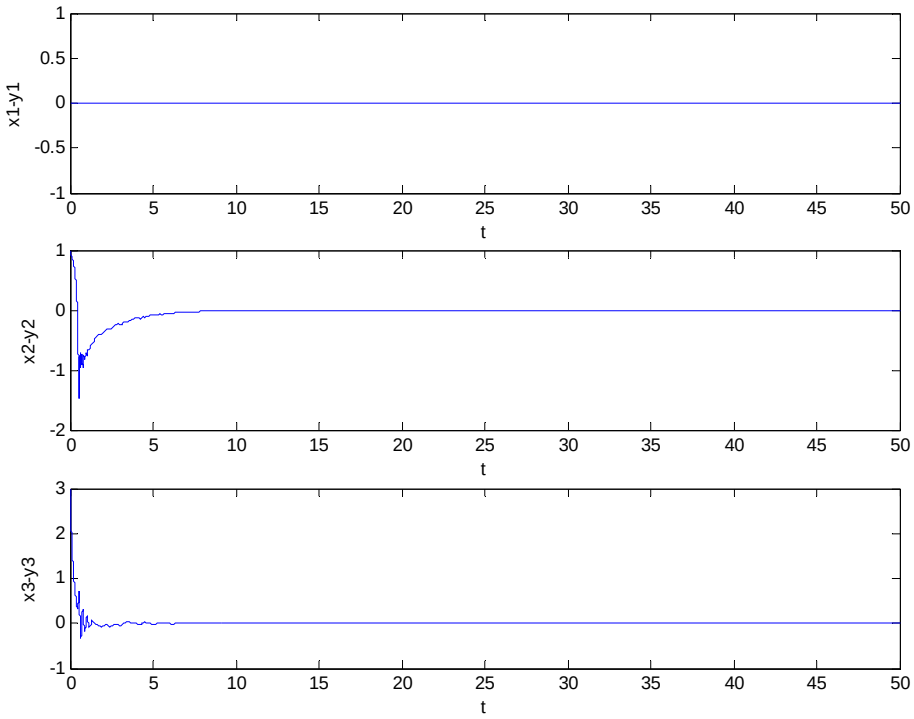

Fig 4.1 Complete synchronization of two BLDCM systems.

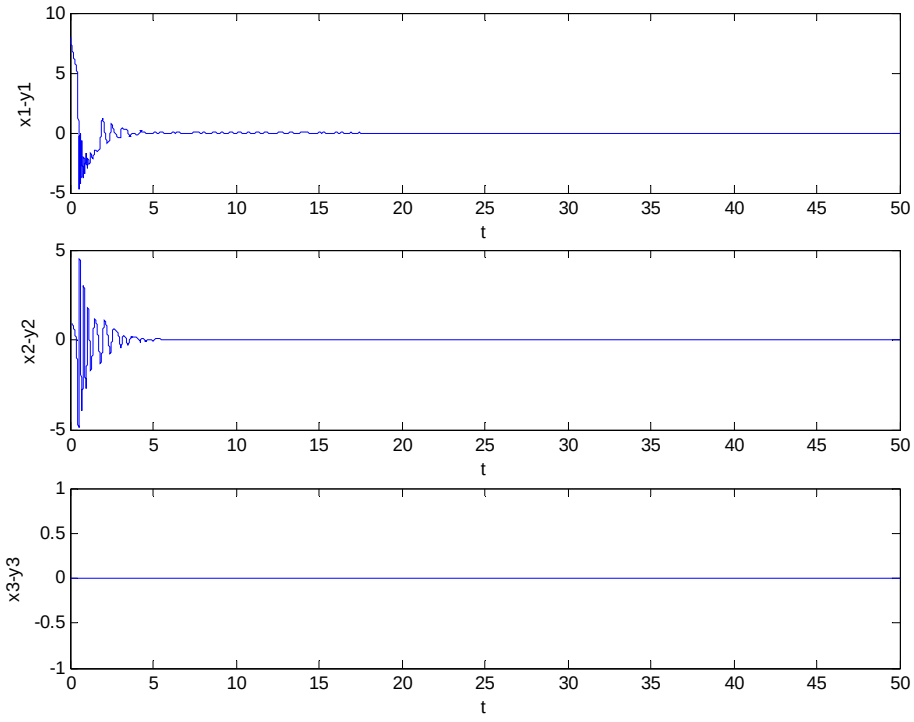

Fig 4.2 Complete synchronization of two BLDCM systems.

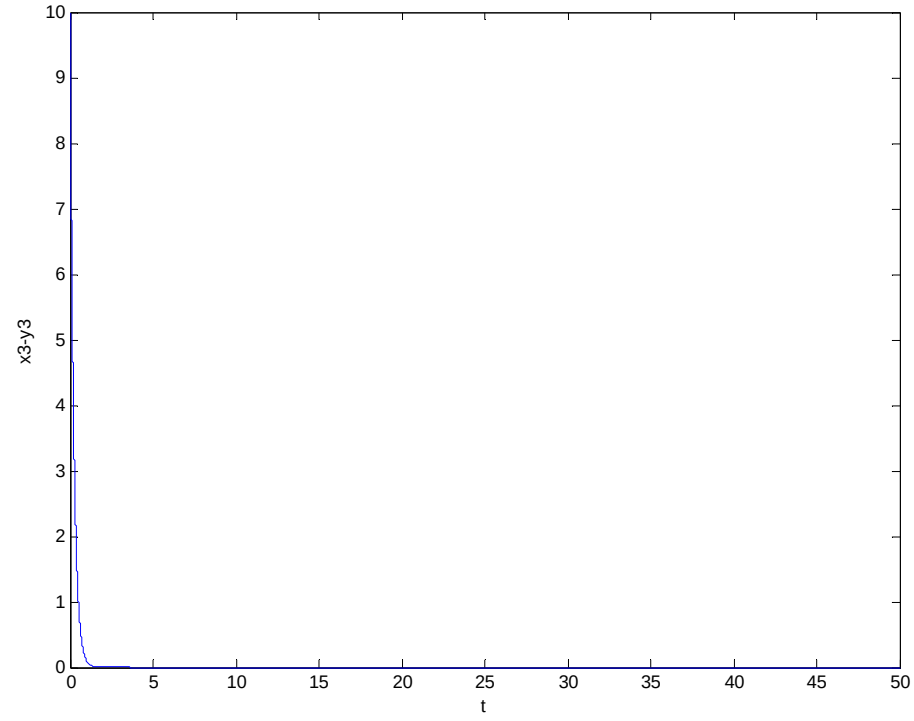

Fig 4.3 Complete synchronization of two BLDCM systems.

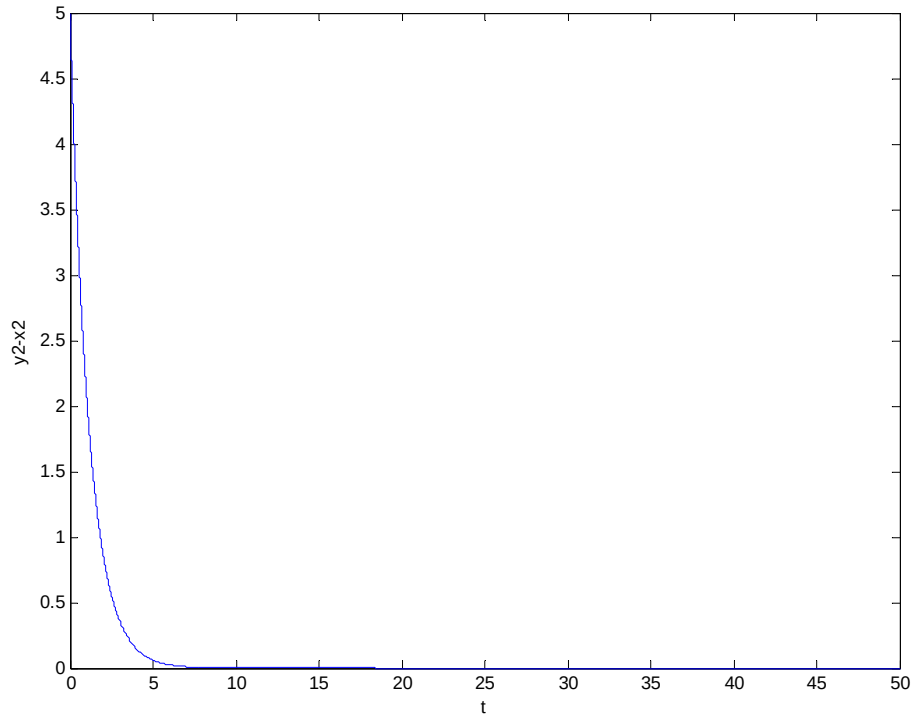

Fig 4.4 Complete synchronization of two BLDCM systems.

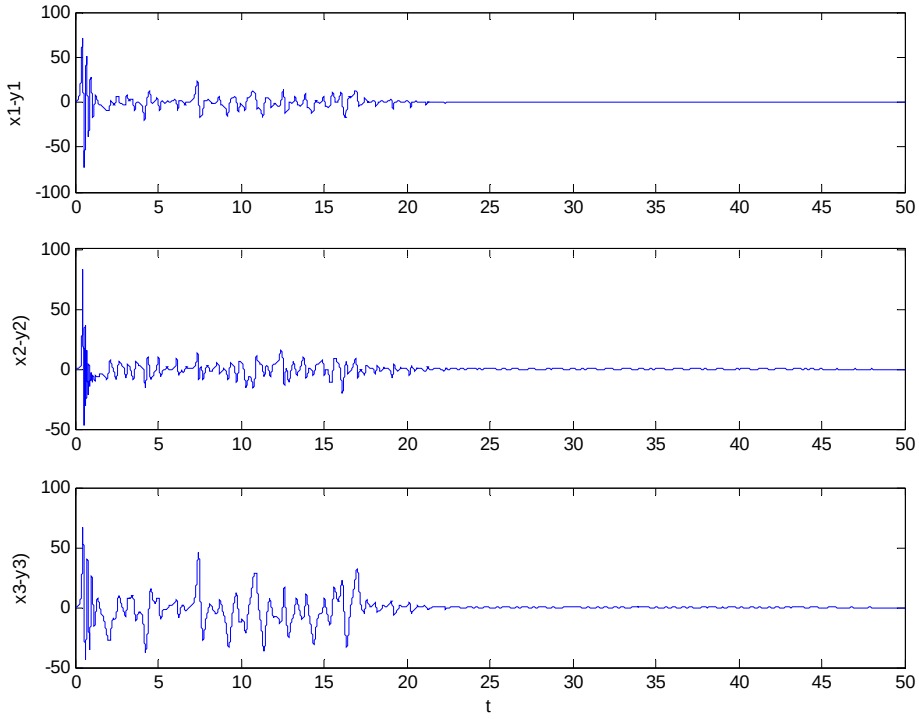

Fig 4.5 Complete synchronization of two BLDCM systems.

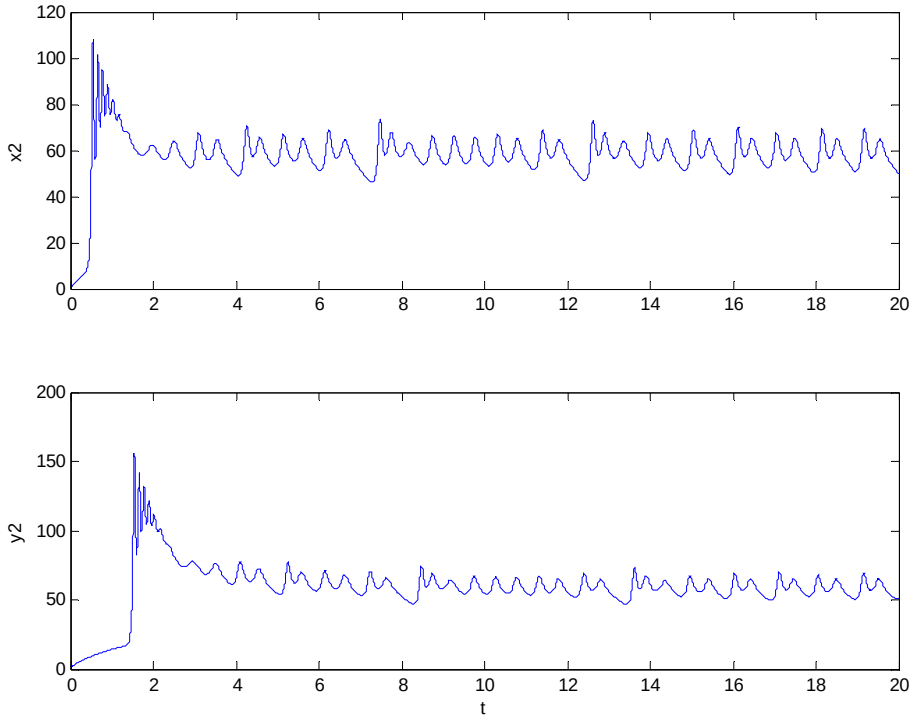

Fig 4.6 Time history of x_2 *and* y_2.

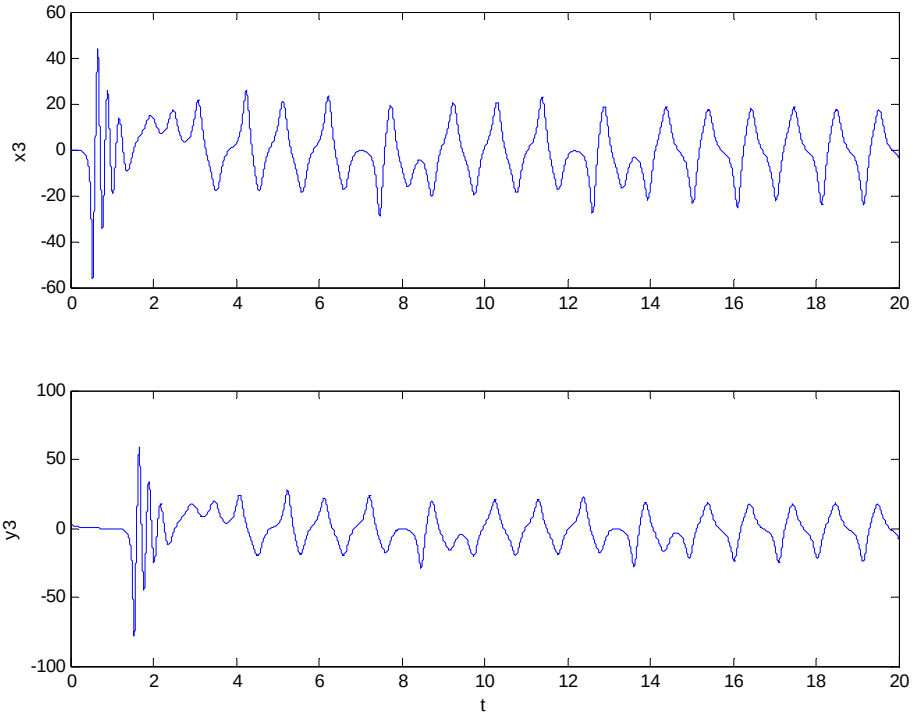

Fig 4.7 Time history of x_3 *and* y_3.

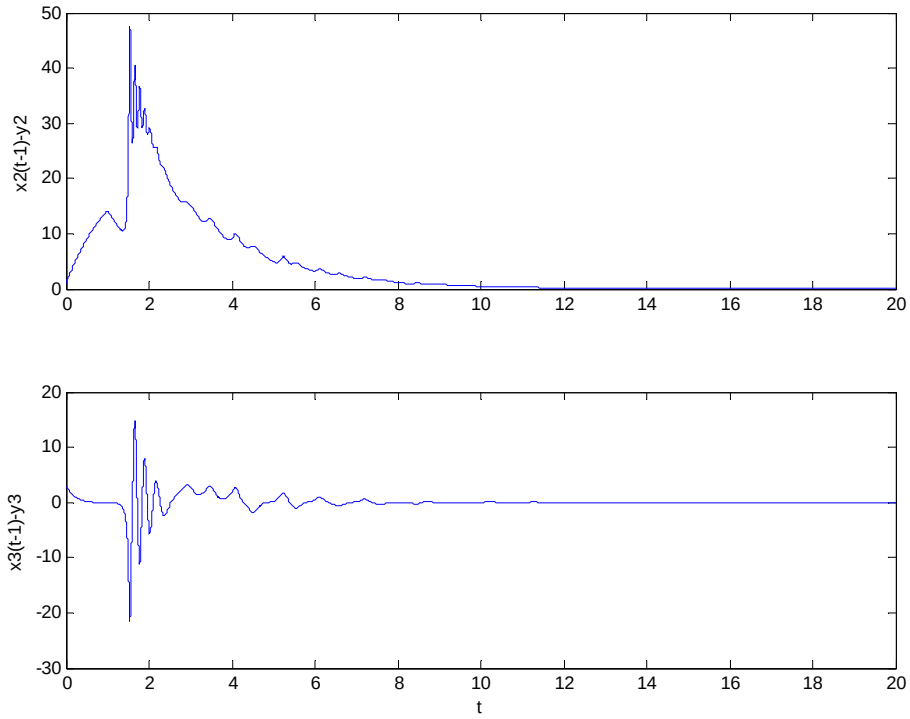

Fig. 4.8 Lag synchronization of two BLDCM systems.

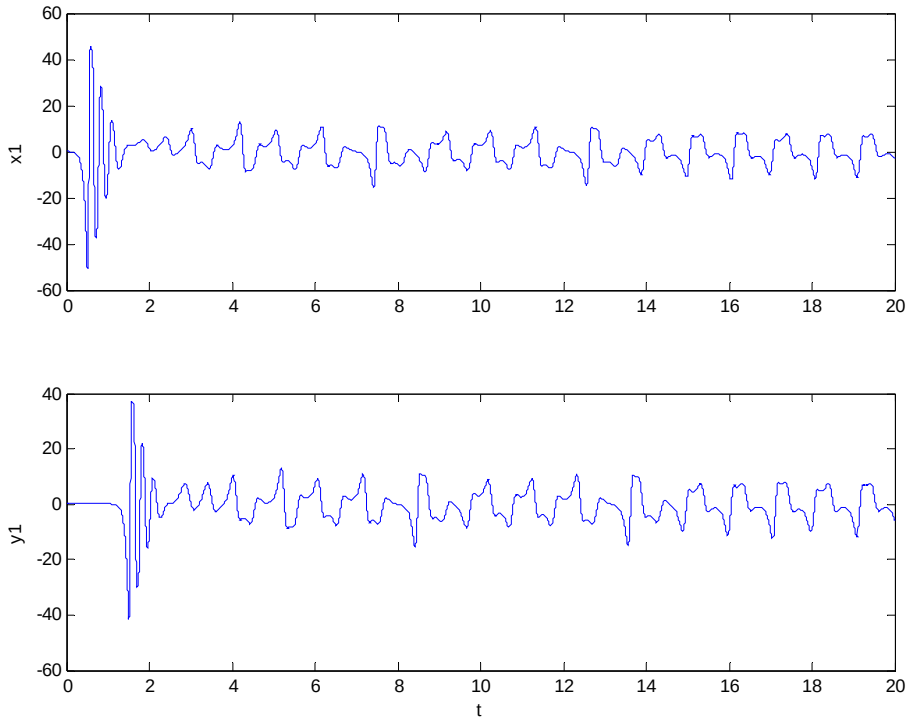

Fig 4.9 Time history of x_1 *and* y_1.

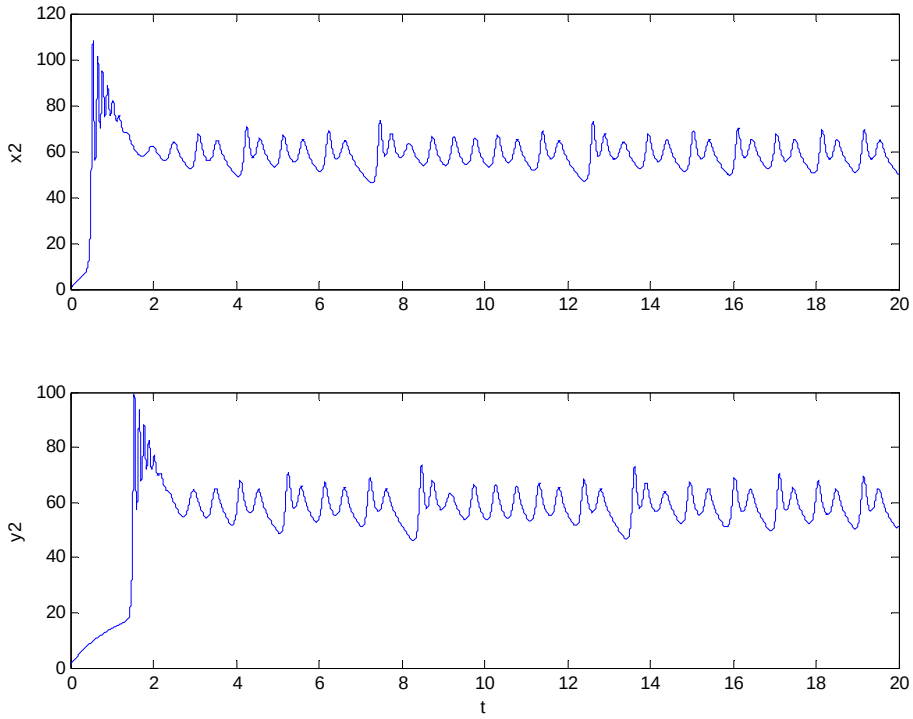

Fig-4.10 Time history of x_2 *and* y_2.

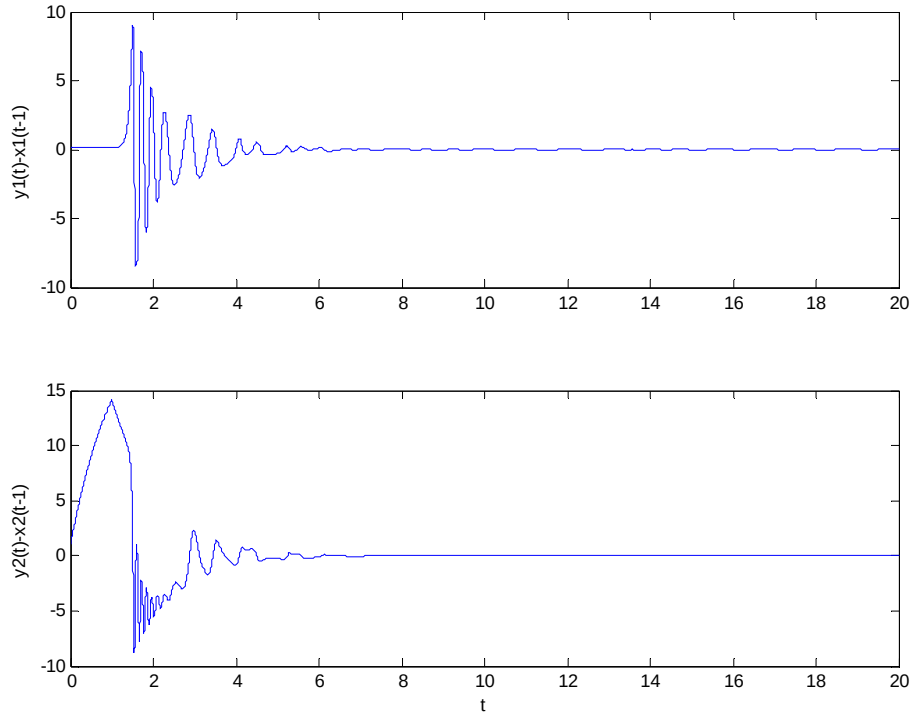

Fig 4.11 Lag synchronization of two BLDCM systems.

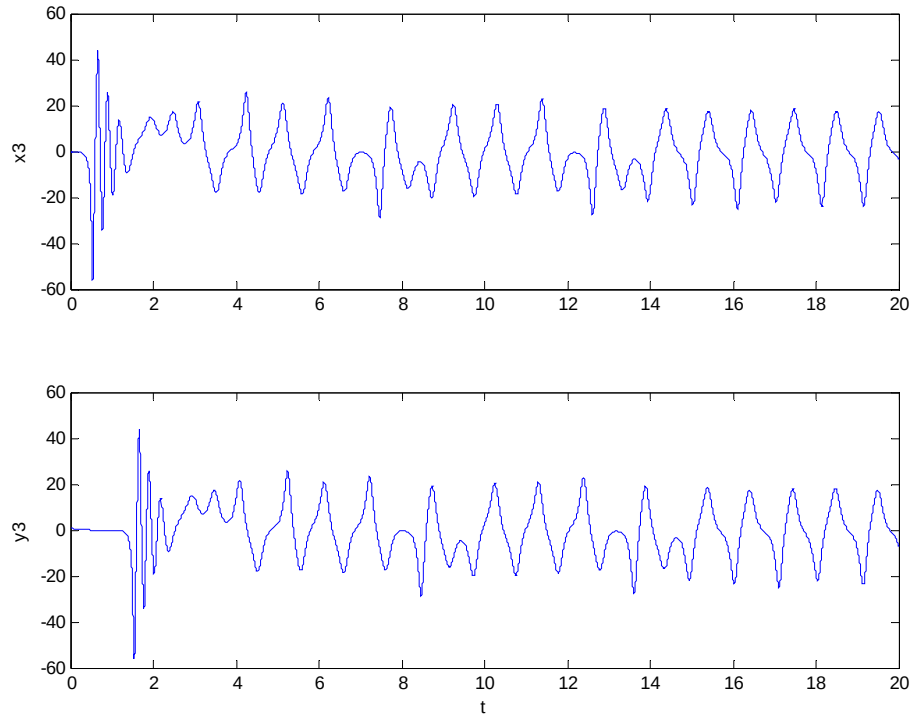

Fig 4.12 Time history of x_3 *and* y_3.

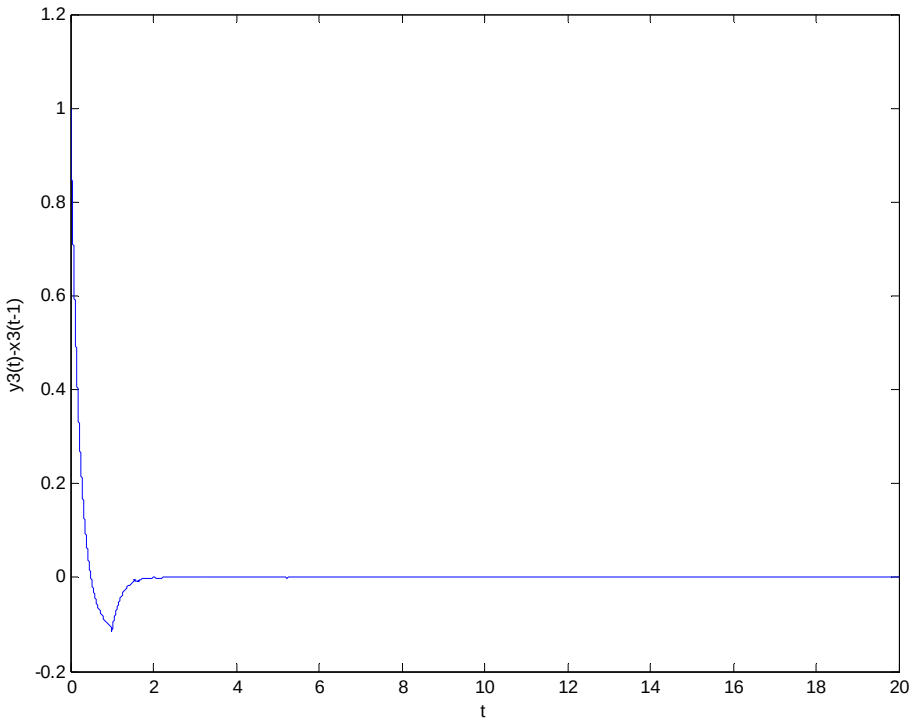

Fig 4.13 Lag Synchronization of two BLDCM systems.

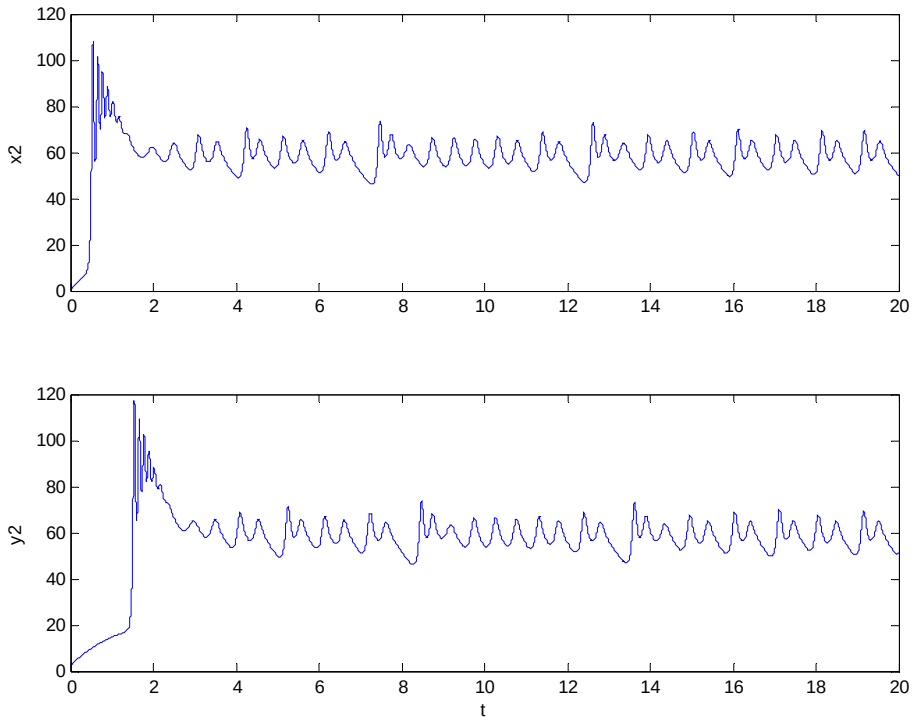

Fig 4.14 Time history of x_2 *and* y_2.

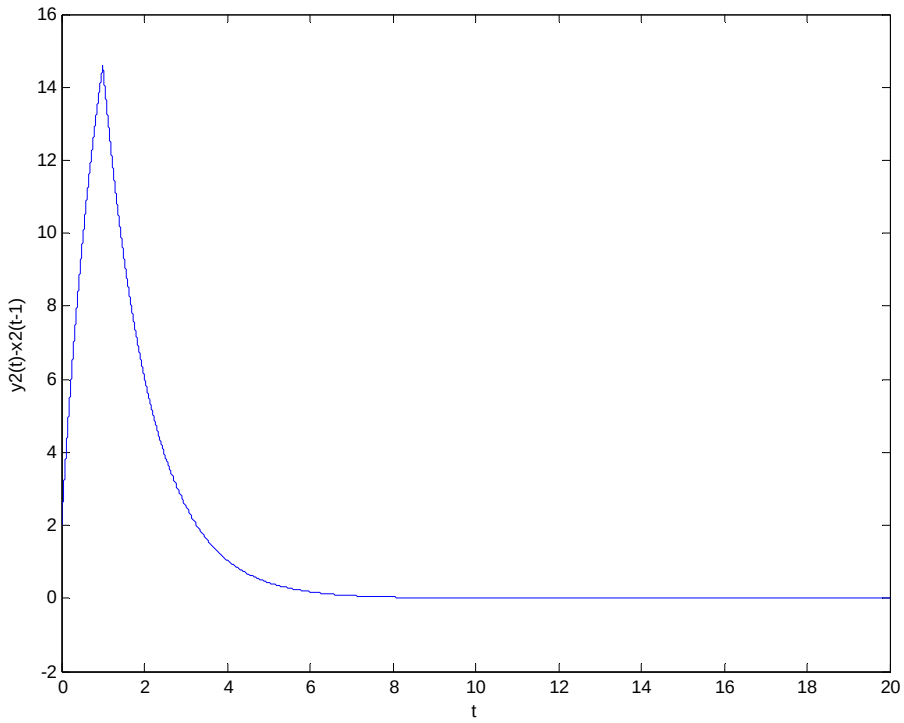

Fig 4.15 Lag synchronization of two BLDCM systems.

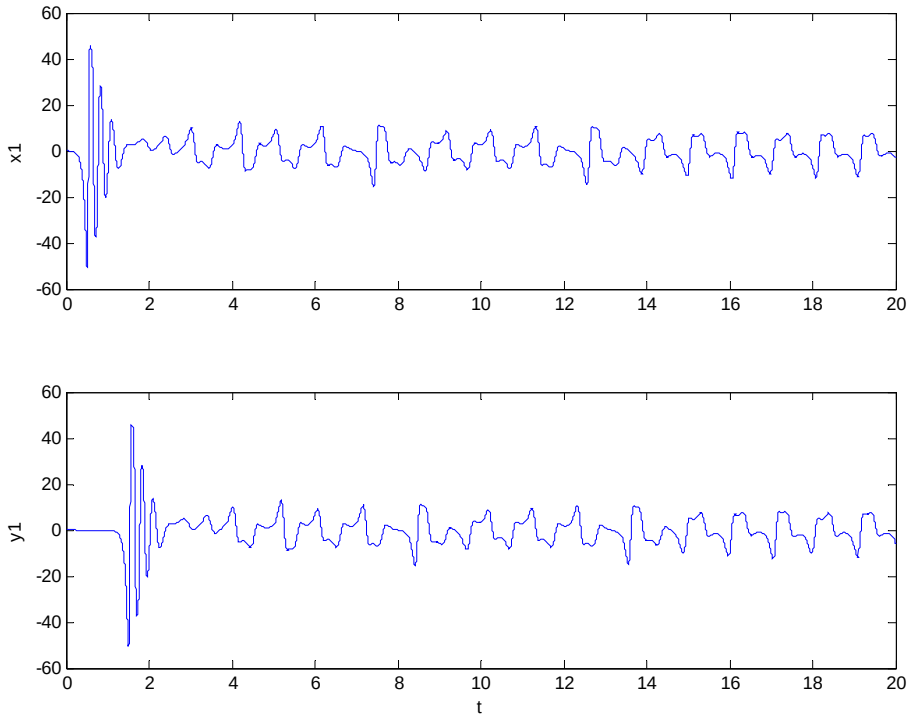

Fig 4.16 Time history of x_1 *and* y_1.

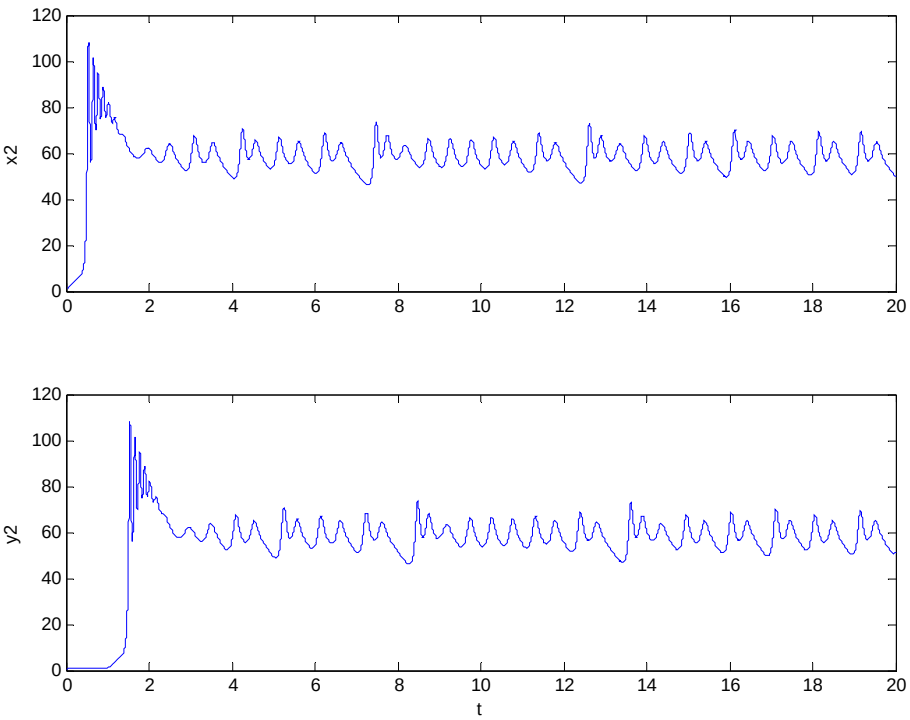

Fig 4.17 Time history of x_2 *and* y_2.

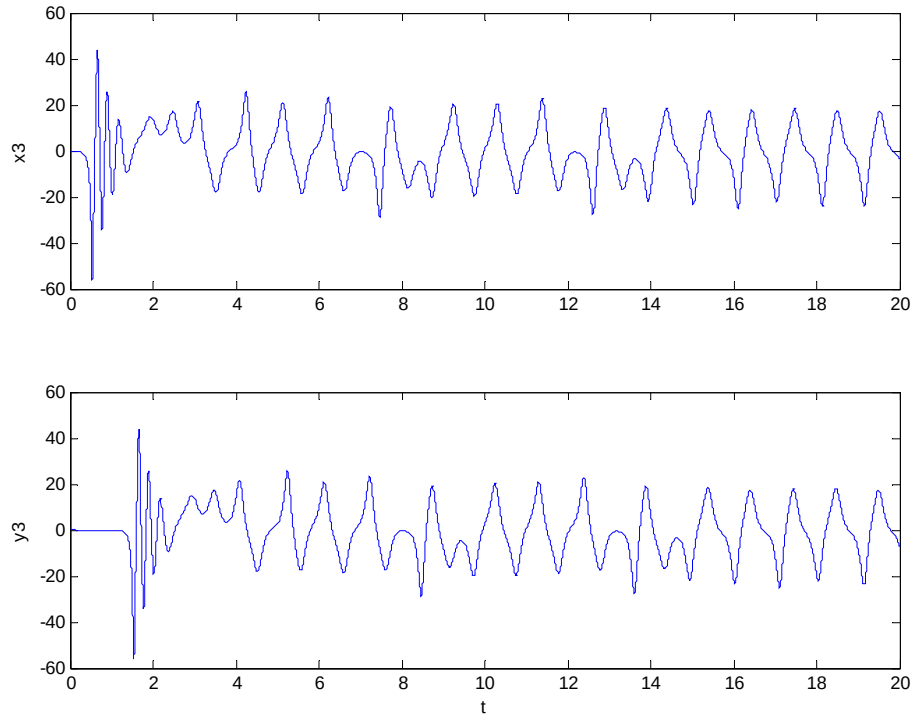

Fig 4.18 Time history of x_3 *and* y_3.

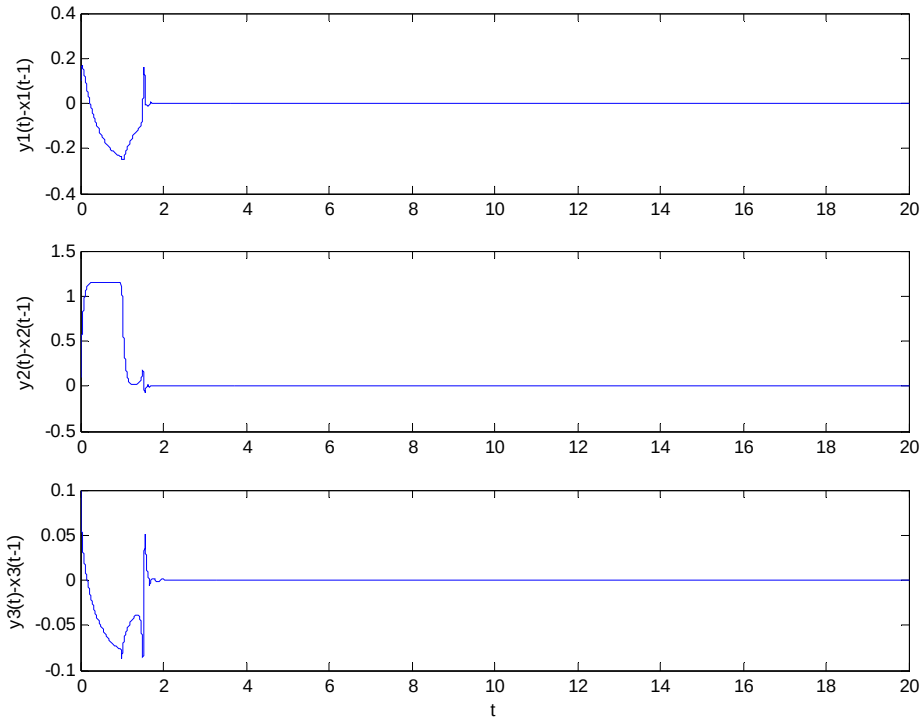

Fig 4.19 Lag synchronization of two BLDCM systems.

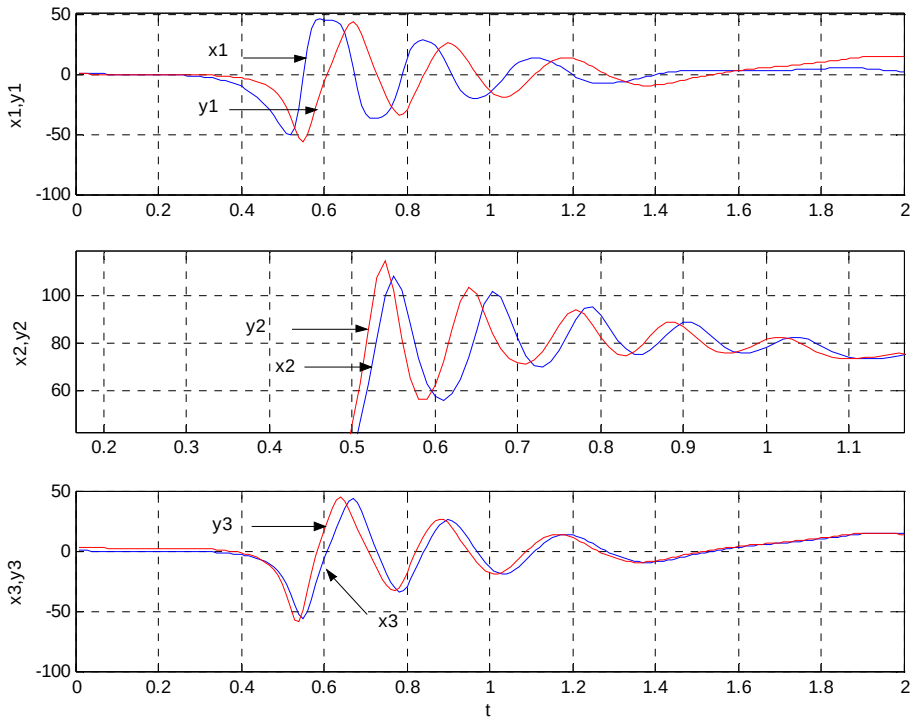

Fig 4.20 Time history of all state.

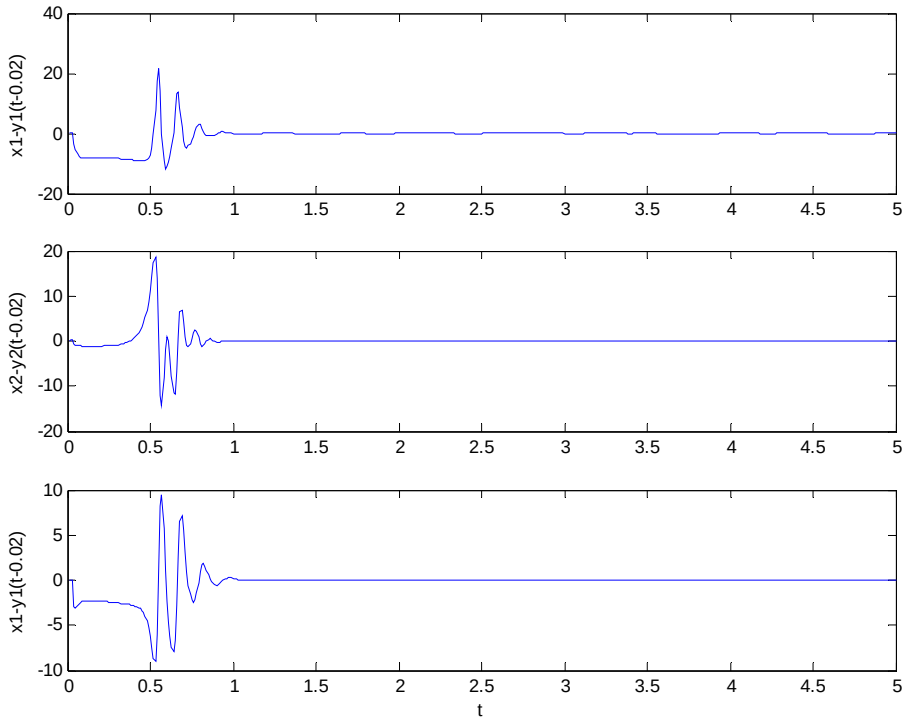

Fig 4.21 Anticipated synchronization of two BLDCM systems.

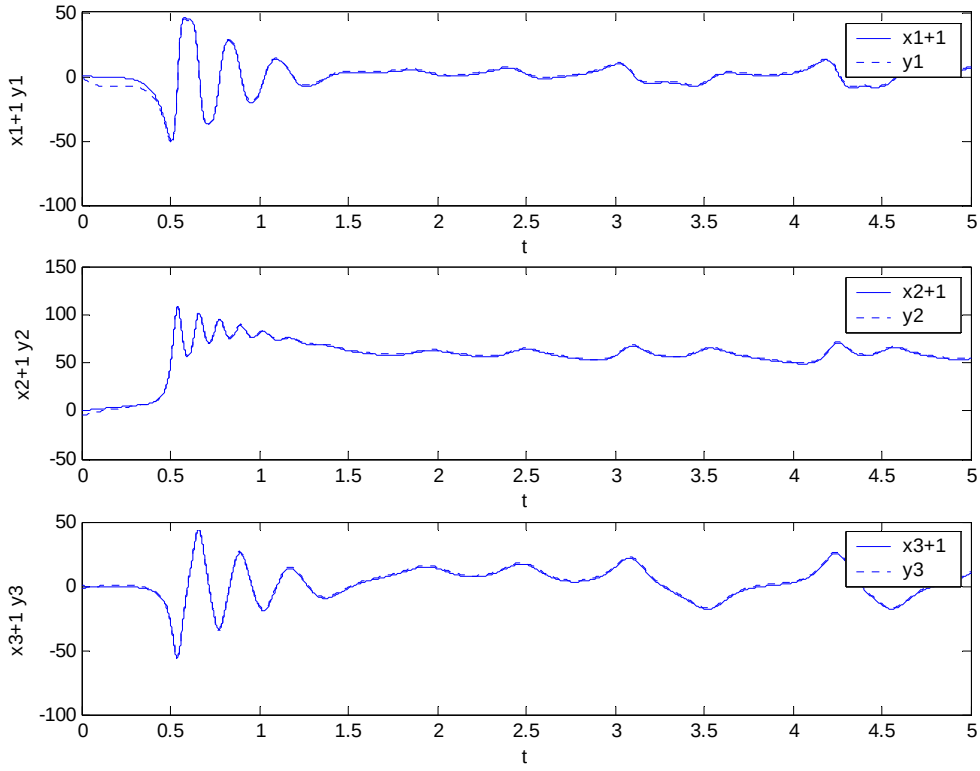

Fig. 4.22 Time history for y_1, y_2, y_3 *and* x_1+1, x_2+1, x_3+1.

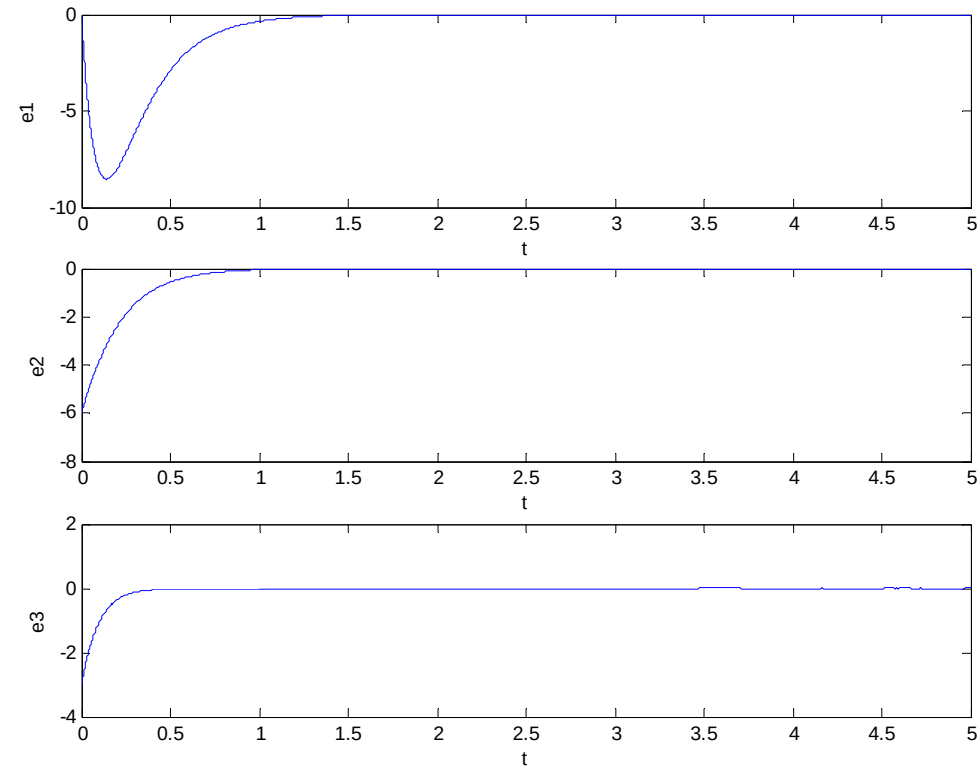

Fig. 4.23 Generalized complete synchronization error for $e = y-(x+1)$.

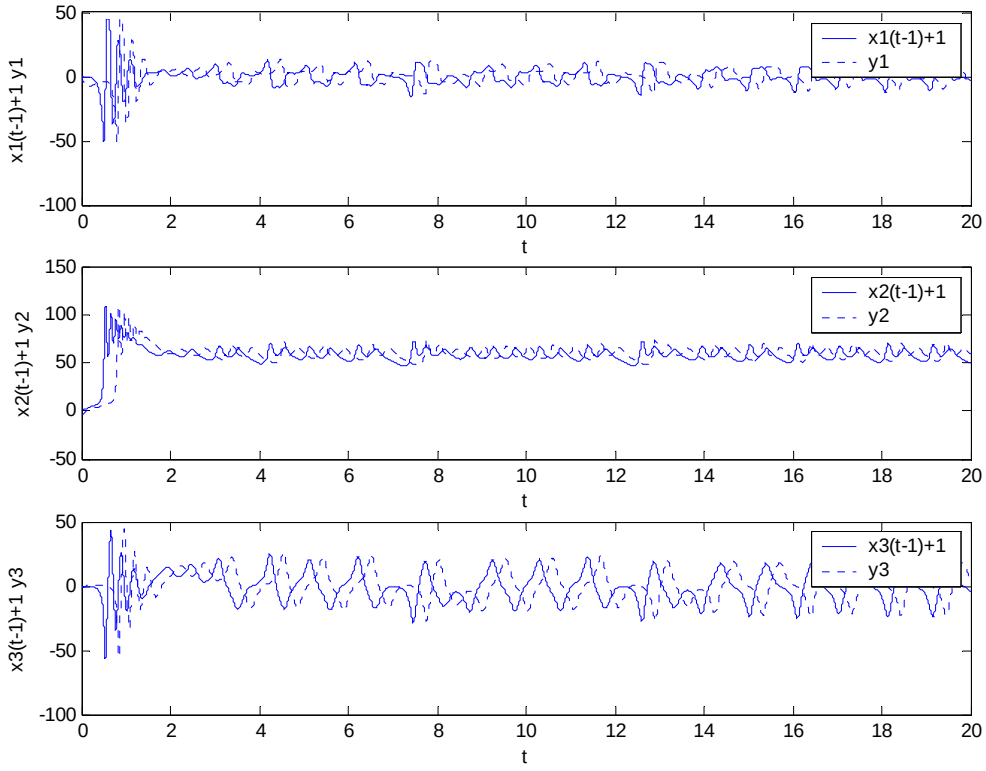

Fig. 4.24 Time history for y_1, y_2, y_3 *and* x_1+1, x_2+1, x_3+1.

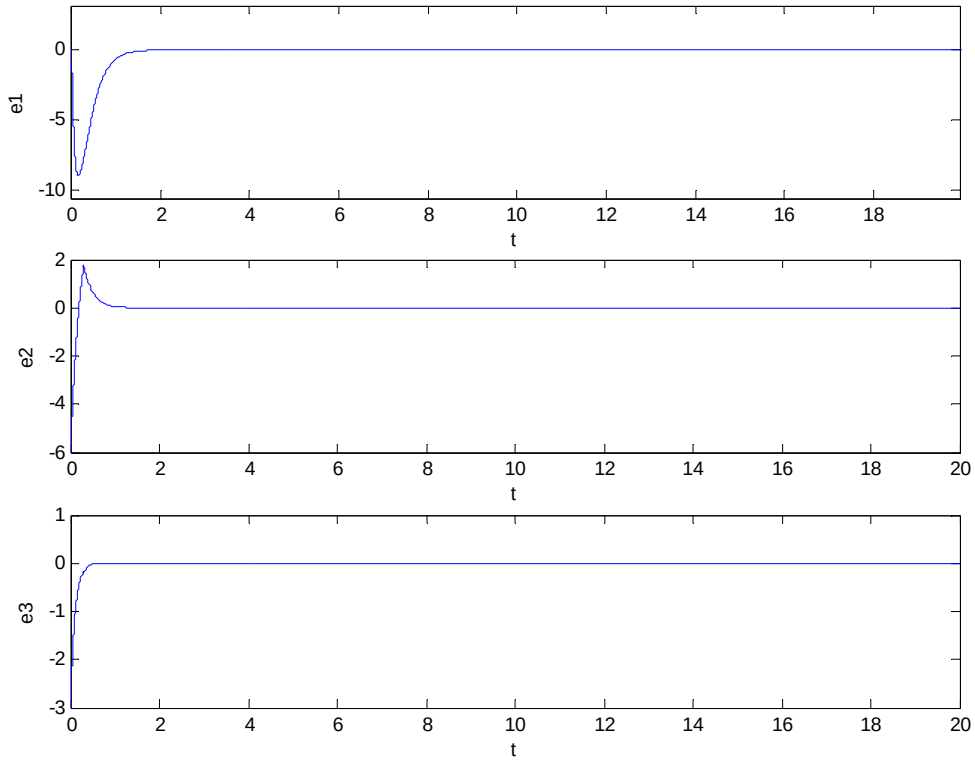

Fig. 4.25 Generalized lag synchronization error for e= $y(t)-(x(t-0.5+1))$.

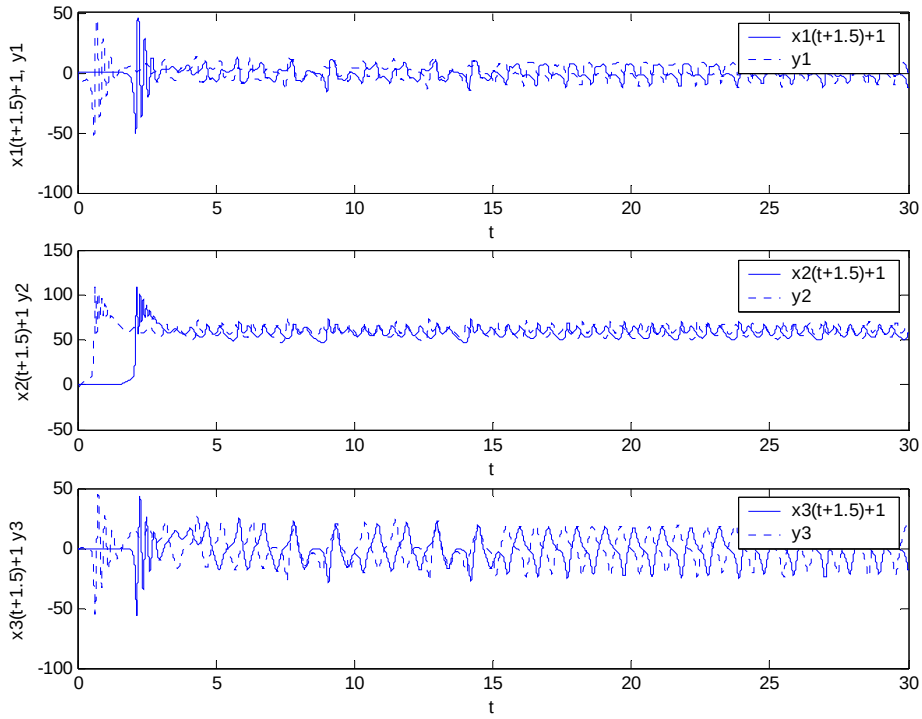

Fig. 4.26 Time history for y_1, y_2, y_3 *and* x_1+1, x_2+1, x_3+1.

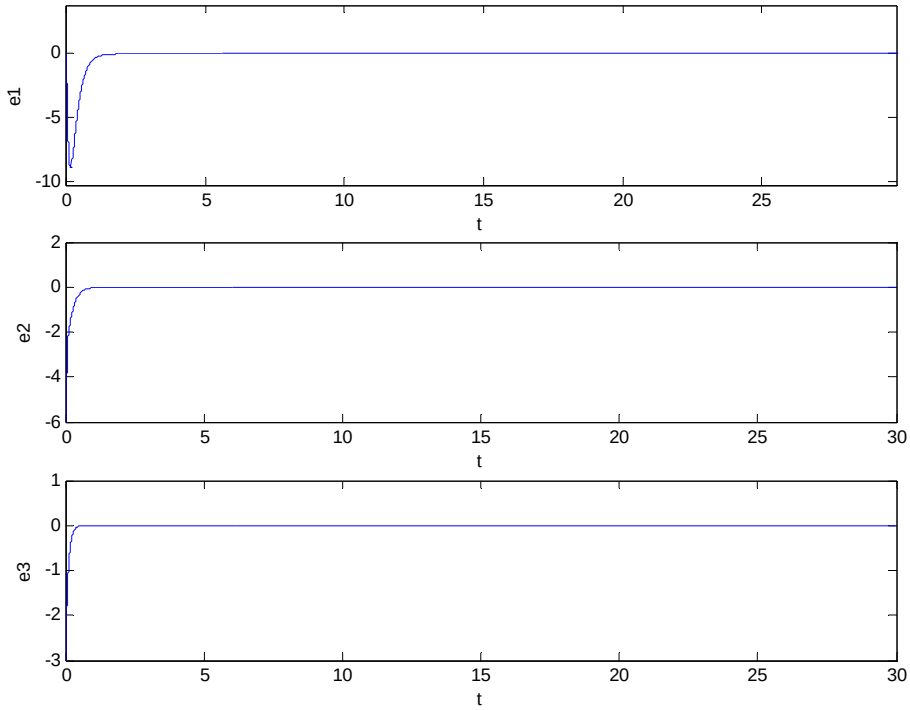

Fig. 4.27Generalized anticipated synchronization error for e= $y(t)-(x(t+1.5)+1)$.

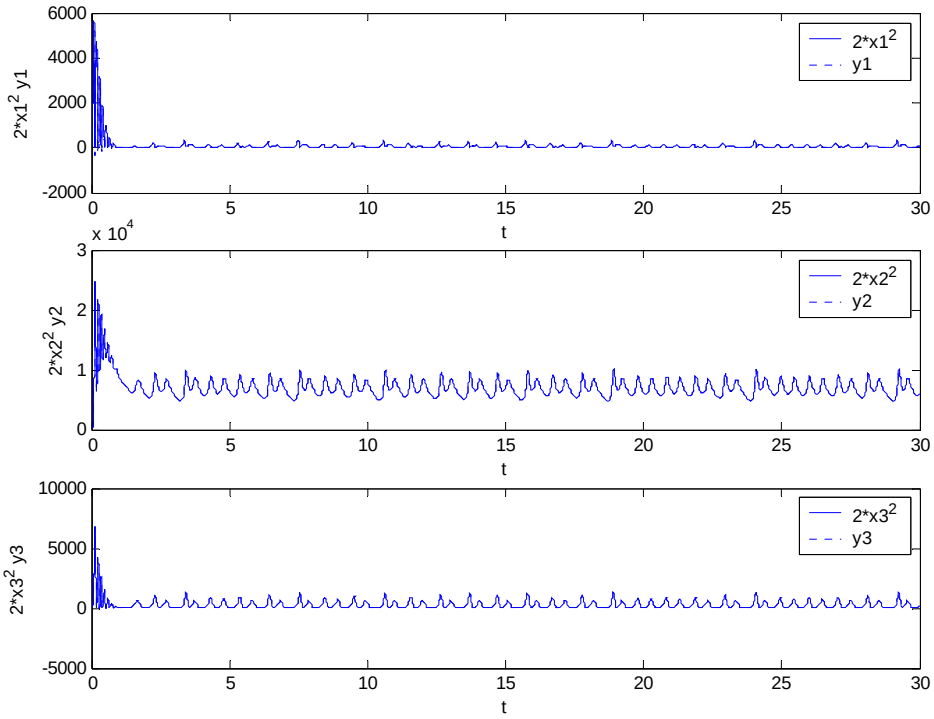

Fig. 4.28 Time history for y_1, y_2, y_3 *and* $2x^2_1, 2x^2_2, 2x^2_3$.

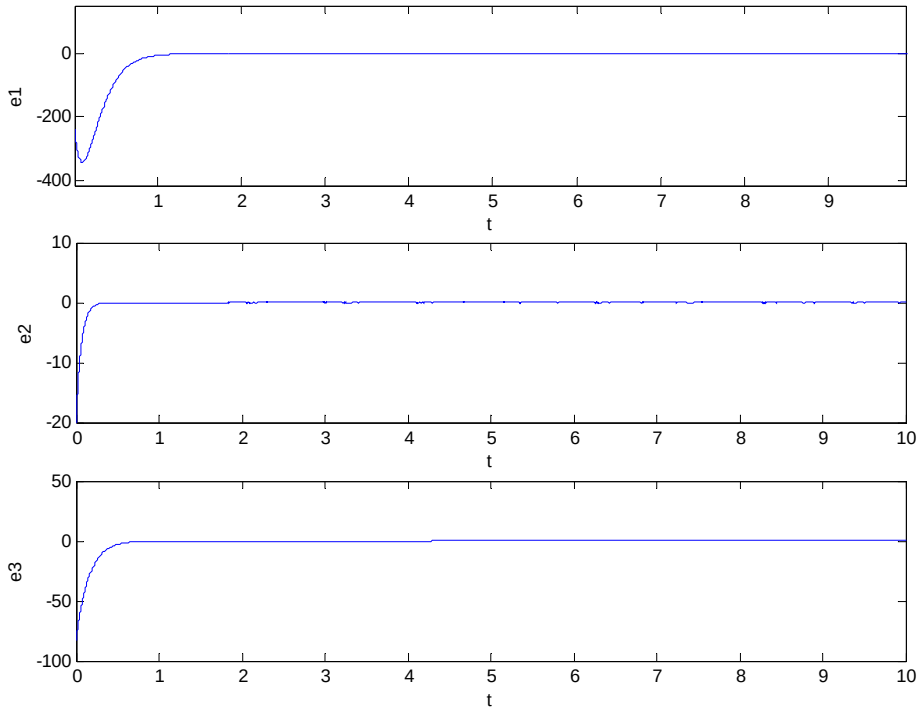

Fig. 4.29 Generalized complete synchronization error for e= $y(t)-(2x^2)$.

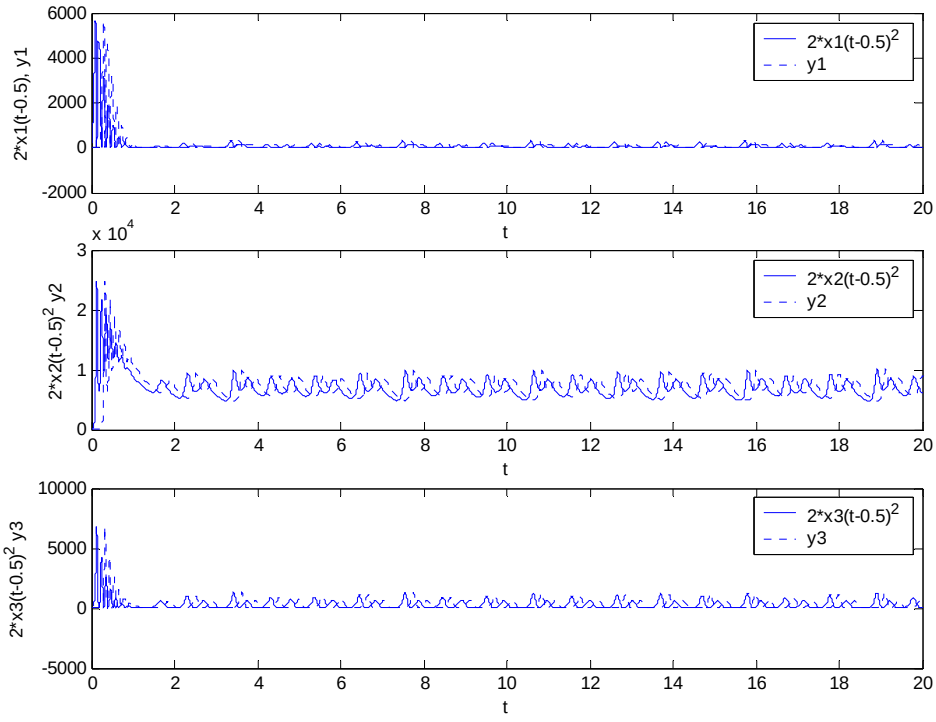

Fig. 4.30 Time history for y_1, y_2, y_3 *and* $2x^2{}_1(t-0.5), 2x^2{}_2(t-0.5), 2x^2{}_3(t-0.5)$.

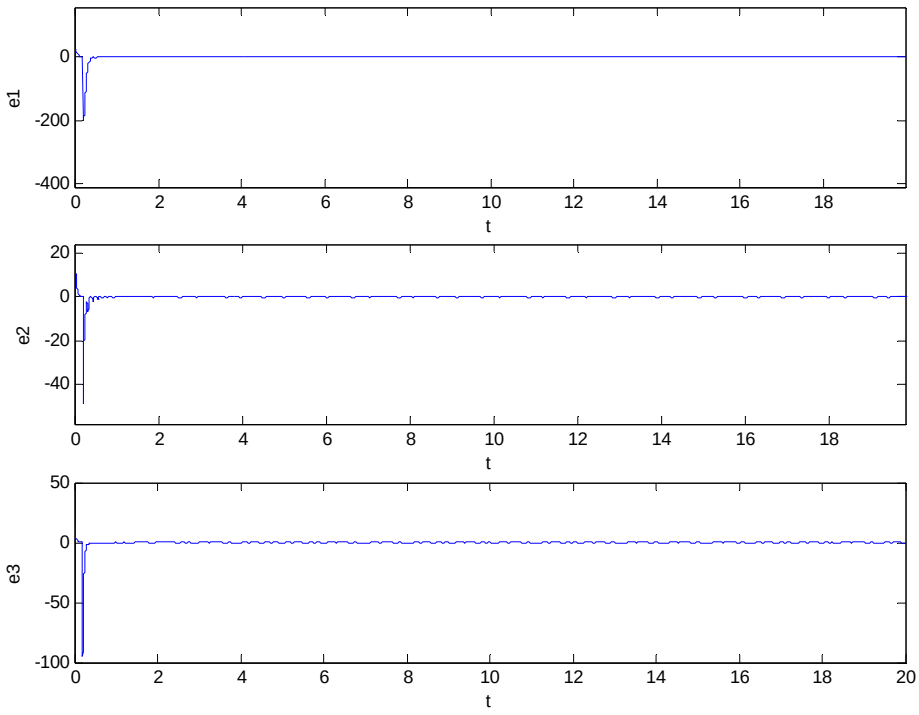

Fig. 4.31 Generalized lag synchronization error with e= $y(t)-(2x^2(t-0.5))$.

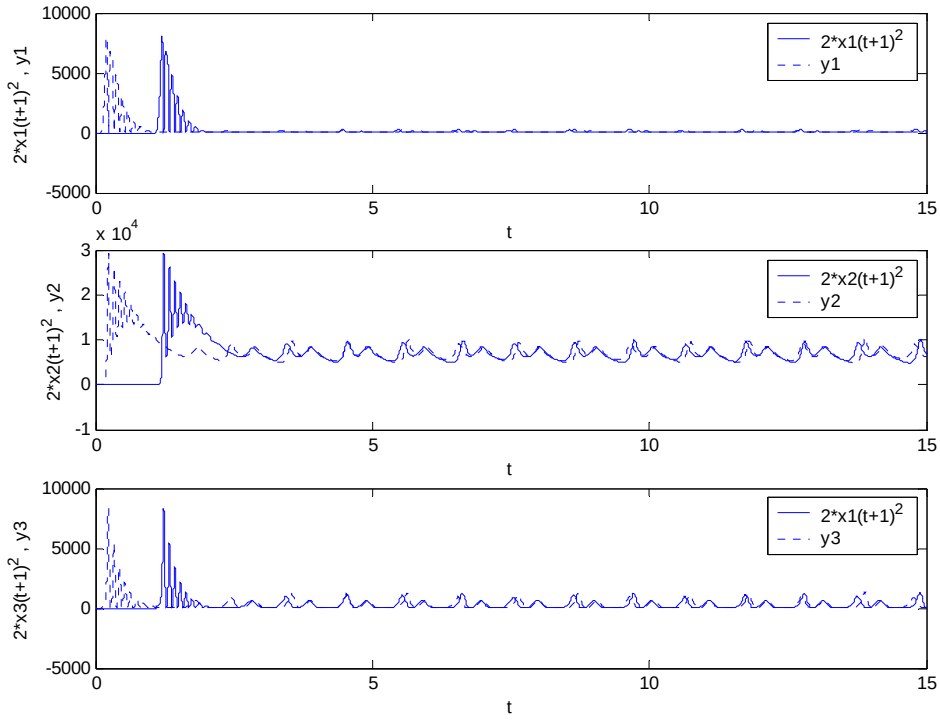

Fig. 4.32 Time history for y_1, y_2, y_3 *and* $2x^2_1(t+1), 2x^2_2(t+1), 2x^2_3(t+1)$.

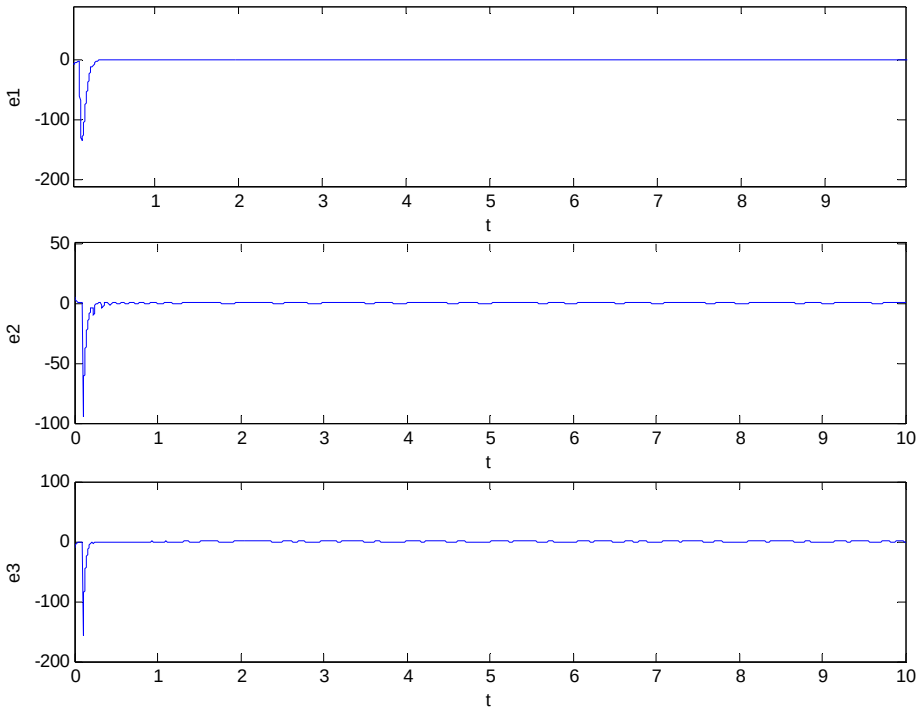

Fig. 4.33 Generalized anticipated synchronization error for e= $y(t)-(2x^2(t+1))$.

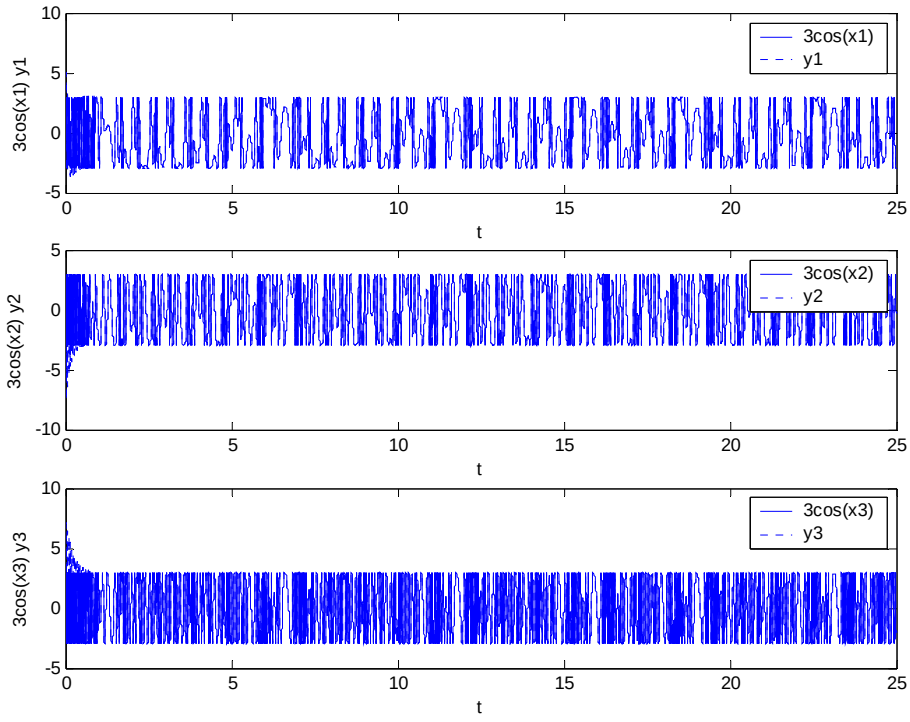

Fig. 4.34 Time history for y_1, y_2, y_3 *and* $3\cos(x_1), 3\cos(x_2), 3\cos(x_3)$.

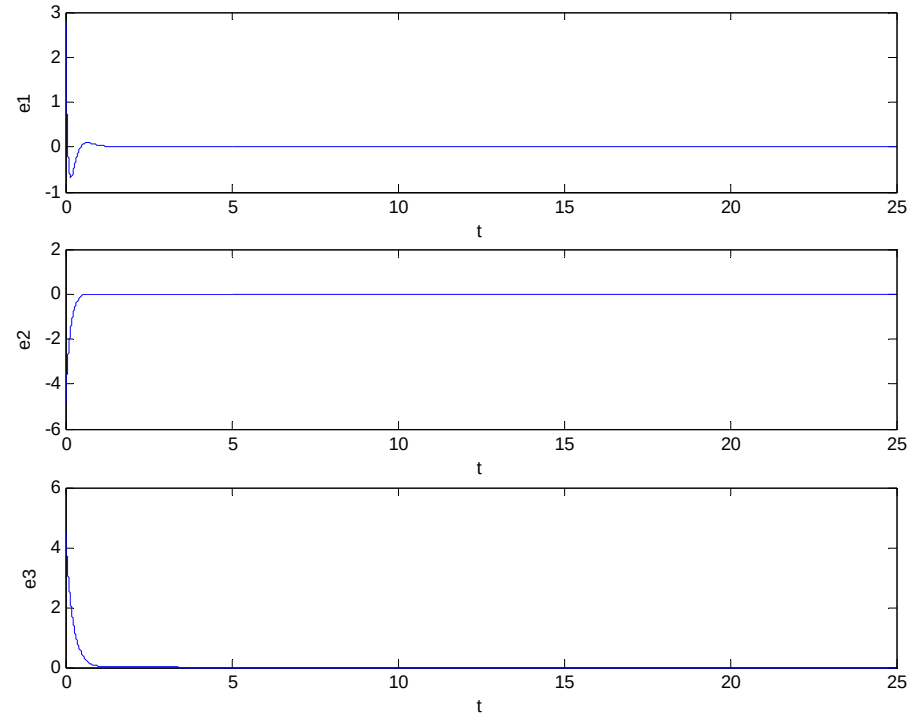

Fig. 4.35 Generalized complete synchronization error for e= $y(t) - 3\cos(x)$.

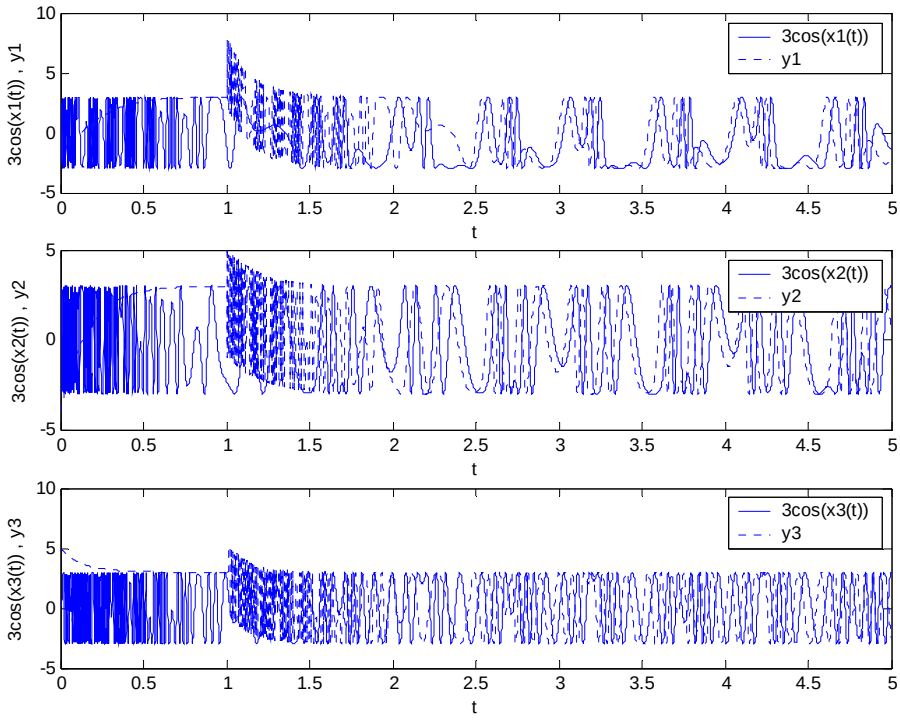

Fig. 4.36 Time history for y_1, y_2, y_3 *and* $3\cos(x_1(t-1)), 3\cos(x_2(t-1)), 3\cos(x_3(t-1))$.

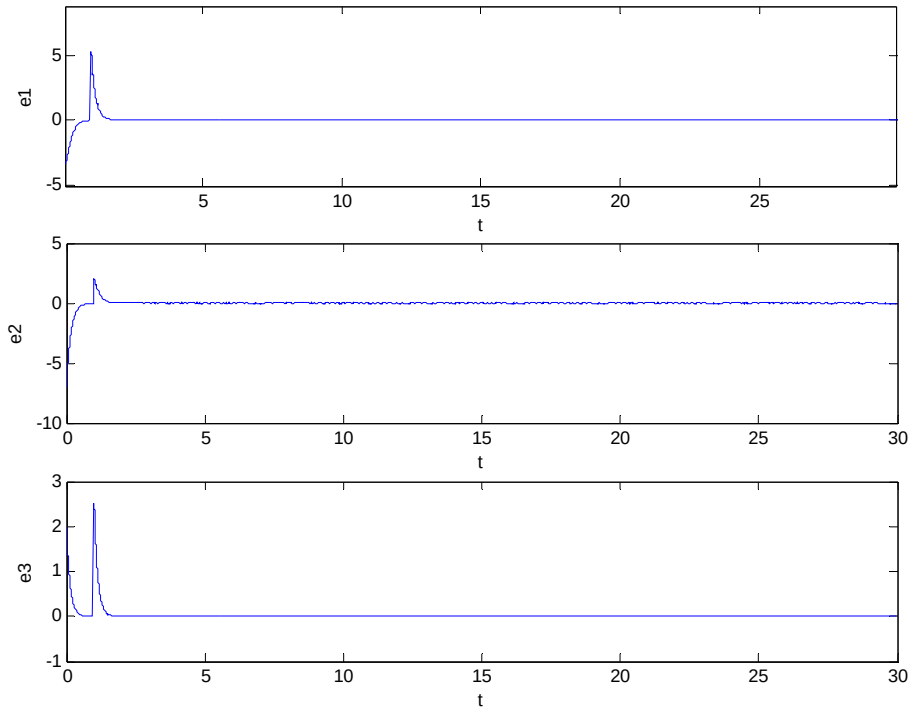

Fig. 4.37 Generalized lag synchronization error for e= $y(t)-3\cos(x(t-1))$.

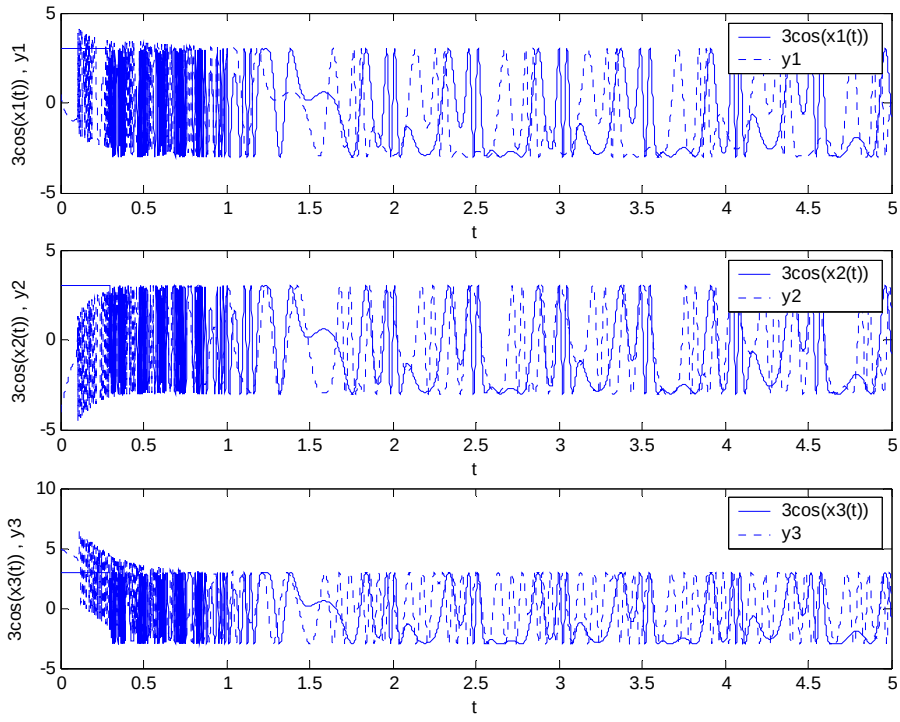

Fig. 4.38 Time history for y_1, y_2, y_3 *and* $3\cos(x_1(t+0.2)), 3\cos(x_2(t+0.2)), 3\cos(x_3(t+0.2))$.

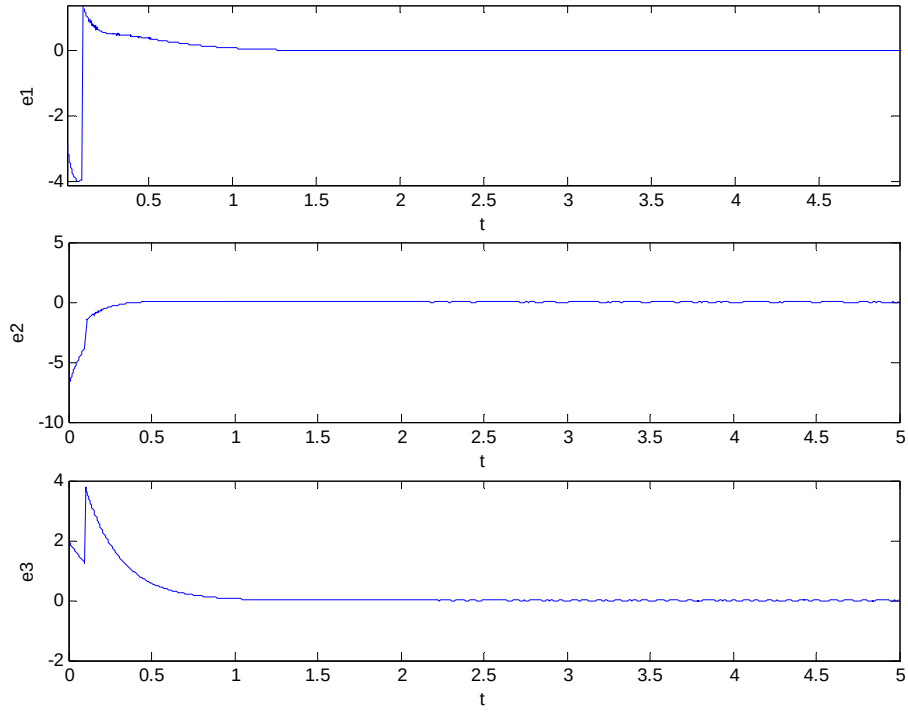

Fig. 4.39 Generalized anticipated synchronization error for e=y(t)-3cos(x(t+0.2)).

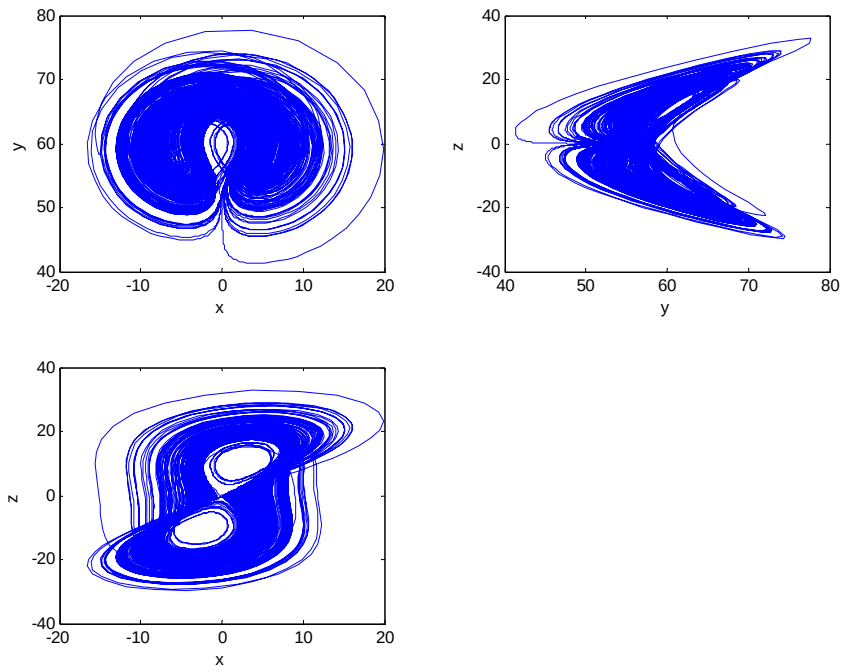

Fig. 5.1 phase portrait of BLDCM with (i, j, k) = (1,1,1) and $\left(V_q, V_d, \delta, \sigma, \eta, T_L\right)$=(0.168,20.66,-0.875,4.55,0.26,0.53).

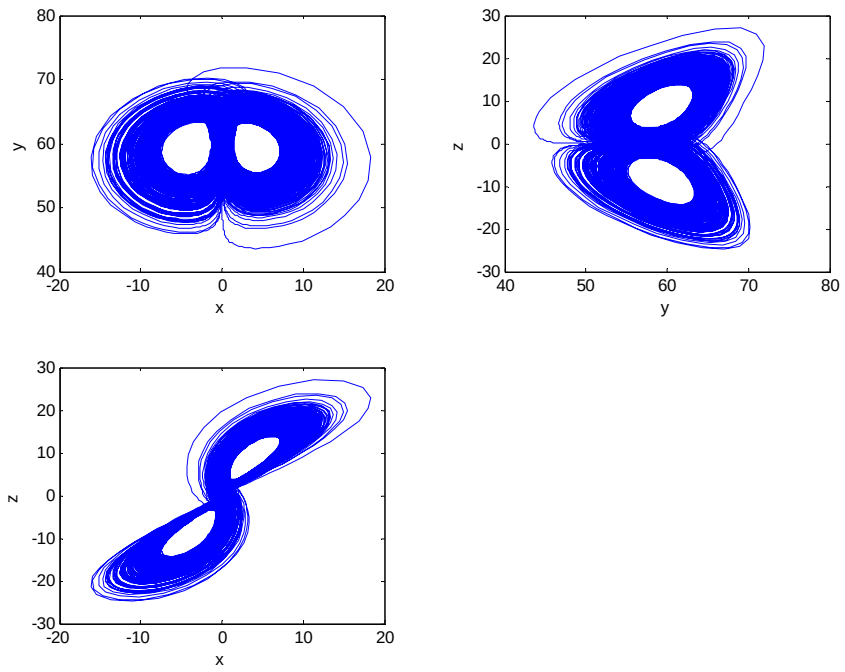

Fig. 5.2 phase portrait of BLDCM with (i, j, k) = (0.9,1,0.9) and $\left(V_q, V_d, \delta, \sigma, \eta, T_L\right)$=(0.168,20.66,-0.875,11,0.26,0.53).

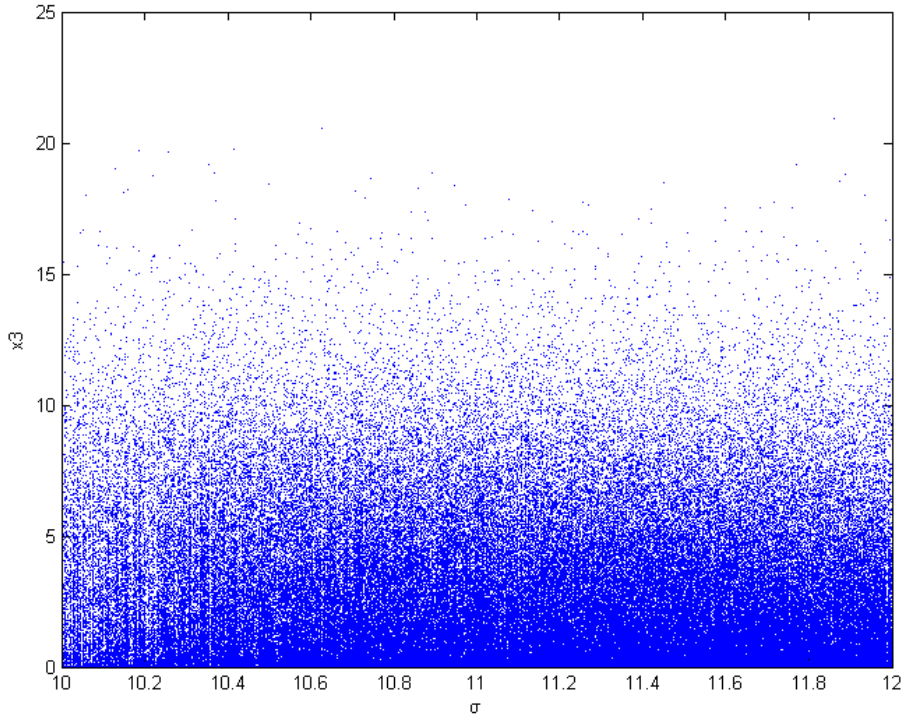

Fig.5.3 Bifurcation diagram for BLDCM with order (i, j, k)=(0.9,1,0.9).

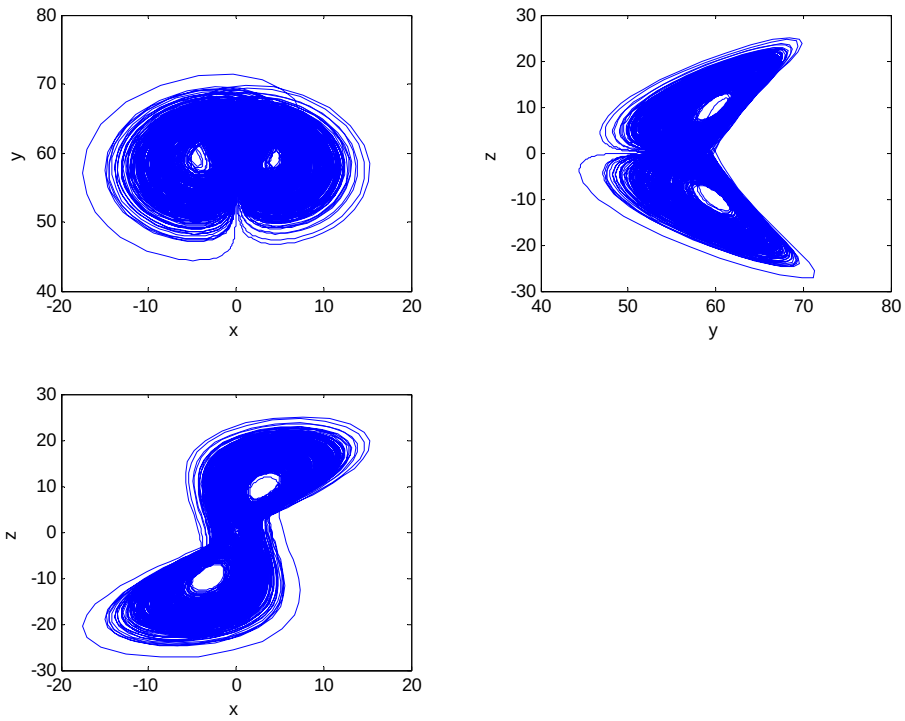

Fig. 5.4 phase portrait of BLDCM with (i, j, k) = (0.9,1,1) and $\left(V_q, V_d, \delta, \sigma, \eta, T_L\right)$=(0.168,20.66,-0.875,7,0.26,0.53).

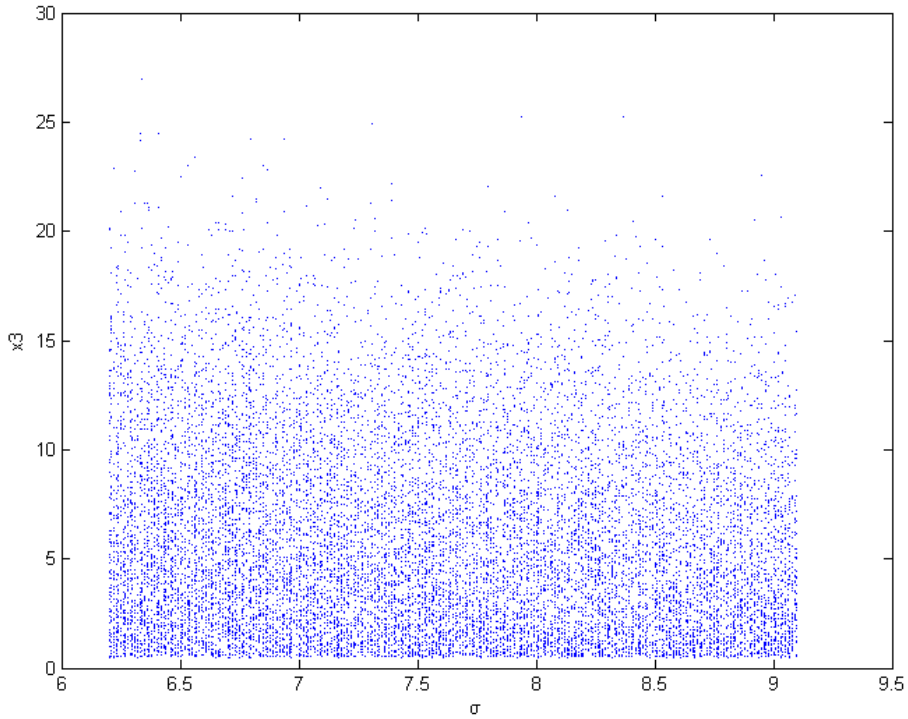

Fig.5.5 Bifurcation diagram for BLDCM with order (i, j, k)=(0.9,1,1).

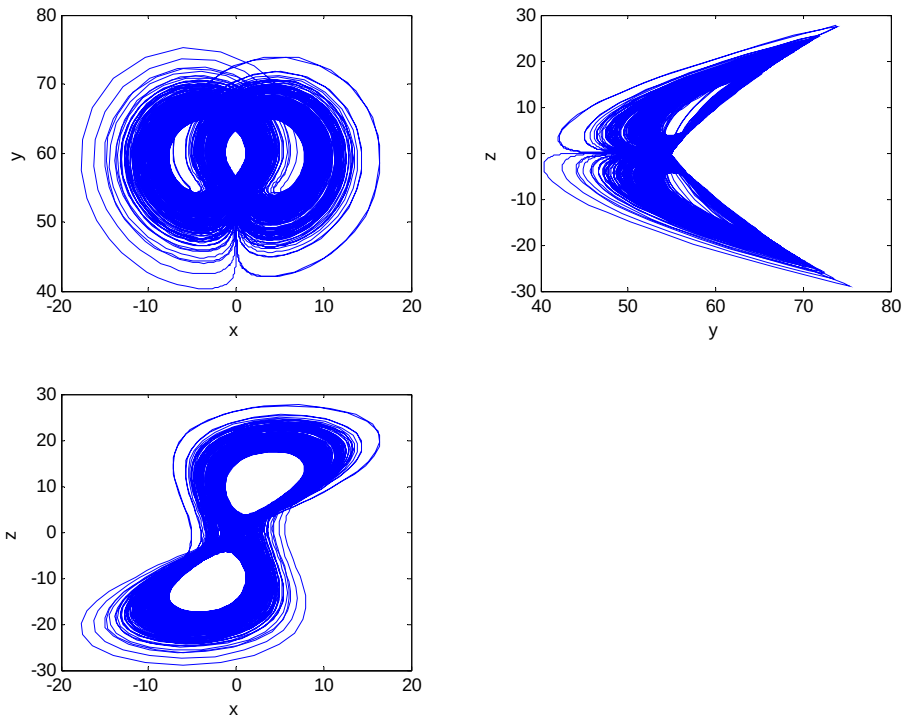

Fig. 5.6 phase portrait of BLDCM with (i, j, k) = (1,0.9, 1) and $\left(V_q, V_d, \delta, \sigma, \eta, T_L\right)$=(0.168,20.66,-0.875,6,0.26,0.53).

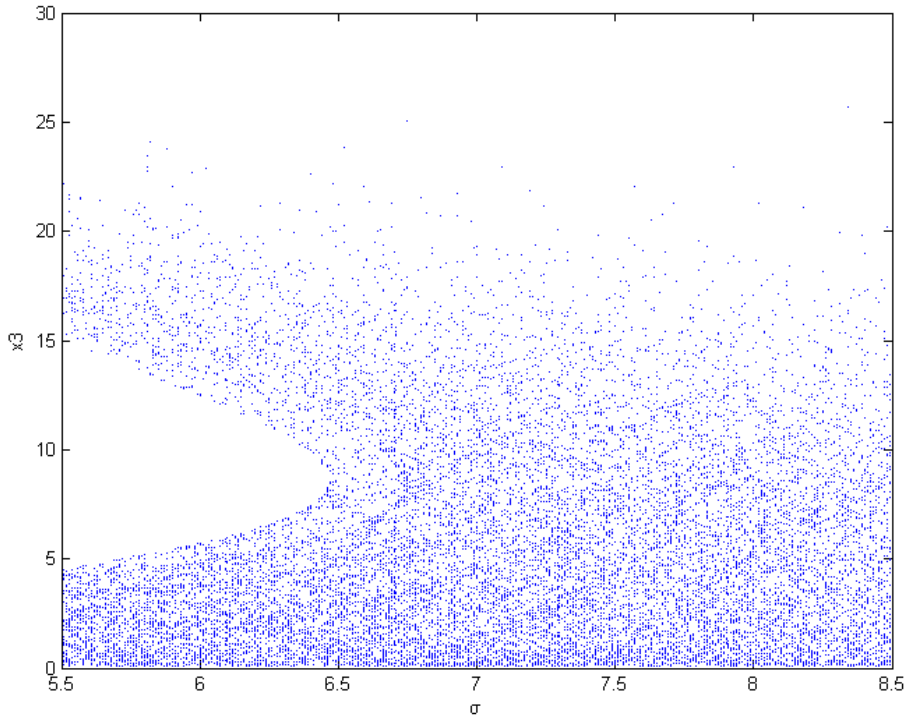

Fig.5.7 Bifurcation diagram for BLDCM with order (i, j, k)=(1,0.9,1).

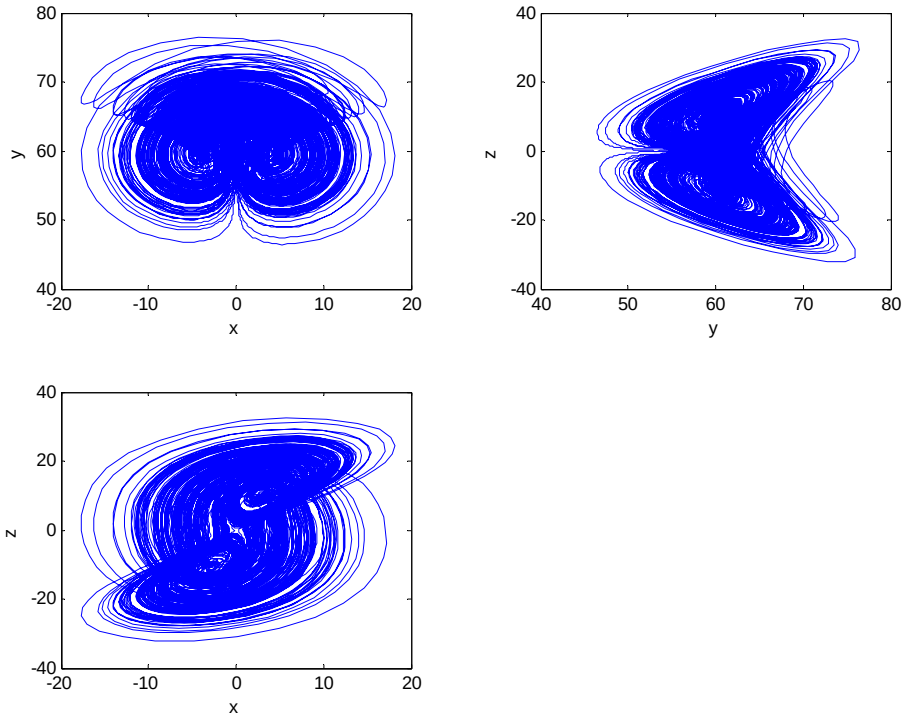

Fig. 5.8 phase portrait of BLDCM with (i, j, k) = (1,1.1, 1) and $\left(V_q, V_d, \delta, \sigma, \eta, T_L\right)$=(0.168,20.66,-0.875,9,0.26,0.53).

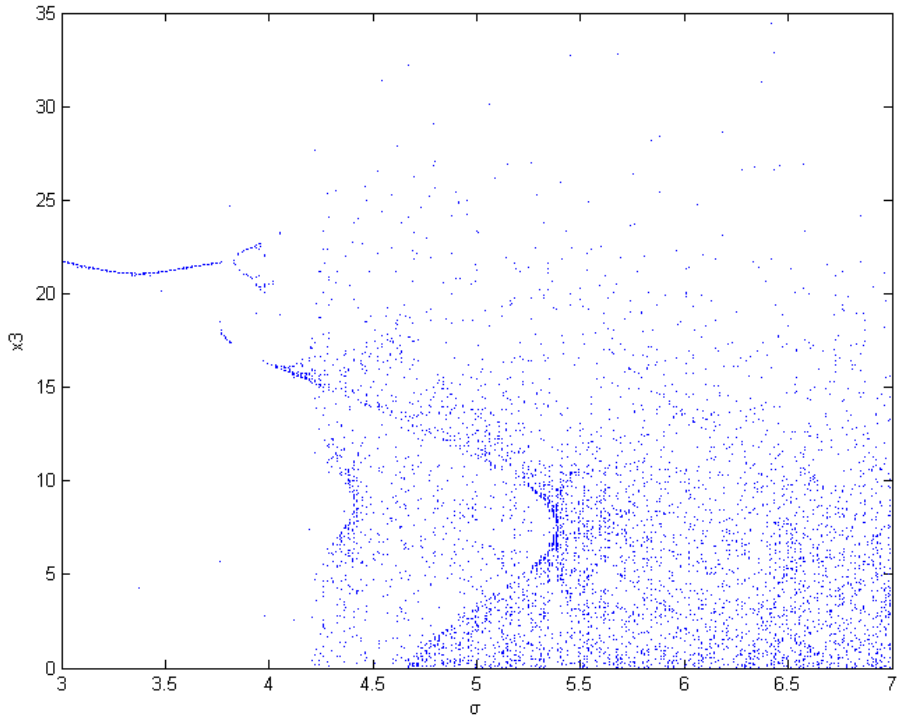

Fig.5.9 Bifurcation diagram for BLDCM with order (i, j, k) = (1,1.1,1).

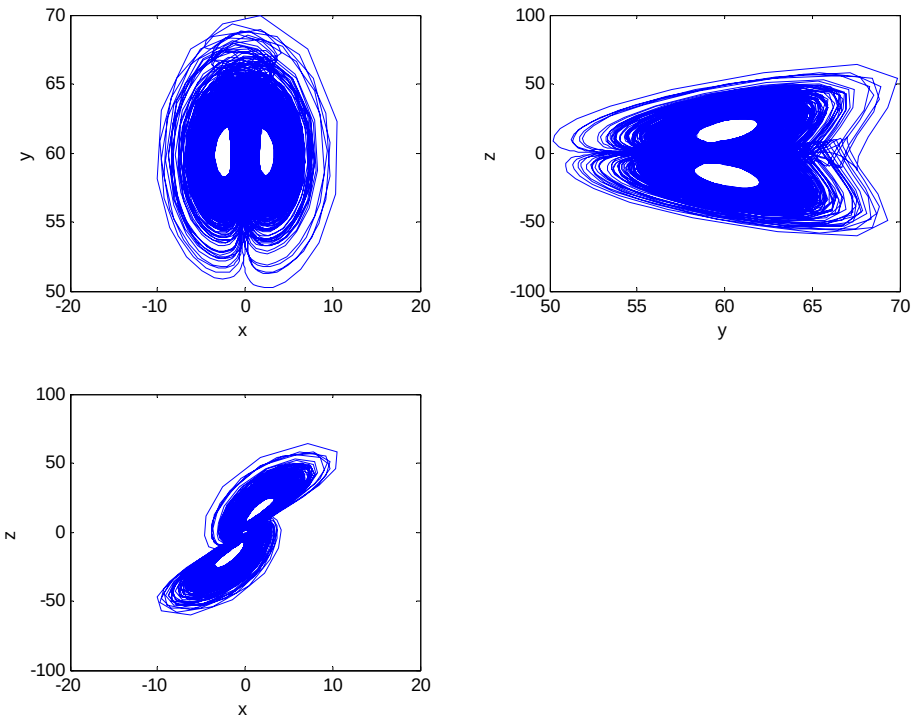

Fig. 5.10 phase portrait of BLDCM with (i, j, k) = (1,1, 0.3) and $\left(V_q, V_d, \delta, \sigma, \eta, T_L\right)$=(0.168,20.66,-0.875,0.2,0.26,0.53).

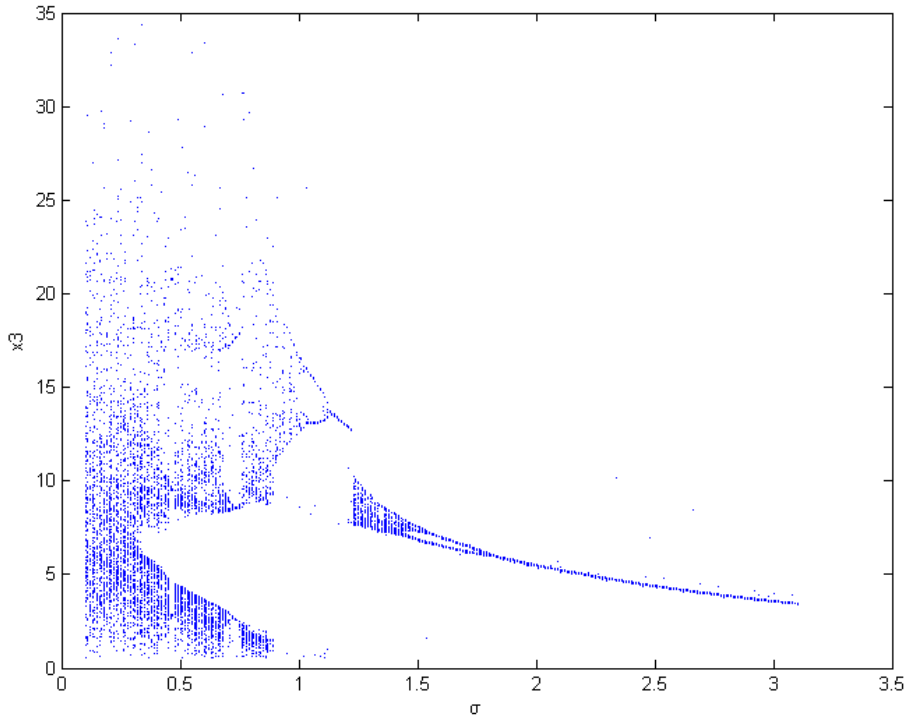

Fig.5.11 Bifurcation diagram for BLDCM with order (i, j, k)=(1,1,0.3).

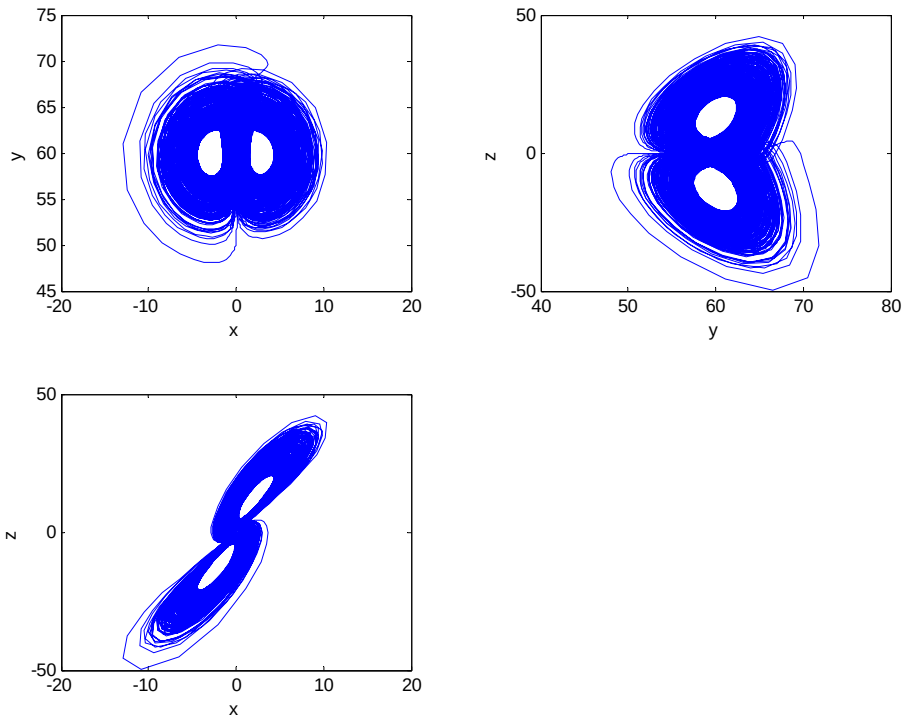

Fig. 5.12 phase portrait of BLDCM with (i, j, k) = (1,1, 0.4) and $\left(V_q, V_d, \delta, \sigma, \eta, T_L\right)$=(0.168,20.66,-0.875,1.5,0.26,0.53).

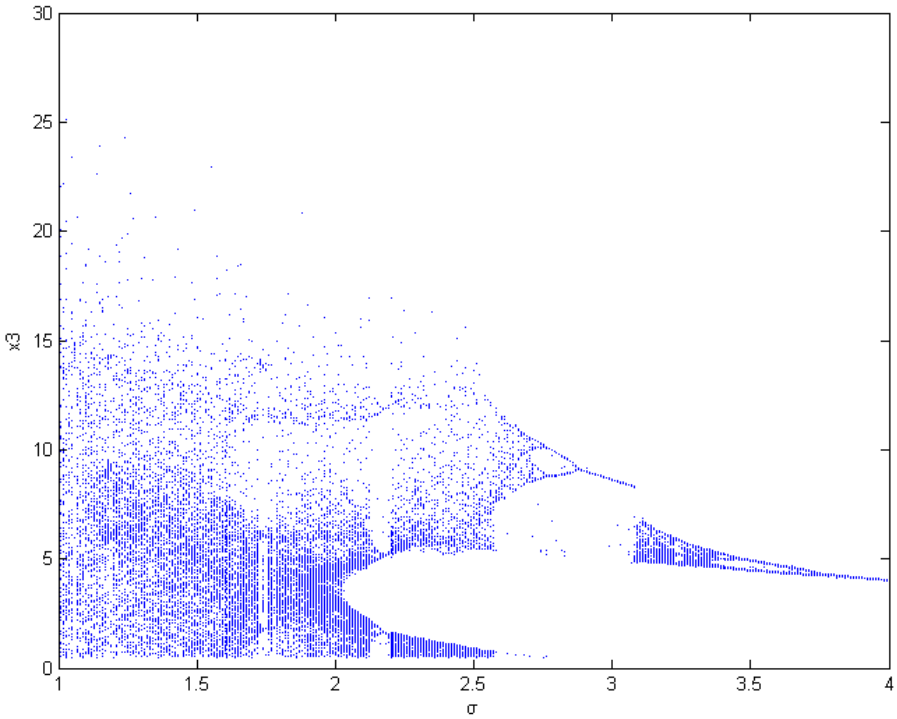

Fig.5.13 Bifurcation diagram for BLDCM with order (i, j, k)=(1,1,0.4).

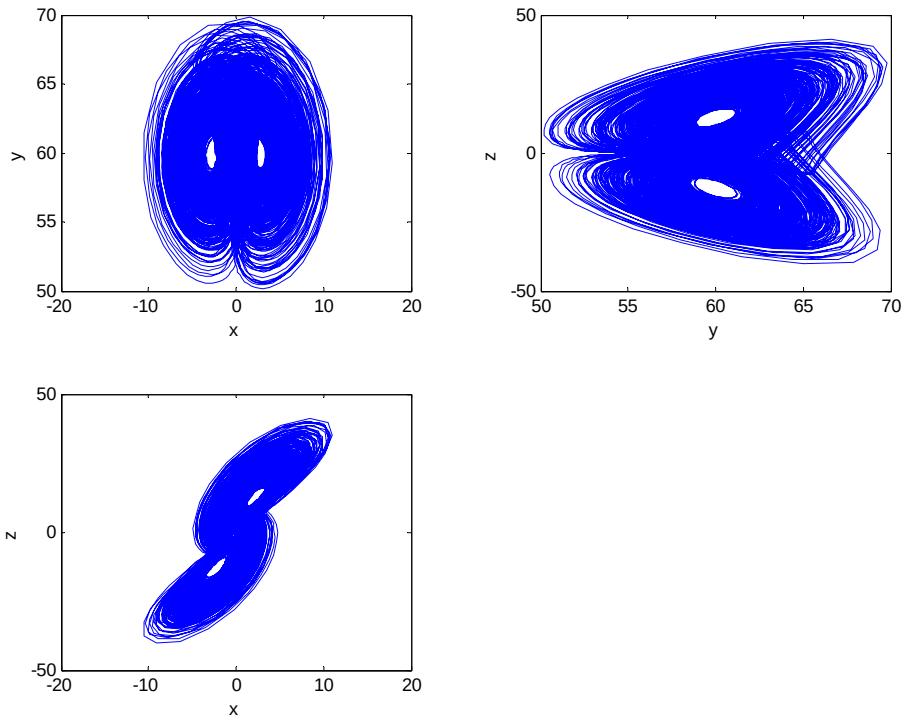

Fig. 5.14 phase portrait of BLDCM with (i, j, k) = (1,1, 0.5) and $\left(V_q, V_d, \delta, \sigma, \eta, T_L\right)$=(0.168,20.66,-0.875,1.5,0.26,0.53).

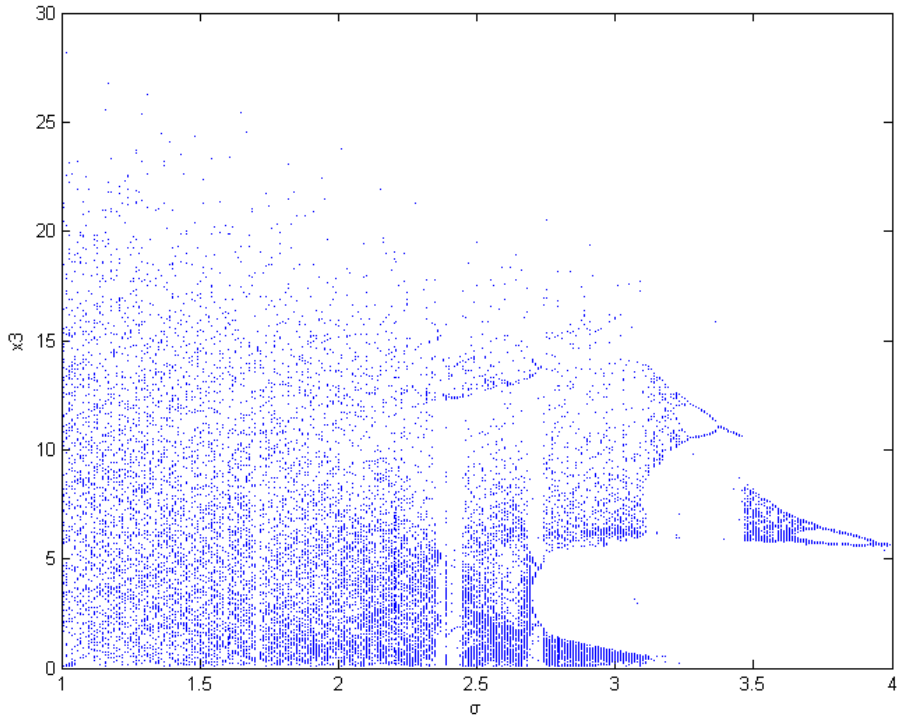

Fig.5.15 Bifurcation diagram for BLDCM with order (i, j, k) = (1,1,0.5).

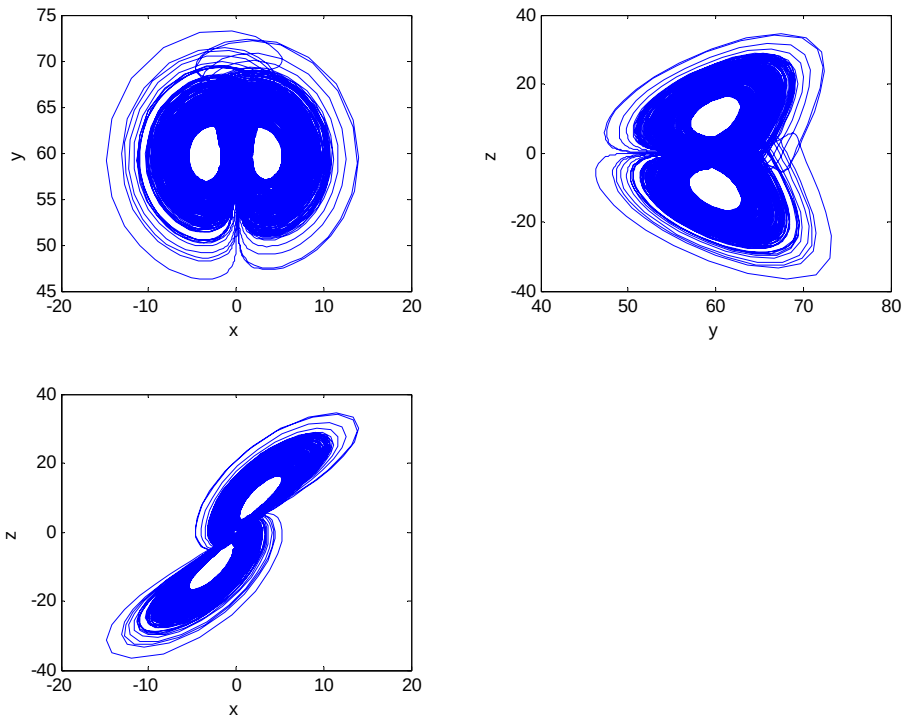

Fig. 5.16 phase portrait of BLDCM with (i, j, k) = (1,1, 0.6) and $\left(V_q, V_d, \delta, \sigma, \eta, T_L\right)$=(0.168,20.66,-0.875,4,0.26,0.53).

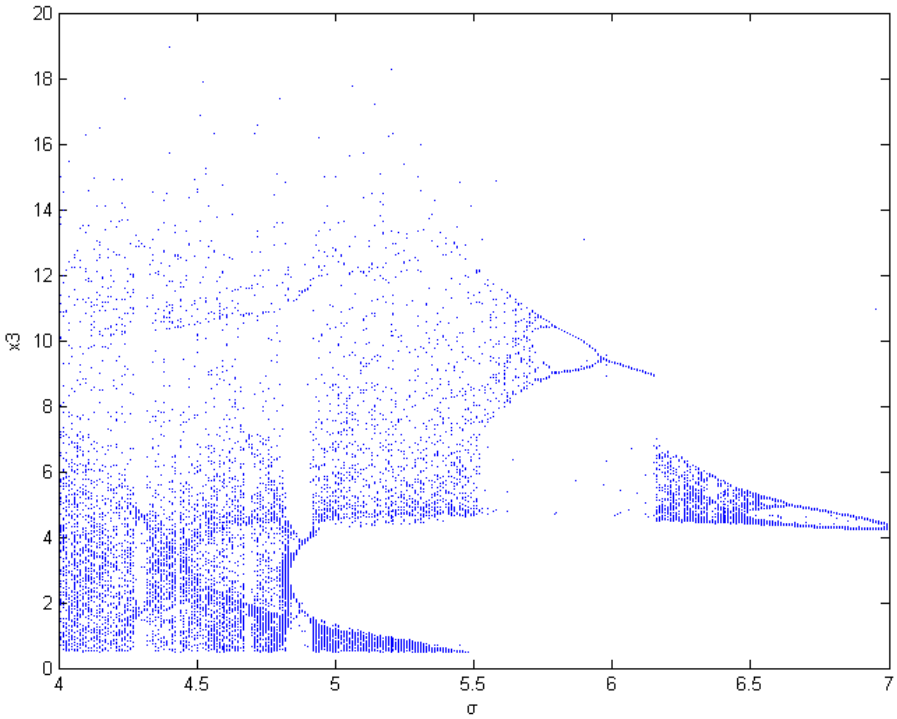

Fig.5.17 Bifurcation diagram for BLDCM with order (i, j, k) = (1,1,0.6).

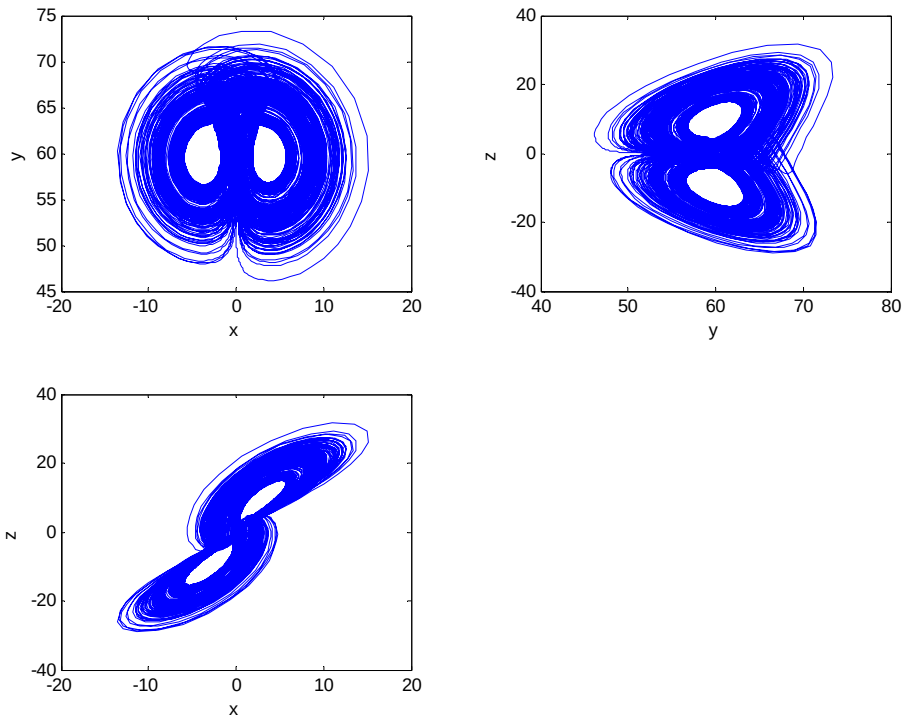

Fig. 5.18 phase portrait of BLDCM with (i, j, k) = (1,1, 0.7) and $\left(V_q, V_d, \delta, \sigma, \eta, T_L\right)$=(0.168,20.66,-0.875,6,0.26,0.53).

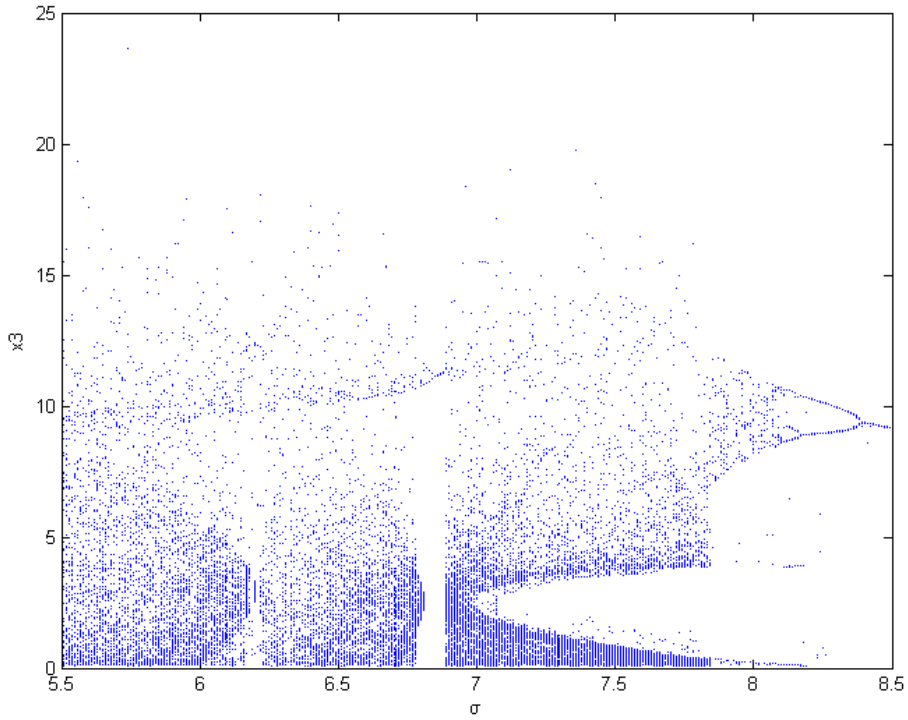

Fig.5.19 Bifurcation diagram for BLDCM with order (i, j, k) = (1,1,0.7).

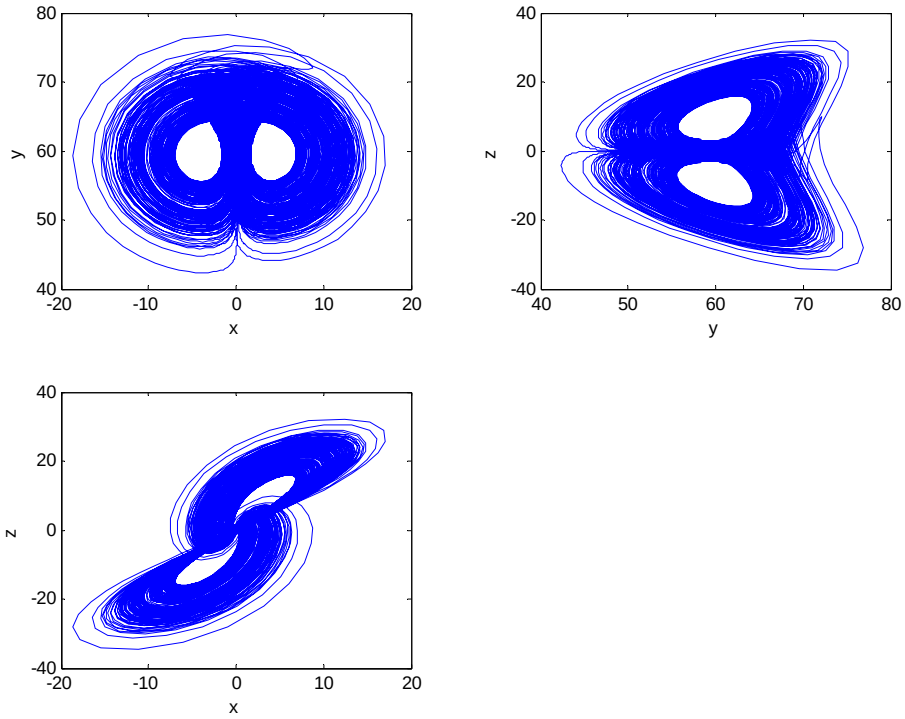

Fig. 5.20 phase portrait of BLDCM with (i, j, k) = (1,1, 0.8) and $\left(V_q, V_d, \delta, \sigma, \eta, T_L\right)$=(0.168,20.66,-0.875,7.2,0.26,0.53).

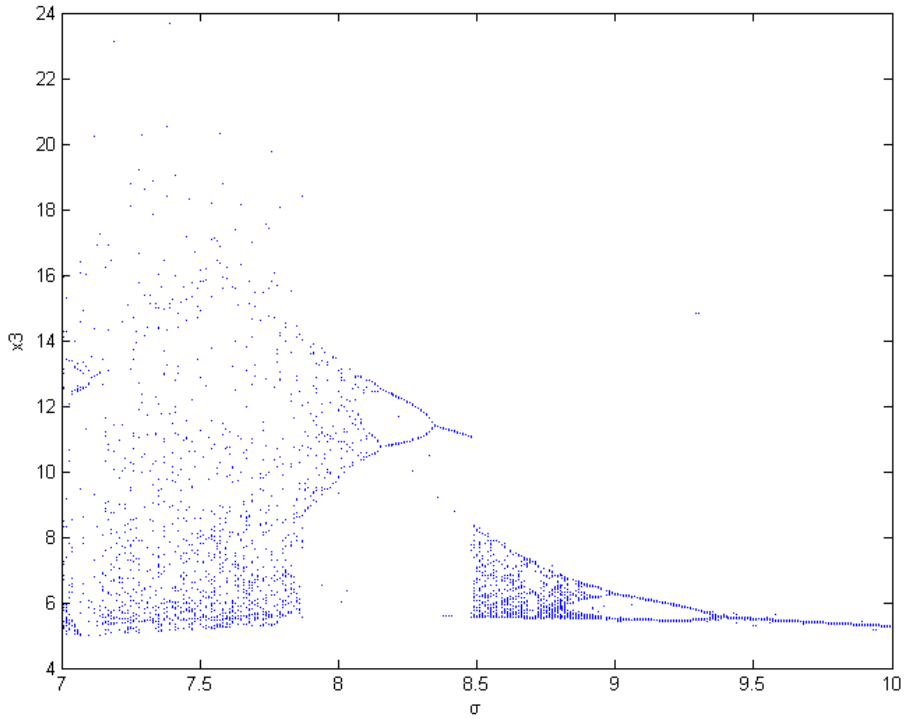

Fig.5.21 Bifurcation diagram for BLDCM with order (i, j, k) = (1,1,0.8).

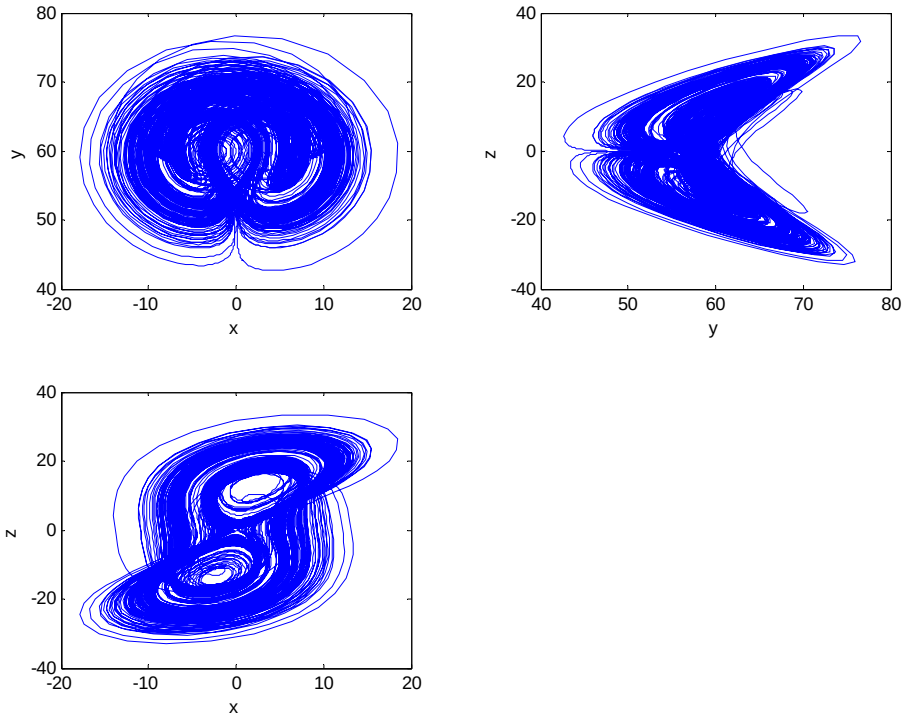

Fig. 5.22 phase portrait of BLDCM with (i, j, k) = (1,1, 0.9) and $\left(V_q, V_d, \delta, \sigma, \eta, T_L\right)$=(0.168,20.66,-0.875,3,0.26,0.53).

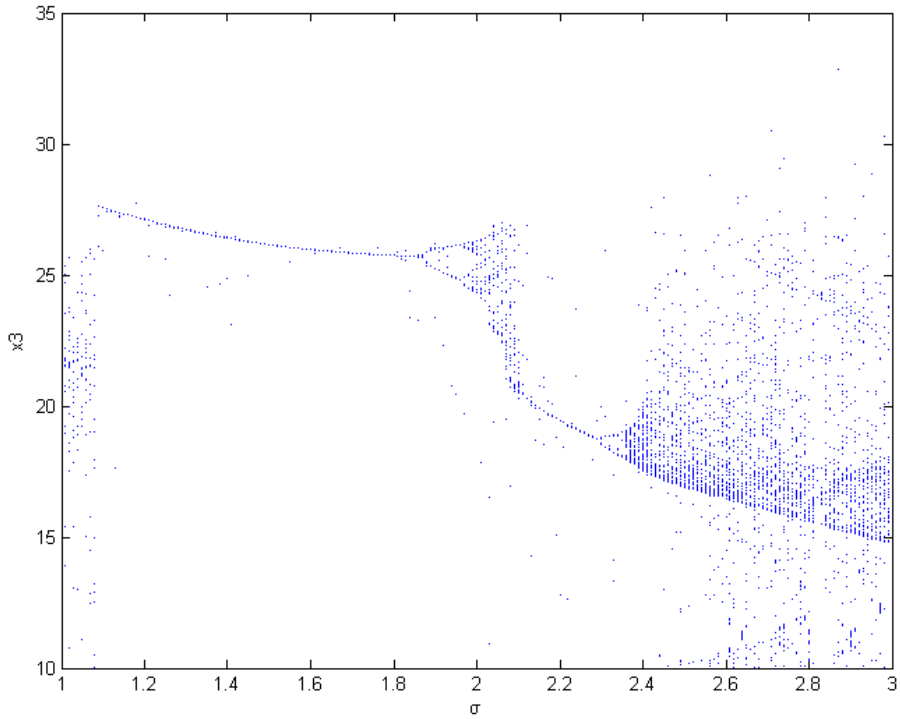

Fig.5.23 Bifurcation diagram for BLDCM with order (i, j, k) = (1,1,0.9).

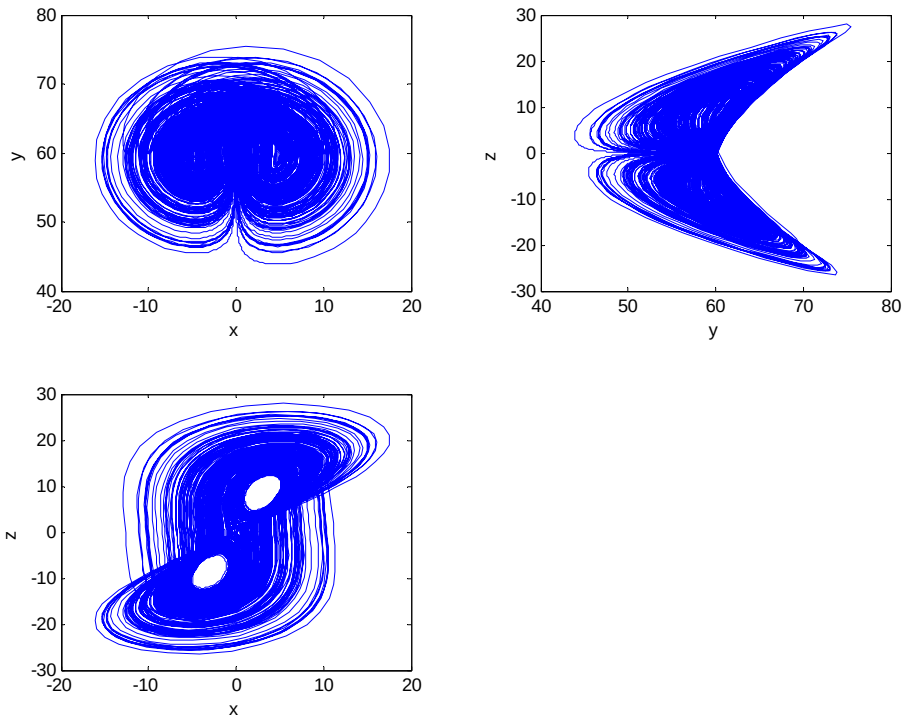

Fig. 5.24 phase portrait of BLDCM with (i, j, k) = (1,1, 1.1) and $\left(V_q, V_d, \delta, \sigma, \eta, T_L\right)$=(0.168,20.66,-0.875,9,0.26,0.53).

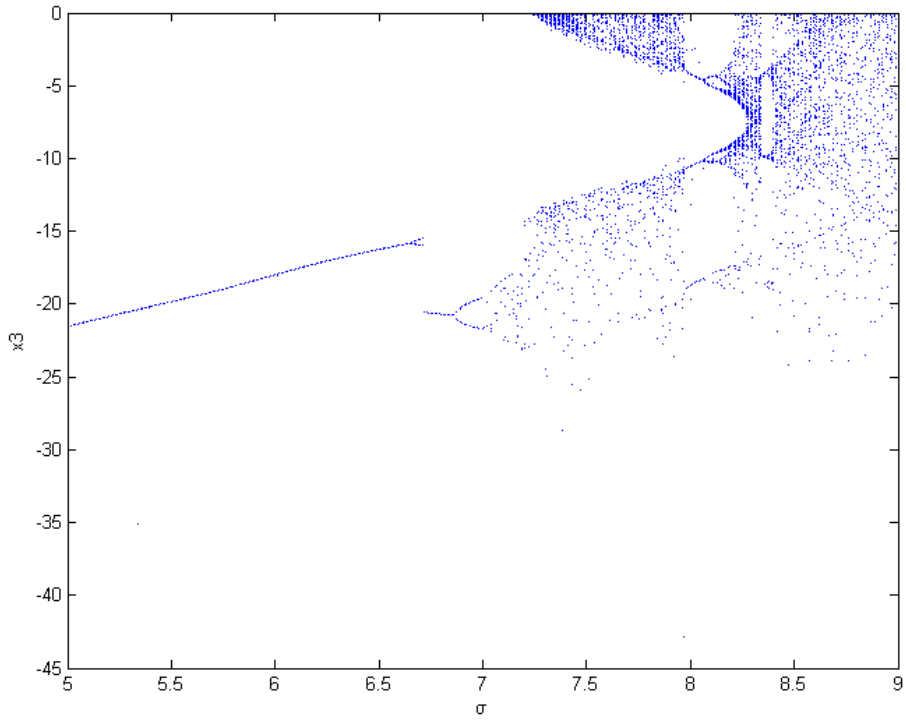

Fig.5.25 Bifurcation diagram for BLDCM with order (i, j, k) = (1,1,1.1).

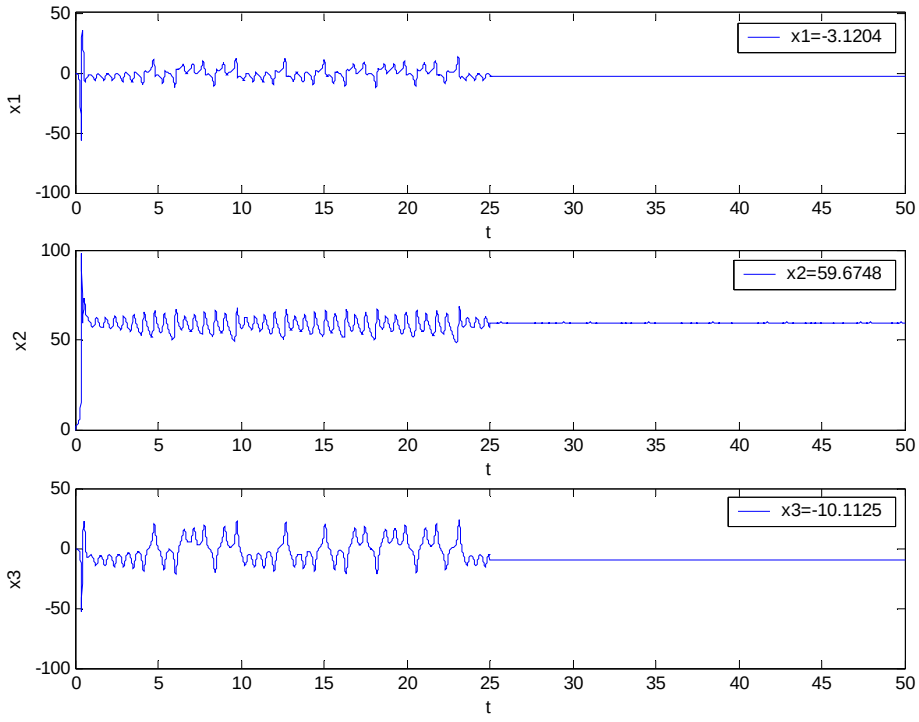

Fig. 5.26. Time history of system state with fractional order (i, j, k)=(0.9,1,1).
The equilibrium point is (x_1, x_2, x_3) =(-3.1204,59.6748,-10.1125).

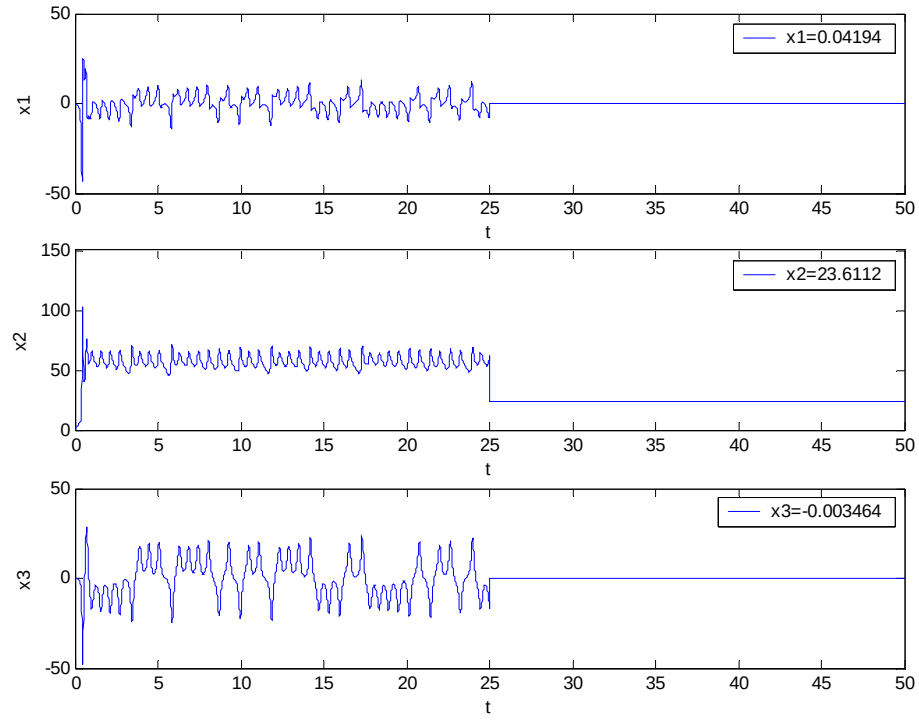

Fig. 5.27. Time history of system state with fractional order (i, j, k)=(1,0.9,1).
The equilibrium point is (x_1, x_2, x_3) =(0.04194,23.6112,-0.003464).

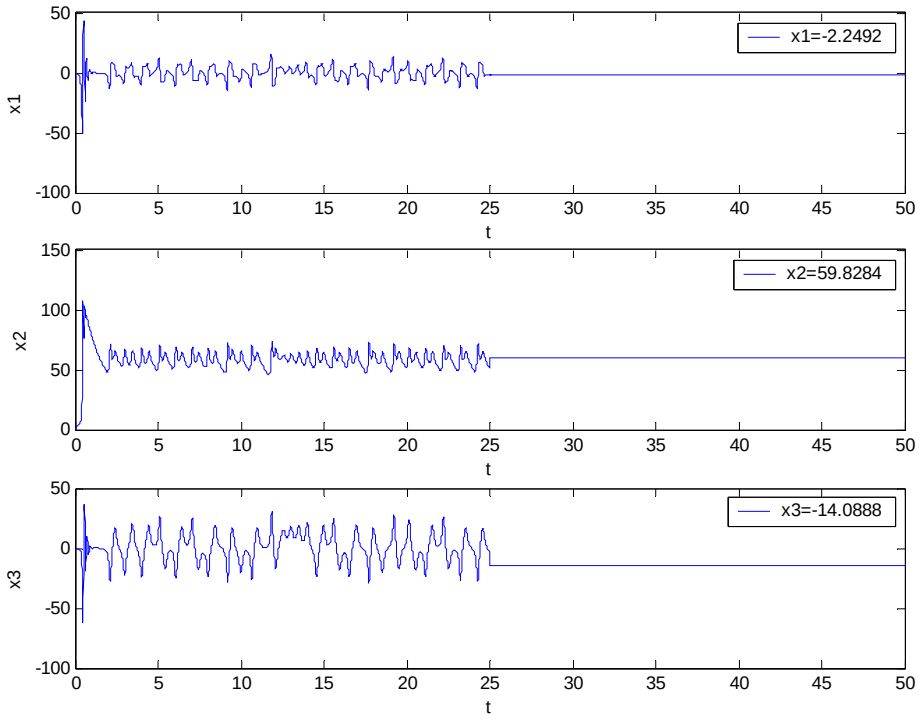

Fig. 5.28. Time history of system state with fractional order (i, j, k)=(1,1,0.9). The equilibrium point is (x_1, x_2, x_3) =(-2.2492,59.8248,-14.0888).

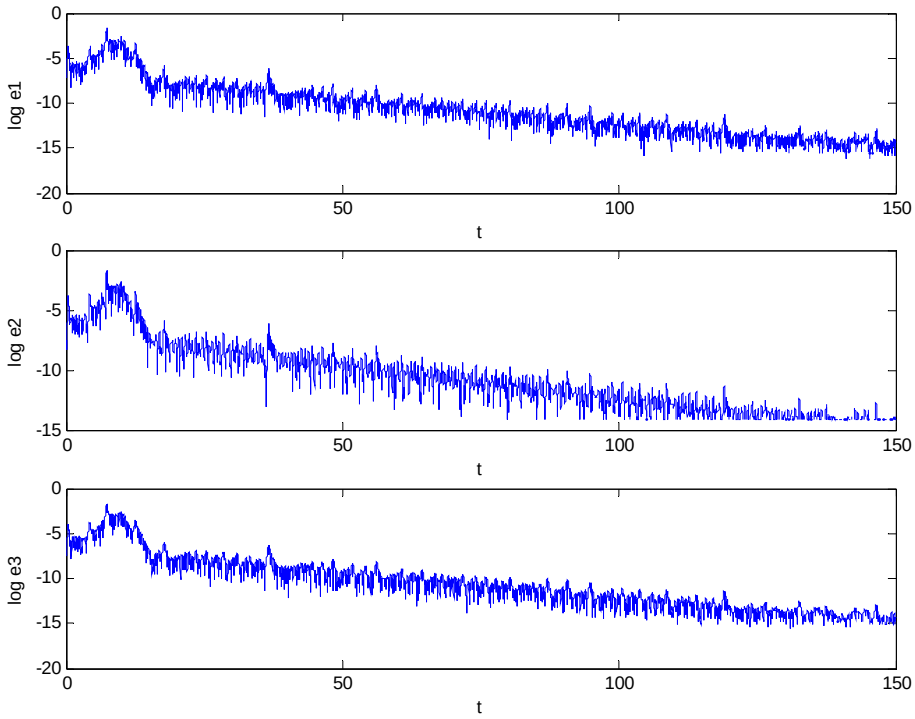

Fig. 5.29 synchronization for fractional order (i, j, k)=(0.9,1,1) and σ =7.

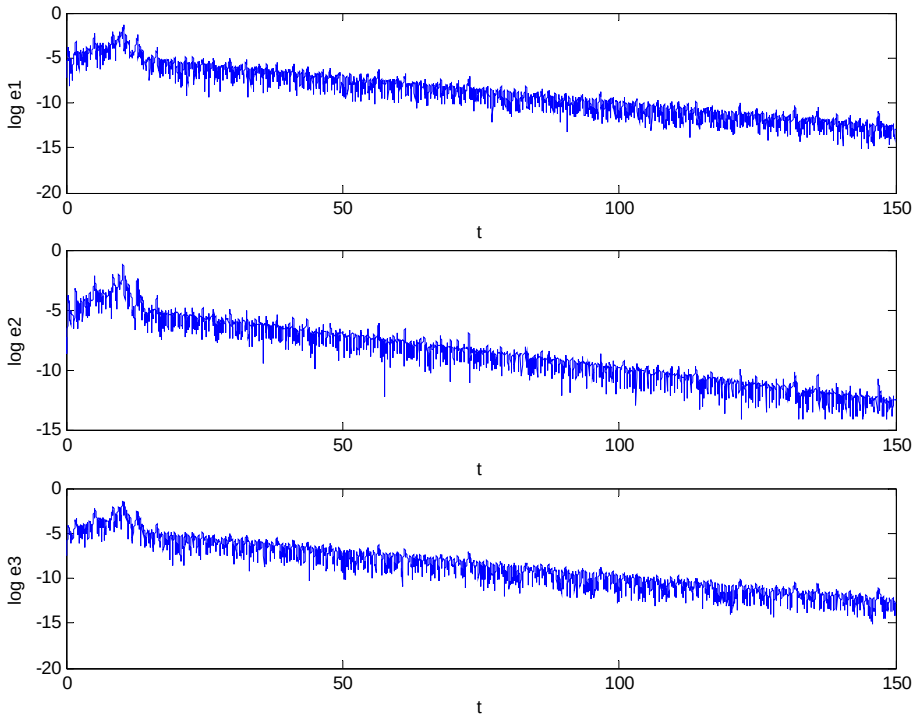

Fig. 5.30 synchronization for fractional order (i, j, k)=(1,0.9,1) and σ =6.

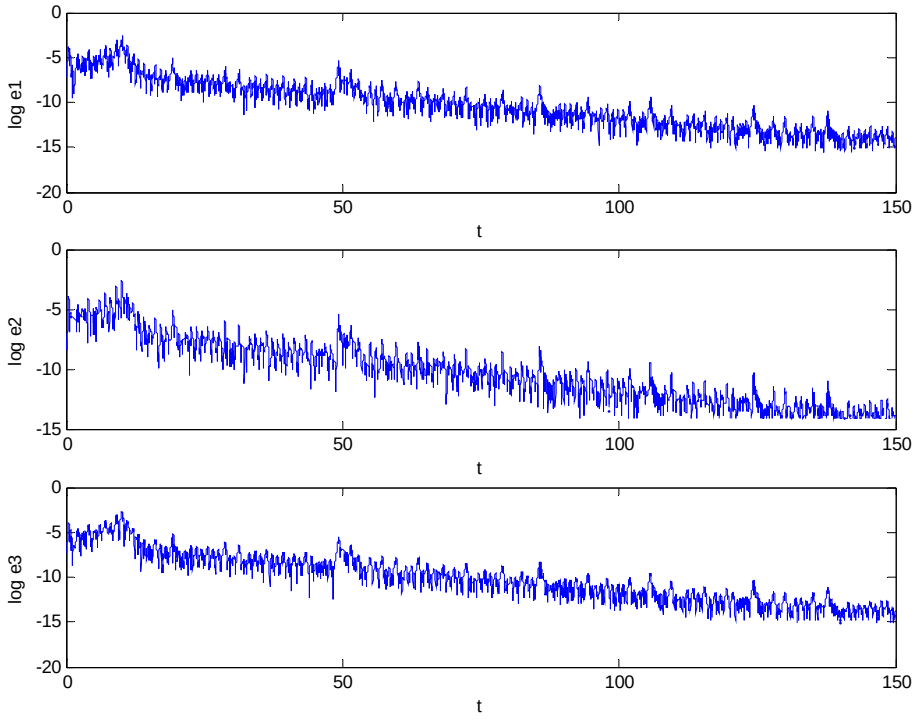

Fig. 5.31 synchronization for fractional order (i, j, k)=(1,1,0.9) and σ =3.

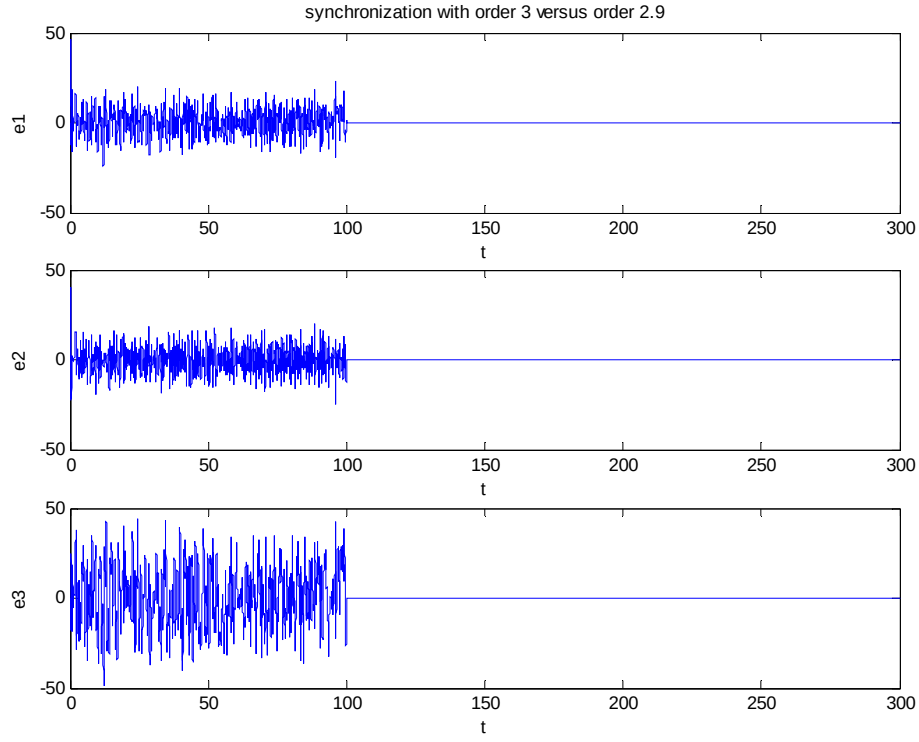

Fig. 5.32. The fractional order BLDCM system with (i, j, k) = (1,1,1), σ =4.55 and (i, j, k) = (1,1,0.9), σ =3.

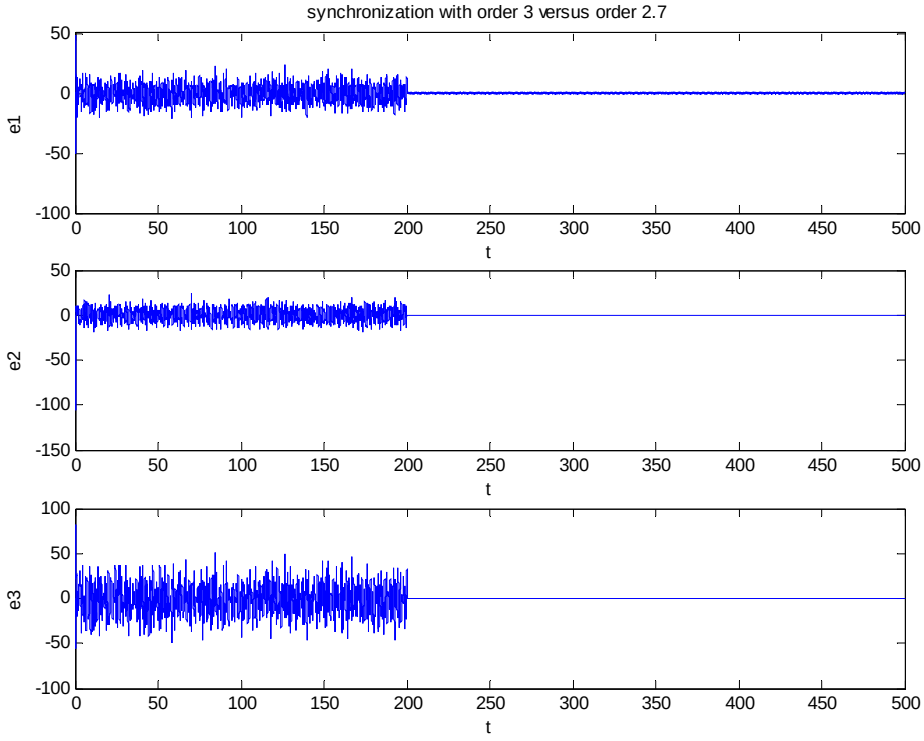

Fig. 5.33. The fractional order BLDCM system with (i, j, k) = (1,1,1), σ =4.55 and (i, j, k) = (1,1,0.7), σ =6.

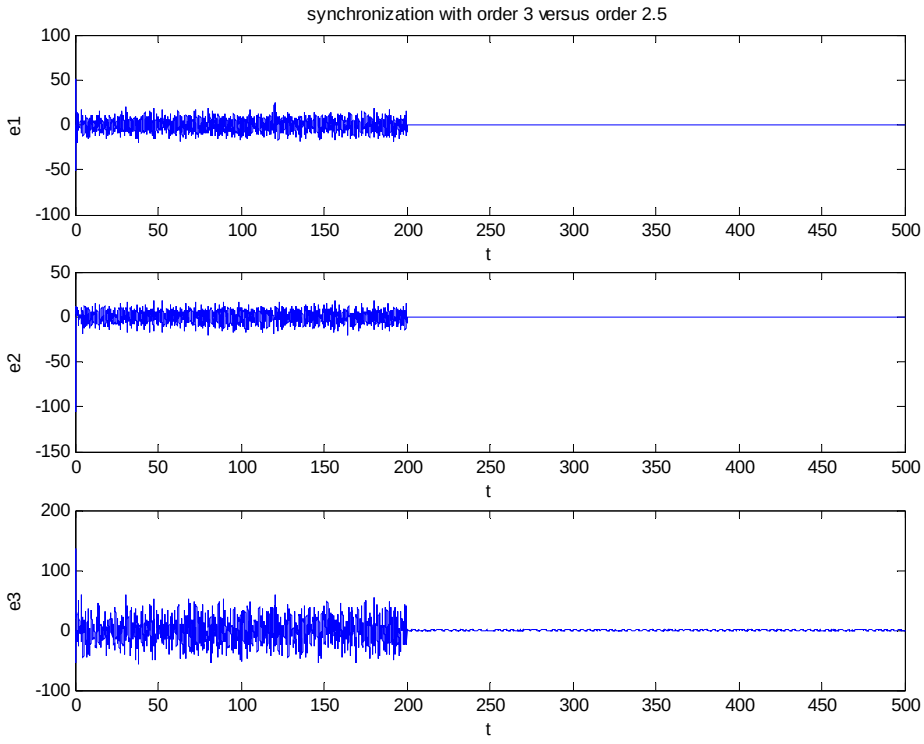

Fig. 5.34. The fractional order BLDCM system with (i, j, k) = (1,1,1), σ =4.55 and (i, j, k) = (1,1,0.5), σ =1.5.

REFERENCES

[1]. J. M. Ottino et al., “Chaos, Symmetry, and Self-Similarity: Exploiting Order and Disorder in Mixing Process”, Science, Vol. 257, pp. 754-760(1992).

[2]. S. J. Schiff, K. Jerger, D. H. Duong, T. Chang, M. L. Spano, and W. L. Ditto, “Controlling Chaos in the Brain”, Nature, Vol. 370, pp. 615-620(1994).

[3]. M. E. Brandt and G. Chen, “Bifurcation Control of Two Nonlinear Models of Cardiac Activity”, IEEE Trans. Circuits Syst., Vol. 44, pp. 1031-1034(1997).

[4]. K. M. Cuomo and V. Oppenheim, “Circuit Implementation of Synchronized Chaos with Application to Communication”, Phys. Rev. Lett., Vol. 71, pp. 65(1993).

[5]. L. Kocarev and U. Parlitz, “General Approach for Chaotic Synchronization with Application to Communication”, Phys. Rev. Lett., Vol. 74, pp. 5028(1995).

[6]. S. K. Han, C. Kerrer and Y. Kuramoto, “Dephasing and Bursting in Coupled Neural Oscillators”, Phys. Rev. Lett., Vol. 75, pp. 3190(1995).

[7]. B. Blasius, A. Huppert and L. Stone, “Complex Dynamics and Phase Synchronization in Spatially Extended Ecological Systems”, Nature, Vol. 399, pp. 359(1999).

[8]. H. Asada and K. Youcef-Toumi, *Direct Drive Robots: Theory and Practice*, Cambridge, MA: MIT Press (1987).

[9]. S. Murugesan, “An Overview of Electric Motors for Space Applications”, IEEE Trans. Ind. Elect. Contr. Instrum., Vol. IECI-28, No. 4(1981).

[10] W. Xie, C. Wen, Z. Li,”Impusive Control For the Stabilization and Synchronization of Lorenz Systems” Phys. Lett. A ;275 67(2000).

[11] Z.-M. Ge ; C.-C. Chang “Chaos Synchronization and Parameters Identification of Single Time Scale Brushless DC Motors” Chaos, Solitions and Fractals Vol.20, No 4, pp.883-903(2004).

[12] M. Rosenblum , A Pikovsky , J. Kurth ” Phase Synchronization in Chaotic Oscillators”.

Phys Rev Lett ;76:1804–7(1996).

[13] M. Rosenblum “A Characteristic Frequency of Chaotic Dynamical System” Chaos, Solitons & Fractals ;3(6):617–26(1993).

[14] D.Xu , Z. Li “Controlled Projective Synchronization in Nonpartially-Linear Chaotic Systems”. Int J Bifurc Chaos ;12(6):1395–402(2002).

[15] D. Xu , C. Chee , C. Li “A Necessary Condition of Projective Synchronization in Discrete-Time Systems of Arbitrary Dimensions”. Chaos, Solitons & Fractals ;22(1):175–80(2004).

[16] Z.-M. Ge ; C.-C.,Chen “Phase Synchronization of Coupled Multiple Time Scales Systems “ Chaos, Solitions and Fractals Vol.20, No 3, pp.639-647(2004)

[17]. P. C. Krause, *Analysis of Electric Machinery*, McGraw-Hill(1986).

[18]. N. Hemati and M. C. Leu, “A Complete Model Characterization of Brushless DC Motors”, IEEE Trans. Ind. Appl., Vol. 28, No. 1, pp.172-180 (1992).

[19]. N. Hemati, “Strange Attractors in Brushless DC Motors”, IEEE Trans. Circuits Syst., Vol. 41, No. 1, pp. 40-45 (1994).

[20]. N. Hemati, “Dynamic Analysis of Brushless Motors Based on Compact Representations of the Equations of Motion”, IEEE Trans. Ind. Appl. Soci. Annual Meeting, Vol. 1, pp. 51-58 (1993).

[21]Yanwu Wang, Zhi-Hong Guan, Hua O. Wang “ Feedback and Adaptive Control for The Synchronization of Chen System Via A Single Variable” Phys.Lett. A312, 34-40(2001).

[22] P. Parmananda, “Synchronization Using Linear and Nonlinear Feedback :A Comparison”Phys. Lett. A 240, 55(1998).

[23] T.-L. Liao, S.-H. Tsai, “Adaptive Synchronization of Chaotic Systems and Its Application to Secure Communications” Chaos ,Solitons and Fractals 11 ,1387(2000).

[24] S. Chen , J. Lu “Synchronization of Uncertain Unified Chaotic System via Adaptive

Control". Chaos, Solitons & Fractal ;14(4):643–7(2002).

[25] C. Wang, S.S. Ge,"Adaptive Synchronization of Uncertain Chaotic Systems Via Backstepping Design" Chaos, Solitons and Fractals 12 ,1199(2001).

[26] H.-T. Yan, "Design of Adaptive Sliding Mode Controller for Chaos Synchronization with Uncertainties", Chaos,Solitons and Fractals 22, pp. 341-347(2004).

[27].Y. Yu and S. Zhang"Global Synchronization of Three Coupled Systems with Ring Connection" Chaos, Solitons and Fractals 24, 1233-1242(2005).

[28] A. Alexeyev , V. Shalfeev "Chaotic Synchronization of Mutually-Coupled Generators with Frequency-Controlled Feedback Loop". Int J Bifurc Chaos ;5:551–8(1995).

[29]. L. M. Pecora and Th. L. Carroll "Synchronization in Chaotic System "Phys. Rev.Letter, volume 64,pp.821-824(1990).

[30]. L. Pecora, T. Carroll, G. Johnson, and D. "Fundamentals of Synchronization in Chaotic Systems,Concepts and Applications" Mar, Chaos **7**, 520 (1997).

[31]. H.U.Voss, "Anticipating Chaotic Synchronization"Phys. Rev. E **61**, 5115 (2000)

[32] S. Taherion , Y. Lai "Experimental Observation of Lag Synchronization in Coupled Chaotic Systems". Int J Bifurc Chaos ;10:2587–94(2000).

[33]. O. Calvo, D. R. Chialvo, V. M. Eguíluz, C. Mirasso, and R. Toral "Anticipated Synchronization : A Metaphorical Liner View" Chaos ,Vol 14,pp 7-13(2004).

[34] Z. Li, D. Xu "A Secure Communication Scheme Using Projective Chaos Synchronization". Chaos, Solitons & Fractals ;22(2):477–81(2004).

[35] C. Masoller, "Anticipation in The Synchronization of Chaotic Time-Delay Systems" Physica A 295 ,301(2001).

[36].Zhenya Yan "A New Scheme to Generalized (Lag, Anticipated and Complete) Synchronization in Chaotic and Hyperchaotic Systems"CHAOS 15, 013101 (2005)

[37] H.N. Agiza, M.T. Yassen, "Synchronization of Rossler and Chen Chaotic

Dynamical Systems Using Active Control" Phys. Lett. A 278 ,191(2001).

[38] X.Yang, G. Chen "Some Observer-Based Criteria for Discrete-Time Generalized Chaos Synchronization". Chaos, Solitons and Fractals ;13(6):1303–8(2002).

[39] N. Rulkov ,K. Sushchik , L. Tsimring , H. Abarbanel . "Generalized Synchronization of Chaos in Directionally Coupled Chaotic Systems".Phys Rev E 1995;51:980–94

[40] G. Chen , S. Liu "On Generalized Synchronization of Spatial Chaos". Chaos, Solitons and Fractals ;15(2):311–8(2003).

[41] L. Kocarev , U. Parlitz . "Generalized Synchronization, Predictability, and Equivalence of Unidirectionally Coupled Dynamics Systems".Phys Rev Lett ;76:1816–9(1996).

[42] G. Jiang, W. Zheng , G. Chen "Global Chaos Synchronization with Channel Time-Delay". Chaos, Solitons and Fractals ;20(2):267–75(2004).

[43]. Chunguang Li and Guanrong Chen system "Chaos in The Fractional Order Chen System and Its Control" Chaos Solitons and Fractals 24, 1233-1242(2004).

[44] A. Oustaloup , J. Sabatier, P. Lanusse "From Fractal Robustness to CRONE Control". Fract Calculus Appl Anal ;2:1–30(1999).

[45] A. Oustaloup, F. Levron , Nanot, B. Mathieu "Frequency Band Complex Non integer Differentiator": characterization and synthesis.IEEE Trans CAS-I ;47:25–40(2000).

[46] YQ. Chen, K. Moore "Discretization Schemes for Fractional-Order Differentiators and Integrators". IEEE Trans CAS-I ;49:363–7(2002).

[47] TT. Hartley , CE. Lorenzo "Dynamics and Control of Initialized Fractional-Order Systems". Nonlinear Dynamics ;29:201–33(2002).

[48] C.Hwang , J.-F.Leu , S.Y. Tsay "A Note on Time-Domain Simulation of Feedback Fractional-Order Systems". IEEE Trans Auto Contr ;47:625–31(2002).

[49] I. Podlubny , I.Petras , BM. Vinagre, O'Leary P, Dorcak L. "Analogue Realizations

of Fractional-Order Controllers". Nonlinear Dynamics;29:281–96(2002).

[50] Li C, Liao X, Yu J. "Synchronization of Fractional Order Chaotic Systems". Phys Rev E ;68:067203(2003).

[51] Tom T. Hartley, Carl F. Lorenzo, and Helen Killory Qammer " Chaos in Fractional Order Chua's System" IEEE, Tran. on circuit and systems,Vol. 42, No 8(1995).